International Journal of Mining and Mineral Engineering

ISSN:

1754-8918

2016-Volume 7 Number 3

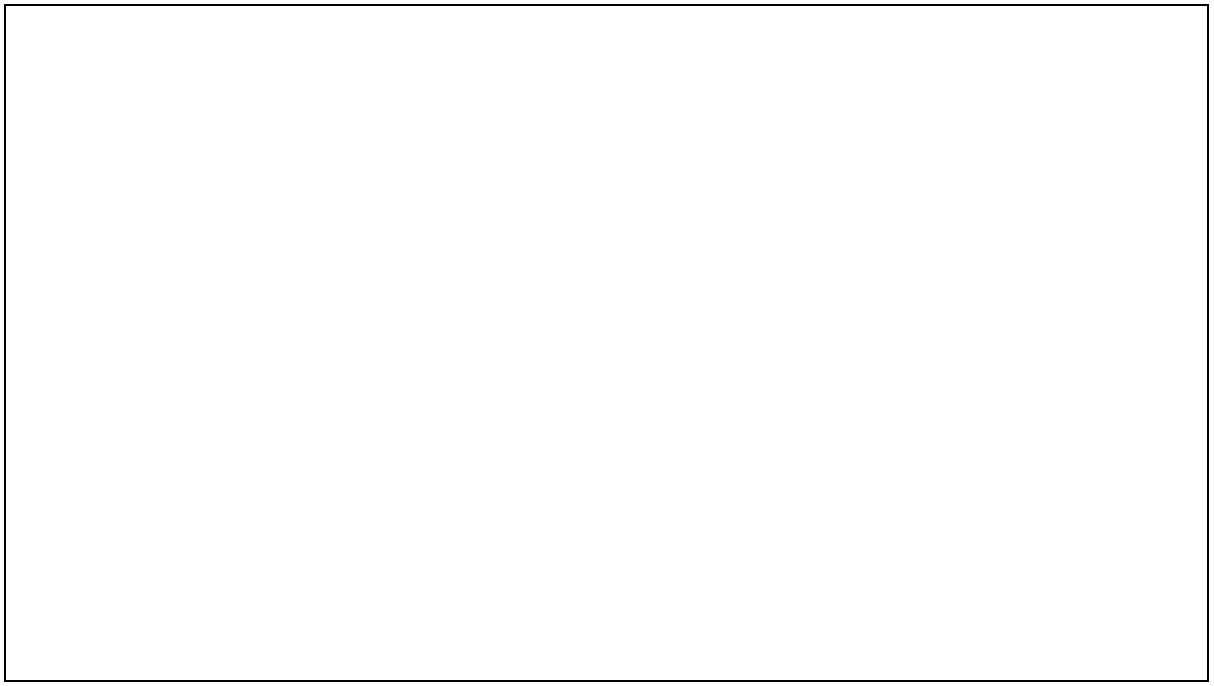

Diggability assessment in open pit mines: a review

Mohammad Babaei Khorzoughi*

Norman B. Keevil Institute of Mining Engineering,
University of British Columbia,
Vancouver, V6T 1Z4, Canada
Email: mbabaei@alumni.ubc.ca
*Corresponding author

Robert Hall

School of Mining and Petroleum Engineering,
University of Alberta,
Edmonton, T6G 2W2, Canada
Email: rhall1@ualberta.ca

Abstract: Loading efficiency has a critical role in increasing production and reducing cost of mining operations. Inefficient loading can significantly increase operational costs. The term diggability index is used to indicate ease of excavation. It also can be related to loading equipment performance and subsequently quality of blast. Several indicators have been defined in the past to assess diggability. This paper mainly focuses on the review of loading equipment based diggability assessment methods. The review highlights that although several indicators for different purposes were proposed in the literature, no universally accepted approach for diggability assessment has been defined which could produce reliable and repeatable results for assessing the muck-pile digging conditions. In addition to muck-pile characteristics and blast quality, operator practice and machine type and conditions have been found to have a significant effect on diggability. Therefore, it is necessary to investigate their effect in any diggability assessment study.

Keywords: diggability index; performance monitoring; muck-pile; loading equipment; electric rope shovel; fragmentation; open pit.

Reference to this paper should be made as follows: Babaei Khorzoughi, M. and Hall, R. (2016) 'Diggability assessment in open pit mines: a review', *Int. J. Mining and Mineral Engineering*, Vol. 7, No. 3, pp.181–209.

Biographical notes: Mohammad Babaei Khorzoughi is a PhD candidate, a Sessional Lecturer and a holder of 4-year Doctoral Fellowship in Mining Engineering at the University of British Columbia. His current research interests and experience include performance monitoring of mining equipment, measurement while drilling techniques, and reliability and maintenance of mining equipment.

Robert Hall is a Professor in the Department of Civil & Environmental Engineering School of Mining and Petroleum Engineering at the University of Alberta. Prior to joining University of Alberta, he spent 15 years at the

University of British Columbia. His areas or research include, mining equipment design and automation, equipment maintenance and reliability, comminution and energy reduction.

1 Introduction

Diggability index can be simply defined as a measure of ease of excavation under specific operating conditions. As a simple, single and easily understandable metric, a diggability index can be used to: provide feedback on drill and blast operations, help to set best operator practices, provide feedback to short range planning and help to improve reliability and availability of loading equipment.

However, one should be cautious when using a 'simple' diggability index as it might be influenced by non-diggability factors; such as operator digging practice, equipment used, and weather. Therefore, it is essential to consider the effect of these factors in a comprehensive diggability assessment study.

In the past, a number of diggability assessment studies have been conducted and several algorithms have been developed. This paper first discusses the importance of determining diggability and having an appropriate metric for it. Then, it gives a review of current approaches in the literature for assessing diggability.

2 Diggability and its importance

Mining operations mainly include two areas: mining and processing. The mining process includes drilling, blasting, loading and hauling and primary crushing (Hustrulid, 1999). Having problems in one stage may lead to inefficiencies in the subsequent stages of the process and therefore affect production. Among the mentioned steps, loading efficiency has a critical role in increasing production and reducing costs as the loading equipment is the source of ore supply (Hustrulid, 1999) or waste removal. For example, according to Scott and McKee (1994), one million dollars can be saved in a surface coal mine with a 1% improvement in digging efficiency, bucket load or cycle time of a dragline. To achieve efficient loading and subsequently hauling and crushing, efficient blasting is required.

Although blasting is one of the lowest cost items in an open pit mine, it has a critical role in the mining cycle. The cost of drilling and blasting is about 15% of the mining cost (crushing, grinding and processing costs have not been included) compared to the costs of loading and hauling which are up to 60% (Allen et al., 1999). Issues in blasting can add extra cost to a mining operation through wasted explosives, dilution, waste of energy in downstream, need for secondary blasting, damage to equipment, inefficient loading and hauling and inefficient processing (Babaei Khorzoughi, 2013). A poor blast design based on using the wrong type and amount of explosive or improper placement in a blast hole combined with inefficient timing design can lead to poor results and thus significantly reduce the overall productivity of an operation. Therefore, the goal of effective blasting is to achieve a good fragmentation and an acceptable amount of material movement which

are shown to be related to diggability by Chung and Preece (1999). The combined impact of such outcomes is more efficient loading as well as lower dilution of the ore and waste products to potentially result in higher productivity and lower cost per tonne (Babaei Khorzoughi, 2013).

To optimise blasting outcomes, it is needed to have quantitative feedback on the outcomes of current blasting practice. Fragmentation analysis, loading equipment performance studies, boulders counting, secondary blasting frequency and crushing performance studies are examples of methods that have been used to assess muck-pile diggability and quality of blast (Brunton et al., 2003; Hendricks, 1990; Jimeno et al., 1995; Koski and Giltner, 2009). Among muck-pile characteristics, such as profile, looseness, swell and size distribution, fragmentation size distribution can be easily quantified to determine the quality of blast. Some methods have been developed in the past to predict or determine fragmentation size distribution and assess muck-pile characteristics including visual assessment, photographic and image analysis methods (Ho Cho et al., 2003; Rholl, 1993; Van Aswegen and Cunningham ,1986), stereo-photogrammetric and machine vision techniques (Andersson et al., 2012; Han and Song, 2014; Han et al., 2011; Tafazoli and Ziraknejad, 2009; Thurley, 2011), loading equipment productivity (Allen et al., 1999; Brunton et al., 2003; Hawkes, 1998; Osanloo and Hekmat, 2005; Sari and Lever, 2007; Singh and Narendrula, 2006; Torrance and Baldwin, 1990; Tosun et al., 2013), partial screening (Ho Cho et al., 2003), high speed photography (Venkatesh et al., 1995) and mathematical modelling such as Kuz-Ram model (Cunningham, 1983, 1987, 2005), CK model (Chung and Katsabanis, 2000), KCO model (Ouchterlony, 2005), JK models (Kanchibotla et al., 1999) and BRW model (Bergmann et al., 1973).

However, these methods are mostly impractical due to production loss, high cost, high error,[1] subjective results and safety issues (Jimeno et al., 1995). For example, operator comments on the same digging conditions can vary from operator to operator (Karpuz et al., 1992). Therefore, many mining operations suffer from the lack of an acceptable and reliable post-blast assessment method to optimise their blasting process. It is believed that a properly measured diggability index can be used as a robust tool for post-blast evaluation. Additionally, a proper diggability index has to be less prone to measurement errors compared to other methods such as fragmentation measurements.

If the diggability index values are spatially plotted for several complete patterns, they could be combined with other available metrics, such as blastability index which is defined as ease of blasting (Babaei Khorzoughi, 2013), to aid the development of an optimum blast design with the proper placement of explosives including the delay, explosive type and amount and the initiation system. The resulting outcome should be a muck-pile that has a more even fragmentation size distribution as well as improved looseness; giving better digging conditions that lead to higher loading equipment productivity, lower machine wear and higher reliability, lower consumed energy per banked cubic metre as well as a reduced need for secondary blasting. In addition, as a result of more efficient use of explosive energy, there is also a potential to enable improved slope stability and wall control through a reduction in blast induced vibration damage. Finally, according to Hansen (2000) a diggability zone map allows mines to balance the cost of drilling and blasting vs. the excavation cost. Figure 1 shows an example of the diggability zone map overlaid on a blast pattern.

Figure 1 Diggability zone map (see online version for colours)

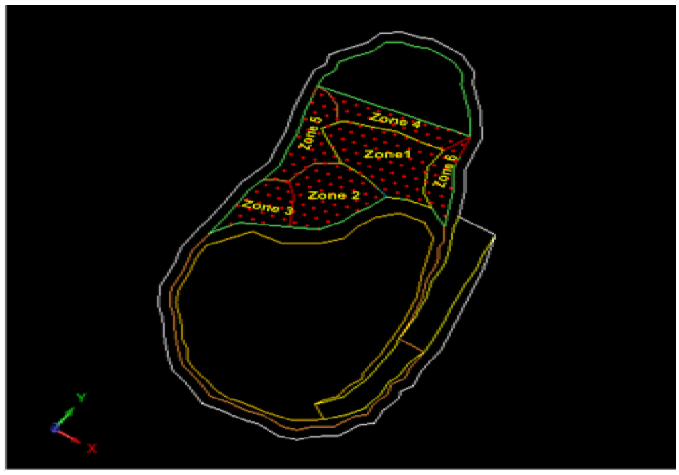

3 Diggability assessment techniques

As mentioned, this paper deals with a review of previous research on diggability. Over the past 40 years, a number of digging studies have been conducted and several diggability indices have been developed (Hendricks, 1990; Mol et al., 1987; Patnayak and Tannant, 2005; Williamson et al., 1983). Early investigations on diggability were related to intact rock or in-situ rock mass characterisation mainly for equipment selection purposes (Franklin et al., 1971; Hadjigeorgiou and Poulin, 1998; Kirsten, 1982; Scoble and Muftuoglu, 1984). However, since the early 80s with the availability of microprocessor technology and instrumentation of mining shovels, researchers have tried to introduce diggability as an index which could be related to loading equipment performance as it interacts with the muck-pile (Hendricks et al., 1990; Karpuz et al., 1992; Patnayak, 2006). In addition, a few attempts have been made in the past decade to study loading equipment digging effort and behaviour through analytical and numerical modelling (Awuah-Offei and Frimpong, 2007; Chung and Katsabanis, 2008; Stavropoulou et al., 2013).

Shovel performance monitoring has been used in the past as a tool to assess diggability based on key shovel performance indicators (KPIs). Cycle and dig time measurements (Allen, 1999; Brandt and Evans, 1998; Brunton et al., 2003; Doktan, 2001; Onederra et al., 2004), dipper fill factor and number of bucket passes (Brandt and Evans, 1998; Brunton et al., 2003; Segarra et al., 2010), dipper payload and power/energy consumption during digging (Hendricks, 1990; Karpuz et al., 2001; Patnayak, 2006) are examples of parameters that have been measured in the past to monitor shovel performance.

One type of mining equipment primarily used in most large, high volume operations as a loading unit is the electric rope shovel. This review mainly focuses on diggability evaluation for electric shovel operations.

3.1 Rock mass diggability classification

To establish a system for equipment and method of excavation selection, Franklin et al. (1971) proposed a graphical rock quality classification based on the fracture spacing and point load strength. Figure 2 shows the prepared chart for excavatability (diggability) classification by Franklin et al. (1971). As this figure shows, excavatability is grouped into the dig, rip, blast to loosen and blast to fracture classes.

Kirsten (1982) introduced an excavation index based on four parameters: mass strength, block size, relative ground structure and joint strength which could be related to the excavation effort. This index was given by:

$$N = a_1 \times a_2 \times a_3 \times a_4 \tag{1}$$

where a_1, a_2, a_3, a_4 are the numerical ratings of the aforementioned parameters. This excavation index was aimed to provide a tool for selecting the appropriate equipment and excavation method.

Similarly, Scoble and Muftuoglu (1984) introduced a diggability metric based on both ground conditions and equipment capabilities. The goal in developing a diggability index in this study was to predict the effect of ground conditions on loading equipment performance. Similar to Kirsten (1982), they proposed four geotechnical parameters to calculate a diggability index. These parameters included rock unit intact strength (*S*), extent of weathering (*W*), joint (*J*) and bedding (*B*) spacing. Finally, the summation of these four parameters as a diggability index was employed to connect machine type and performance and ground conditions to geotechnical features. The diggability index rating and the relevant classification are presented in Tables 1 and 2, respectively.

Table 1 Diggability index rating

	Class				
Parameters	*Rating*				
Weathering	Completely	Highly	Moderately	Slightly	Unweathered
Rating (W)	<0	5	15	20	25
Strength MPa (UCS)	<20	20–60	40–60	60–100	>100
Is MPa (50)	<0.5	0.5–15	15–20	20–35	>35
Rating (S)	0	10	15	20	25
Joint spacing (m)	<0.3	0.3–0.6	0.6–1.5	1.5–2	>2
Rating (J)	5	15	30	45	50
Bedding spacing (m)	<0.1	0.1–0.3	0.3–0.6	0.6–1.5	>1.5
Rating (B)	0	5	10	20	30

Source: After Scoble and Muftuoglu (1984)

Hadjigeorgiou and Poulin (1998) summarised various classifications that can be related to diggability. In this study an empirical ground classification for excavation in surface mines was presented which could be used for equipment selection. Table 3 shows different rock classifications for excavation purposes presented by Hadjigeorgiou and Poulin (1998).

Table 2 Diggability classification

Class No.	*Ease of digging*	*Index* ($W + S + J + B$)	*Plant which could be used without blasting*
1	Very easy	<40	Hydraulic backhoe <3 m^3
2	Easy	40–50	Hydraulic shovel <3 m^3
3	Moderate	50–60	Hydraulic shovel >3 m^3
4	Difficult	60–70	Hydraulic shovel > 3 m^3
5	Very difficult	70–95	Hydraulic shovel > 3 m^3
6	Extremely difficult	95–100	Hydraulic shovel > 7 m^3
7	Marginal without Blasting	>100	Hydraulic shovel > 10 m^3

Source: After Scoble and Muftuoglu (1984)

Table 3 Rock classification schemes for excavation purposes © [Elsevier]

Classification	*Franklin et al.*	*Weaver*	*Read et al.*	*Kristen*	*Scoble and Mouftouglou*	*Singh et al.*	*Smith*	*Scoble et al.*	*Karpuz*
Uniaxial comp. strength	✓	✓		✓	✓		✓		✓
Point load strength	✓		✓		✓	✓`		✓	
Schmidt hammer									✓
Tensile strength						✓			
No of joint sets				✓					
Rock quality designation				✓					
Volumetric joint count				✓				✓	
Joint roughness				✓					
Joint alteration				✓					
Joint orientation		✓	✓	✓			✓	✓	
Bedding spacing					✓				
Joint spacing	✓	✓	✓	✓	✓	✓	✓		✓
Joint continuity		✓	✓				✓		
Joint gouge		✓	✓				✓		
Weathering	✓	✓	✓		✓	✓		✓	✓
Seismic velocity		✓	✓			✓			✓
Abrasivity						✓			

Source: After Hadjigeorgiou and Poulin (1998)

To develop a comprehensive classification, data was collected from several mines in Canada about their equipment, geology and operating conditions. Hadjigeorgiou and Poulin (1998) defined ease of excavation as a characteristic of rock mass determined by its strength, structural features and weathering severity. As a result, point load strength of material and block size, derived from the number of joints per cubic metre or from visual

review, as well as variation in weathering conditions and relative ground structure were chosen to derive an excavation index (EI). Different classes of EI values show different degrees of ease of excavation from easily excavated to ground conditions necessitating blasting. Tables 4 and 5 show the EI rating and the relevant classification respectively.

Figure 2 Rock quality classification system

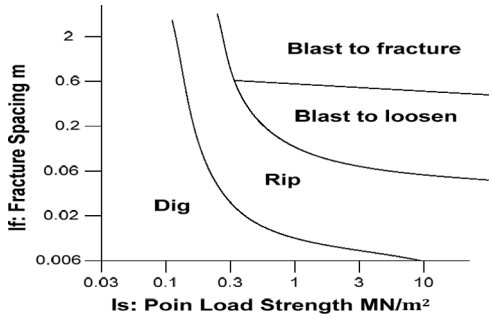

Source: After Franklin et al. (1971)

Table 4 Excavating index rating

	Class				
Parameters	*Rating*				
Weathering	Completely	Highly	Moderately	Slightly	Unweathered
Rating (W)	0.6	0.7	0.8	0.9	1.0
Rock strength Is MPa (50)	0.5	0.5–1.5	1.5–2.0	2.0–3.5	>3.5
Rating (Is)	0	10	15	20	25
Block size	Very small	Small	Medium	Large	Very large
Volumetric joint count (Joint/m^3)	30	10–30	3–10	1–3	1
Rating (Bs)	5	15	30	45	50
Relative ground structure	Very favourable	Favourable	Slightly favourable	Unfavourable	Very unfavourable
Rating (Js)	0.5	0.7	1.0	1.3	1.5

Source: After Hadjigeorgiou and Poulin (1998)

Table 5 Excavating classification

Class No.	*Ease of digging*	*Excavating index* ((*Is* + *Bs*) × *W* × *Js*)
1	Very easy	<20
2	Easy	20–30
3	Moderate	30–45
4	Difficult	45–55
5	Blasting required	>55

Source: After Hadjigeorgiou and Poulin (1998)

The EI developed in this study was applied to 49 case studies which showed that if material diggability could be estimated to a desirable degree of confidence, the excavation equipment then would be properly sized and fully utilised.

In addition to experimental classifications, some diggability indices and classifications have been proposed in the past decade using data processing techniques such as fuzzy logic and artificial neural network. Iphar and Goktan (2006) applied fuzzy theory set to the diggability classification system developed by Scoble and Muftuoglu (1984). They showed that fuzzy set theory could overcome the uncertainties associated with conventional classifications. Haghir Chehreghani et al. (2011) used artificial neural network to estimate rock mass excavatability. They aimed to establish a predictive relationship between rock mass and intact rock properties and excavatability of rock mass. This relationship could be a tool to predict rock excavatability and performance of machine at the design and planning stage. Input parameters to the model in this study were uniaxial compressive strength, tensile strength and discontinuities spacing of rocks and the output was volume of extracted rock (in cubic metre) per unit of power as the productivity indicator.

Rock mass classifications such as those mentioned in this paper can only help to gain an initial understanding of actual conditions and they are mainly used at the preliminary stages for equipment selection. However, to assess muck-pile digging conditions for operational activities, other methods such as shovel instrumentation and loading equipment performance assessment are required which will be discussed next.

3.2 Loading equipment performance studies

The performance of mining equipment such as electrical cable shovels may vary with the diggability characteristics of the muck-pile, operator practice and machine type. Using loading equipment performance for assessing muck-pile conditions is based on the assumption that the digging rate (productivity) is inversely proportional to the muck-pile coarseness and is directly proportional to the looseness (Jimeno et al., 1995). Previous research attempts have shown that loading equipment productivity declines as average particle size distribution increases (Osanloo and Hekmat, 2005; Singh and Narendrula, 2007). However, in addition to muck-pile conditions, operator proficiency and skills play a significant role in productivity of loading equipment (Hendricks, 1990; Jessett, 2001; Onederra et al., 2004; Patnayak et al., 2008; Awuah-Offei and Summers, 2010; Vukotic, 2013; Oskouei and Awuah-Offei, 2014, 2015); therefore, it is important to understand this parameter to isolate the effect of variation in muck-pile digging conditions on the shovel digging behaviour and effort.

Past studies presented in the literature are mainly grouped into three categories: shovel instrumentation, productivity monitoring and numerical and dynamic modelling. Research in these three areas is presented next.

3.2.1 Diggability assessment through shovel instrumentation

In the past studies, crowd, hoist and swing motor responses have been used to assess diggability of blasted and in-situ materials through shovel instrumentation. Williamson et al. (1983) conducted the first performance monitoring study to assess blast efficiency in an iron ore mine in Australia by monitoring of DC motors in a P&H 1900 and a P&H 2100 electric shovel. Crowd armature voltage and current, swing armature voltage,

hoist brake relay, crowd propel transfer relay and dipper trip were recorded during the shovel operation. Williamson et al. (1983) used the crowd motor voltage signal to derive a diggability index which was the ratio of change in the voltage and the area under the signal trace. This diggability index is given by:

$$\text{Diggability Index} = \frac{\sum|\delta V|}{\int_{t_1}^{t_2} V \mathrm{d}t} \tag{2}$$

where V is voltage, t_1 and t_2 are start and end of the digging respectively and δV is change in voltage values. The estimated diggability index values were found to vary from 1 to 10 with higher values representing harder digging conditions.

In this study the swing voltage signal was used to determine different activities and to isolate the dig cycle. Swing voltage was assumed to be static over the digging cycle. Figure 3 illustrates an example of their analysis including the crowd and swing motors responses for easy and hard digging conditions.

Figure 3 Monitored signals for easy and difficult digging conditions (see online version for colours)

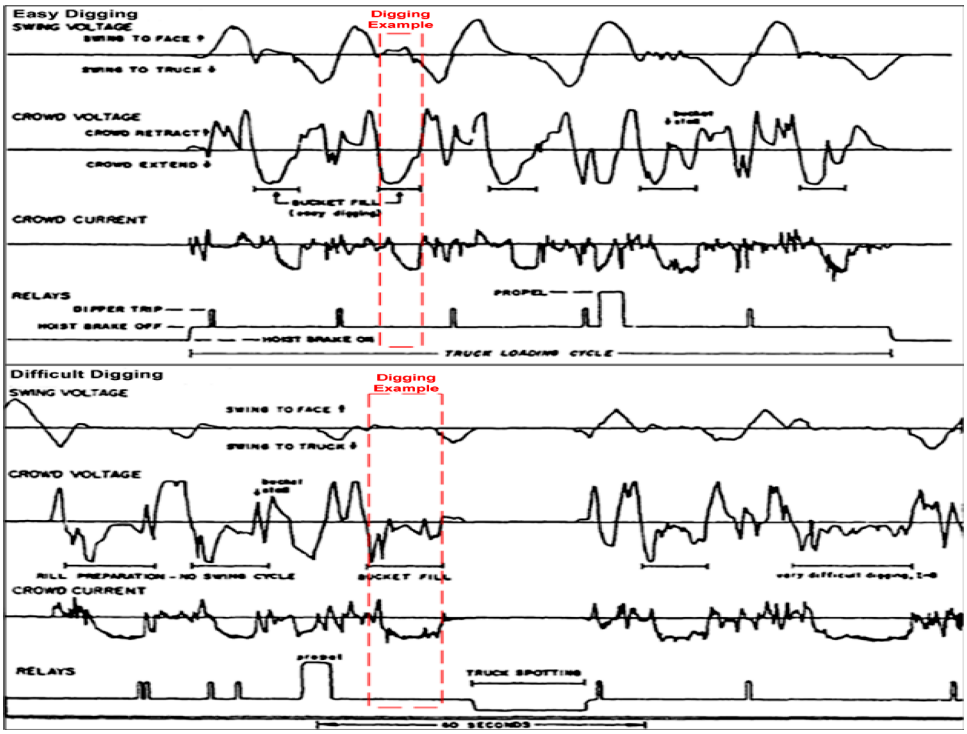

Source: Modified from Williamson et al. (1983)

As Figure 3 demonstrates, crowd voltages as well as current become more ragged in harder digging conditions. In spite of the fact that Williamson et al. (1983) used crowd voltage to assess diggability, they concluded that crowd power does not correlate well with actual digging conditions.

Mol et al. (1987) reported performance monitoring of P&H2300 electric shovels used for blasted overburden removal at an open cut coal mine in Australia. They measured crowd armature voltage and current, swing armature voltage, hoist armature voltage and current, dipper trip and crowd/propel relays. Similar to Williamson et al. (1983), in this study the swing motor was used to determine dig cycle, and crowd motor responses (volts and amps) were used to assess material diggability. Finally, a combination of crowd voltage, crowd current and dig time was used to derive a diggability metric. For different dig time intervals different definitions were proposed to estimate the diggability index. Estimated values were found to vary from 0 to 10. Table 6 presents diggability classification based on the proposed diggability index.

Table 6 Diggability index classification

Index value	*Digging condition*
<1.0	Extremely easy
1.0–2.0	Very easy
2.0–4.0	Easy
4.0–6.0	Normal
6.0–8.0	Difficult
8.0–9.0	Very difficult
>9.0	Extremely difficult

Source: After Mol et al. (1987)

In the study performed by Hendricks (1990), a P&H 2800XP shovel was monitored while loading blasted material in a coal mine in Canada. He used crowd armature voltage and current, hoist rope position and crowd arm extension signals to identify different shovel activities (digging, swinging and dumping). In contrast to Williamson et al. (1983) and Mol et al. (1987), he showed that swing voltage was not useful to determine dig cycle, and concluded that crowd motor responses were not sensitive to different digging conditions (from easy to very difficult). He stated that digging action primarily is accomplished by hoist motors, and that the crowd motor only assists to maintain a suitable depth of dipper penetration into the bank.

A post blast analysis was performed to quantify muck-pile conditions by using photographic methods. Moreover, shovel activities were identified through video tape records. To isolate the dig cycle from other activities, Hendricks (1990) used hoist rope position and crowd arm extension as well as hoist field current. The proposed algorithm was based on some if-then rules. Hendricks identified the beginning of digging when the hoist rope extension and crowd arm retraction are at a maximum and he identified end of digging when the crowd arm extension is at a maximum. However, Jessett (2001) in part of his study showed that this is a rigid procedure which may result in erroneous conclusions since in normal digging operation operators may follow different tactics.

Contrary to Williamson et al. (1983) and Mol et al. (1987), Hendricks (1990) showed that crowd motor's responses are not strongly related to digging conditions and he used hoist voltage and current signals to estimate muck-pile diggability. The established diggability index by Hendricks (1990) is given by:

$$\mathrm{DI} = \frac{\sum_{i=1}^{n} \left| \mathrm{HV}_{i+1} - \mathrm{HV}_i \right|}{\sum_{i=1}^{n} \left| \mathrm{SR} \times \mathrm{HV}_i \right|} \times \frac{\sum_{i=1}^{n} \left| \mathrm{HI}_{i+1} - \mathrm{HI}_i \right|}{\sum_{i=1}^{n} \left| \mathrm{SR} \times \mathrm{HI}_i \right|} \tag{3}$$

where

n: number of readings taken during the dig cycle

DI: diggability index

HV: hoist armature voltage

HI: hoist armature current

SR: sampling rate.

Equation (3) was used to determine the raggedness in hoist armature voltage and current signals. It was shown that in difficult digging conditions the DI is high while in easy digging conditions it is low. Table 7 shows diggability classification proposed by Hendricks (1990) based on the DI values.

Table 7 DI classification

Digging condition	*DI range*
Easy digging	0.4–0.8
Average digging	0.8–1.2
Difficult digging	1.2–1.6

Source: After Hendricks (1990)

It was also indicated that using average current and voltage values could be misleading. In difficult digging conditions, the hoist current average would be low compared to an easy digging condition because of high raggedness of the signal. Figure 4 compares examples of hoist current and voltage signals for easy and hard digging conditions. Hendricks (1990) concluded that using the average value for calculating power consumption gives a lower value for difficult digging conditions which is not expected. Additionally, he considered the influence of digging trajectory on diggability assessment. It was shown that the digging trajectory represented by a cut ratio (a ratio of crowd to hoist motion during the digging) has a significant influence on the motors responses and so DI values. But owing to the presence of complicating factors such as variation in muck-pile characteristics through its height, the accurate distance between shovel and muck-pile and variations in muck-pile profile during different cycles, he was unable to normalise diggability index on the basis of digging trajectory or operating practice.

Hunter et al. (1990) developed a cost reporting system to optimise blast and therefore to achieve minimum mining cost. By closely monitoring each blast and subsequent operations, it is possible to measure the effect of blasting on cost. Production variables, current operation costs and survey data were collected in this study. An image analysis system was also used to measure size distribution of dumps in the passing haul truck box, and a shovel monitoring system was employed to assess diggability. Finally maintenance and reliability information was collected to estimate maintenance cost under different digging conditions.

Figure 4 Example of hoist motors responses for easy and difficult digging conditions

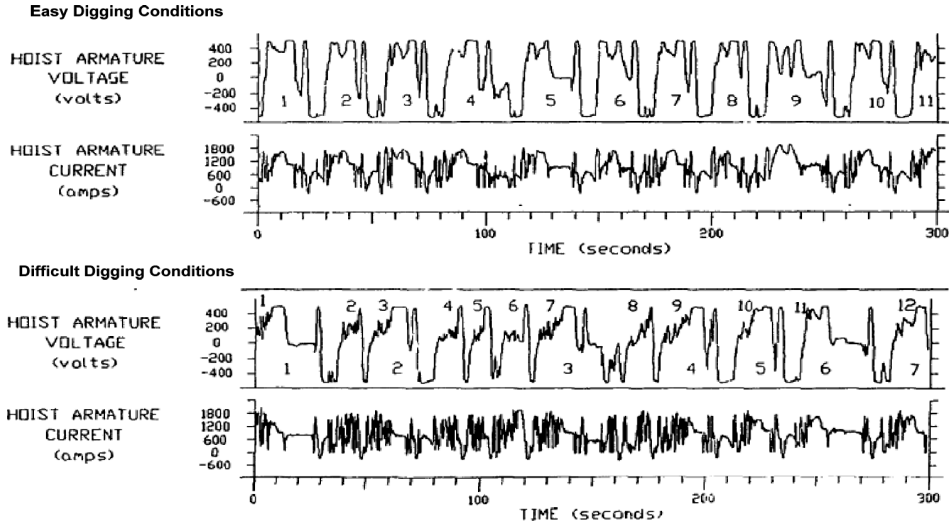

Source: Modified from Hendricks (1990)

In this study, a prototype monitoring system was used to monitor a P&H2100 shovel for diggability assessment. The system included a set of rotary transducers and a central computer along with an operator console. The operator manually recorded the end of loading a haul truck and downtimes. A tilt sensor was mounted on the boom to record boom jacking and vibrations. Thus, crowd current and voltage, vertical and horizontal tilt signals and crowd, hoist and swing positions were recorded at 0.1 second intervals. An example of data collected over a 200 seconds period is illustrated by Figure 5.

Figure 5 Shovel monitoring data

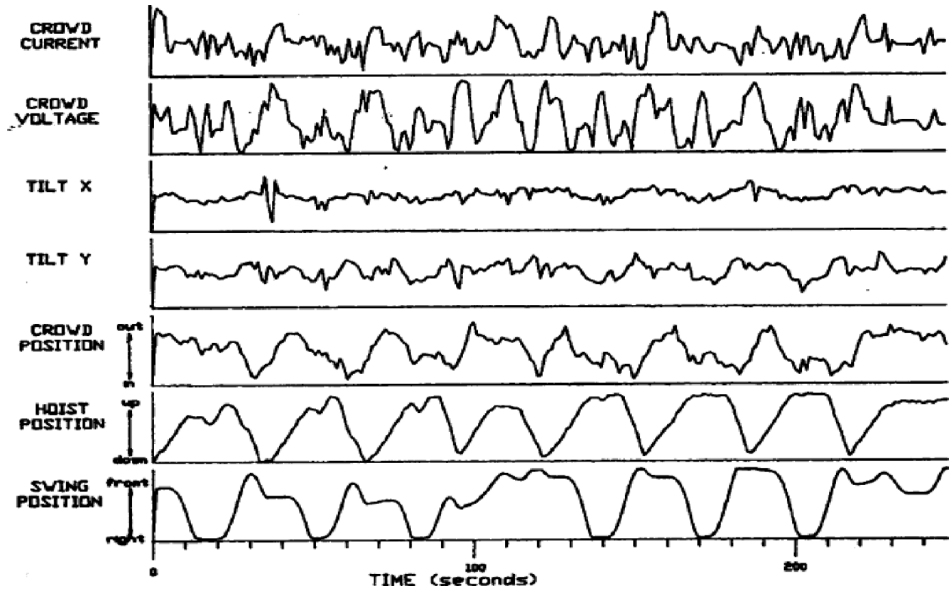

Source: After Hunter et al. (1990)

Load time per truck, time per dig cycle, waiting time for truck, downtime, diggability index, boom vibration index and swing angle are examples of estimated indices from this study. Diggability index was based on the Williamson et al.'s (1983) diggability index and boom vibration index was based on the longitudinal tilt signal and was defined as the number of peaks above a given threshold during loading of one haul truck. Hunter et al. (1990) concluded that tilt signals (Figure 5) are the direct measure of loading severity on the boom's mechanical structure and could be related to digging conditions and operator characteristics. In the proposed vibration index, mechanisms of excitation, operator proficiency and variations in muck-pile digging conditions were not considered which might cause various inaccuracies. In addition to shovel monitoring data and fragmentation analysis, maintenance operation data and costs were collected. It was shown that failure of a shovel's major components such as boom, dipper handle and crowd gear box is directly affected by digging conditions. Finally, based on the collected data, the mining cost imposed by blasting results was calculated which included primary and secondary drilling and blasting cost, loading cost, hauling cost and crushing costs. It was concluded that the proposed system could be used to optimise blasting based on the estimated mining cost.

Karpuz et al. (1992) presented performance monitoring of the P&H 2100BL electric shovels in Turkey surface coal mines. They compared cycle time, dig time, dipper fill factor and power on the main drive A.C. motor for four rock types with and without blasting under different depth of cut classifications. As a result, the influence of depth of cut and blasting on shovel performance was revealed. In this study, the average power of digging, energy consumption of digging and specific digging energy values were calculated to detect relative changes in the diggability of rock units and to examine effect of depth of cut. It was shown that large depth of cuts will result in higher power consumption. Karpuz et al. (1992) concluded that based on their results from different dig cycles, the specific digging energy which depends on power consumption, digging time and amount of excavated material was the best indicator which could reflect influence of depth of cut as well as ground characteristics. To measure power, a system was developed comprising mainly of a wattmeter and a data logger.

Similarly, in another paper, Karpuz et al. (2001) presented a quantitative determination of depth of cut and its relationship with performance parameters by monitoring dipper motion over digging activities. Depth of cut is one of the operational parameters which significantly affects parameters such as dig time, fill factor and dig energy that could be used in the diggability studies. Depth of cut was defined as the shortest distance between the initial face profile and the digging trajectory. An example of the typical motion trajectory of the dipper in the x-y space during the digging is illustrated by Figure 6.

They concluded that a low depth of cut value may result in a dipper which is not full at the end of the dig cycle. This would increase the dig time significantly. Alternatively, a high value of depth of cut may cause higher consumption of energy to fill the dipper.

In this study the dipper position was determined by using crowd angle and length. These parameters were measured using electrical transducers. Similar to the other research, in addition to performance parameters, a video tape of shovel activities was recorded at the same time. Also, before initiating the monitoring, excavation face properties were recorded including rock type, fracturing, weathering, and blast parameters such as blasting quality, block dimensions and swell factor. The post-blast quality was assessed by employing image analysis techniques. Consequently, based on

the several monitored dig cycle data, they concluded that energy consumption while digging per unit of time (time normalised digging energy) is strongly correlated with depth of cut as illustrated in Figure 7. Additionally, based on the results of different tests it was concluded that normalised digging energy is also strongly correlated with rock digging characteristics.

Figure 6 Example of digging trajectory and depth of cut

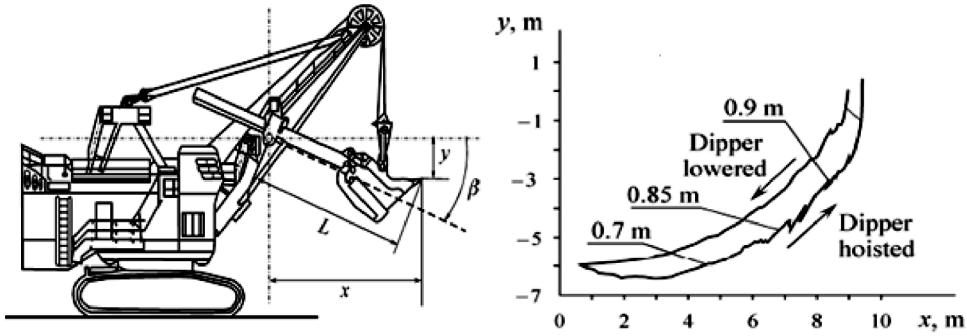

Source: Modified from Karpuz et al. (2001)

Figure 7 Time normalised digging energy against average depth of cut

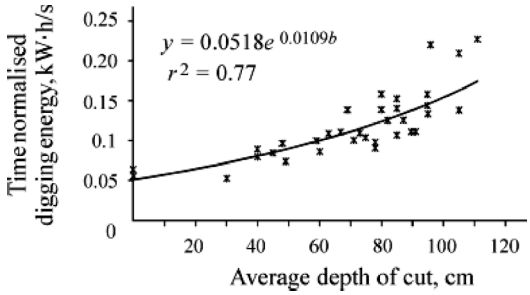

Source: Karpuz et al. (2001)

Kumar et al. (2000) reported performance monitoring of electric mining shovels using microprocessor technology in surface coal mines. The hoist and crowd motor responses were recorded under two different digging conditions-soft and hard-for up to four digging cycles. They concluded that hoist motor voltage and current are more sensitive to digging characteristics of muck-pile than crowd motor responses. Similar to Hendricks (1990) and contrary to Williamson et al. (1983) and Mol et al. (1987), they introduced hoist current signal as representative of the actual work done during digging. Also, they noted that besides crowd and hoist motor responses, shovel performance is a function of dipper position from the toe in the bank and muck-pile characteristics. In addition to this, they also studied the harmonic spectrum of voltages and concluded that an increase in the difficulty of digging resulted in a rise in the harmonic voltages.

Jessett (2001), in his master thesis presented a tool for performance monitoring of electric rope shovels. The data was collected from a P&H 5700 shovel operating in the Hunter Valley, NSW, Australia. The data was recorded at the rate of 100 Hz including stress state of the boom and boom suspension rope, boom dynamics, the main operator commands and analogue electrical signal from the shovel's primary drive systems.

To record the stress state and boom dynamics, he used eight accelerometers mounted to the boom as well as 16 strain gauges fitted to the boom and boom support ropes. Statistically comparing measured data for different operators, Jessett (2001) concluded that operator style affects shovel productivity. However, the variation in muck-pile digging conditions was not considered in comparing different operators' performance.

As part of this research, a framework was developed to monitor different shovel activities based on the electrical signals of the drive systems. To develop this framework, first, using a self-organising algorithm, it was shown that a structure exists in the sampled data from a shovel's electric drives, and data makes different clusters for different shovel activities. Then, employing Fisher's linear discriminant functions in a hypothesis testing strategy, an algorithm was presented and tested to track different shovel activities(digging, swinging, dumping, returning to dig and waiting for haul truck) and to detect events that result in significant duty loading. These events include: swing-during-dig, hoist stall and jacked boom. It was shown that on average, 30% of loading cycles include swing during digging. Figure 8 shows an example of a linear discriminant set's output for one loading cycle of the shovel. Jessett (2001) concluded that using this approach, shovel activities could be monitored with an accuracy of about 90%.

Figure 8 The output of a linear discriminant set for one loading cycle

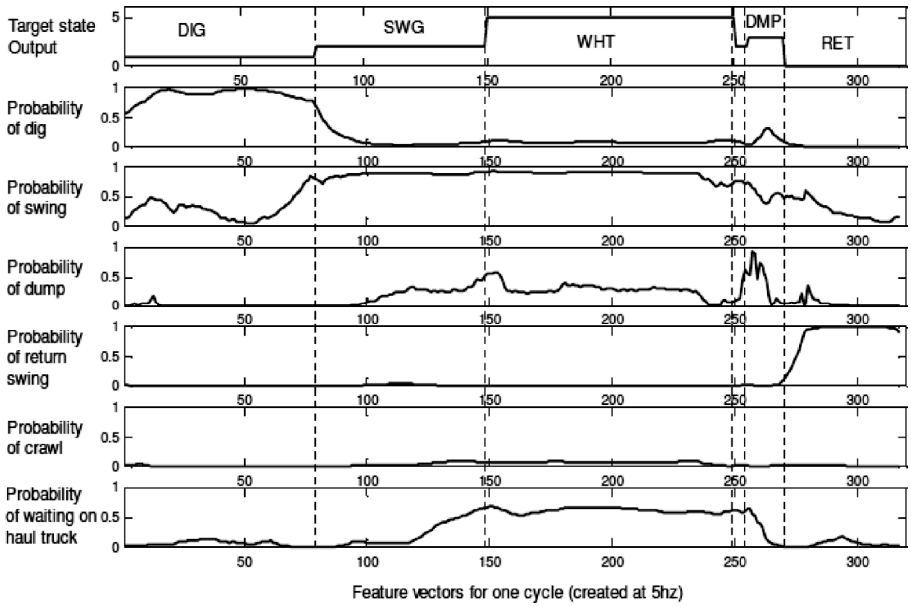

Source: After Jessett (2001)

Similar to Jessett (2001) and Joseph and Hansen (2002) introduced an algorithm to isolate different shovel activities. They recorded hoist motor current and voltage, swing motor current and voltage and dipper trip current and voltage. Then to isolate different shovel activities over a loading pass, variation in the hoist power consumption was used. These activities include dipper trip, dipper rebound, swinging to face, positioning the dipper, preparing to dig, digging in face and hoist drum braking.

Most of the studies presented so far were based on the digging of broken rocks. Patnayak (2006) monitored the performance of P&H4100 series shovels in an oil

sand operation. He used a set of recorded data including date and time, hoist armature voltage and current, hoist field current, crowd armature voltage and current, crowd field current, and swing voltage and current for eight different shovels including two models: TS and BOSS. The data sampling rate was 1 Hz. Dig cycle time, digging energy and digging power were used as the KPIs. As addresses by several researchers, digging trajectory has an important role in assessing material diggability (Hendricks, 1990; Karpuz et al., 2001). Patnayak (2006) showed that average hoist power (equation (4)) is less sensitive to digging trajectory and could be a useful metric to assess muck-pile diggability though he did not have any data to quantify variations in digging trajectory. Table 8 compares the variability between different performance indicators. The coefficient of variation values confirm that hoist power has the lowest variability.

$$\text{Average hosit power} = \frac{\sum_{i=1}^{n} \text{Hoist energy for individual dig cycle}}{\sum_{i=1}^{n} \text{Dig time for individual dig cyle}} \tag{4}$$

where n is the number of dig cycles. Hoist power energy for individual dig cycle in equation (3) is also given by:

$$\text{Hoist power} = \frac{0.5\sum_{i=1}^{n} |\,\text{HV}_{i+1} \times \text{HI}_{i+1} + \text{HV}_i \times \text{HI}_i\,|}{\text{Dig time}} \tag{5}$$

where

HV: hoist armature voltage

HI: hoist armature current.

He also monitored KPIs over different digging conditions to find the relationship between his KPIs and material diggability. For example, he postulated that digging time in similar operating conditions (trajectory and operator) could be used as a diggability metric. In the difficult digging conditions the digging time would be expected to be longer than easy digging conditions. However, it was shown that dig time between individual dig cycles in the same operating condition could vary due to the different digging height, depth of dipper penetration into the bank and digging trajectory. Therefore, he concluded that dig time is not a good indicator to assess diggability.

Table 8 Variability analysis of different performance indicators for 440 cycles of one shift

	Dig cycle time (s)	*Hoist energy* (kJ)	*Hoist power* (kW)	*Crowd energy* (kJ)	*Crowd power* (kJ)
Minimum	6	70	12	0	0
Maximum	24	28,210	1450	8500	657
Range	18	28,141	1438	8500	657
Mean	12	11,599	963	2928	246
Standard deviation	4	5011	262	2044	168
Coefficient of variation	36	43	27	70	68

Source: After Patnayak and Tannant (2005)

During this study, besides performance data, digital video recordings of different operating shovels were taken to identify different activities (especially dig cycle). By comparing these video records with performance data, it was concluded that in contrast to previous research, swing voltage is less sensitive to different shovel activities. Finally, Patnayak (2006) used hoist and crowd motor responses to isolate the dig cycle based on several if-then rules. However, the developed algorithm to isolate dig cycle was site specific.

3.2.2 Shovel performance study

In addition to the diggability studies through shovel instrumentation, some attempts have been made to relate shovel productivity to muck-pile digging conditions. As a result, some indicators such as dipper fill factor, dig time, cycle time, mucking rate and payload were evaluated in the past. Hawkes et al. (1995) presented a review of available methods of monitoring of equipment productivity operating in mines. According to Hawkes et al. (1995), the complete assessment of mining process of a surface coal mine involves determination of KPIs in the process, a methodology for recording and assessing the data and determination of suitable measurements.

In this study, methods for shovel monitoring were also discussed. On the basis of the work published by Williamson et al. (1983), Kennedy (1995) and Hawkes et al. (1995) named the principal requirement of shovel monitoring system:

> "minimal rock handling, minimal interruption to production, accuracy and reproducibility of results, relatively low cost, suitability for routine use, real time data output, minimal subjective input, data quality to reflect true shovel performance and resulting size parameters which can be related to a blast design model." (Hawkes et al., 1995, p.129)

As a case study, they conducted a manual time and motion study for a truck/shovel operation in a coal mine in Australia. They aimed to find the relationship between powder factor and size of blast and shovel productivity; however, the quality of collected data was poor. Therefore, no correlation was evident. They concluded that shovel monitoring should be controlled and well understood to draw precise conclusion on the success of any blast practices.

A document published by P&H MinePro Services (2003) defines the diggability as the ease of excavation in working face which is a function of material hardness, weight, density, grain size, moisture content, fragmentation and several other factors. In this document fill factor was reported as a diggability metric which shows how easily materials flow into the dipper. Fill factor is defined as:

$$\text{Fill factor} = \frac{\text{Loose volume per load}}{\text{Dipper rated volume}} \tag{6}$$

It is important to consider that fill factor could vary by different dipper designs and machine conditions as well as operator practice and skills. A shovel with a custom designed dipper operating in well-fragmented and loosened enough materials can achieve fill factors of 100–120% and more (P&H MinePro Services, 2003). Table 9 shows the material diggability classification based on the dipper fill factor for electric rope and hydraulic shovels presented by P&H MinePro Services (2003).

Table 9 Diggability classification based on fill factor

	Approximate dipper fill factor	
Material diggability	*Electric rope shovel*	*Hydraulic shovel*
Easy digging	1.05–1.20	0.95–1.05
Medium digging	1.00–1.15	0.90–1.00
Hard digging	0.90–1.00	0.85–0.95
Very hard digging	0.85–0.95	0.80–0.90

Source: After P&H MinePro Services (2003)

Onederra et al. (2004) presented outcomes of a comprehensive study called Shot to Shovel. In this study the influences of muck-pile characteristics and operator skills on shovel productivity was investigated using a drill and blast information management system, high precision GPS and modular's dispatch system. Although the data was collected from a hydraulic shovel, because of its importance this study is included here.

During the course of the project a set of performance data was collected including number of bucket passes, dig, swing, dump and return time. The results showed a high degree of variability in all of the loading cycle components, especially dig time. This can be explained by variation in muck-pile characteristics and different digging tactics. To examine the impact of muck-pile characteristics on shovel performance, they monitored fragmentation, muck-pile shape, swell and looseness. They chose these parameters because of their ease of measurement and their reported impacts on loading equipment productivity. To assess fragmentation, Onederra et al. (2004) employed split desktop image processing system and the photographs were taken of the truck box when it was full.

Using HPGPS, modular's dispatch system and GIS based software, the profile of the muck-pile was generated. It was shown that muck-pile shape has a direct impact on the diggability. In the lower (flatter) regions of the muck-pile, dig rate was below average. Also, it was observed that dig rate decreases in the corner regions of muck-piles. They stated that this occurred due to loading geometry limitations and/or decreases in material looseness as the burden relief decreases.

Similarly, Clark et al. (2004) investigated the effect of muck-pile characteristics on the performance of electric rope shovel by using scale model technology to emulate actual field conditions in the laboratory. The modelled machine type in this study was P&H4100XPB and muck-pile independent variables were size distribution, compaction, height and cohesion, but in the presented paper only muck-piles with high oversize size distribution were tested which could affect the results. A dig algorithm was also used to simulate operator performance. Measured dig response also includes dig energy, dig time and dipper payload. They modelled oversize piles with three compaction degree (loose, compact and very tight) made up of two pile height (37.5 ft and 50 ft) compared against two cohesions (high cohesion with clay fines and low cohesion with sandy dirt fines). They concluded that muck-pile height does not have any significant effect on shovel productivity. High cohesion material increased the dig time, increased energy consumption and increased the payload. However, compaction was reversely proportional to payload. Figure 9 shows a reproduction of their results.

To further investigate the relationship between muck-pile characteristics and loading equipment performance, Segarra et al. (2007) investigated the effects of blasting

parameters on loading equipment's efficiency. They used mucking rate (amount of rock excavated per unit of time) and mean bucket load (bucket load per pass) as key excavator efficiency indicators for rope shovels and front-end-loaders. During the course of this project, rock characteristics, blasting parameters (drill pattern, explosive energy and charging) and the loading equipment's performance (truck loading time and number of buckets to fill a truck) were measured in an open pit iron mine. To characterise rock properties, point load test and rock density measurements were carried out for different samples from different benches.

Figure 9 Main effect plots (data means)

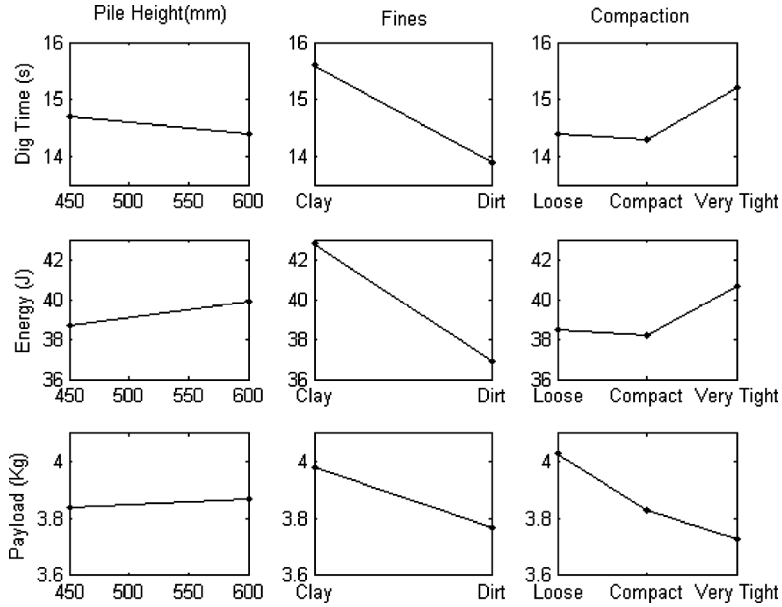

Source: Modified from Clark et al. (2004)

They introduced excavator (rope shovel and front-end-loader) efficiency as a measure of muck-pile diggability which is a function of rock movement and fragmentation. Although there are several factors such as muck-pile profile, operator proficiency and machine type that may affect the relationship between blasting performance and loading equipment's productivity, in this study similar to most of the published work only the effect of blast parameters were investigated. Blasthole length, burden at the crest of the block, spacing, stemming, sub-drilling length, mass of explosive, charge length and energy of explosive were recorded during this project.

They concluded that there is no strong correlation between mean bucket load and blasting parameters, whereas there is a positive correlation between mucking rate and explosive energy. Also, it was shown that there is no significant correlation with rock characteristics. Segarra et al. (2007) suggested that mucking rate is a non-monotonic function of the useful work of the explosive per unit volume of rock (specific energy, J/m^3).

On the basis of the results of this work, Segarra et al. (2010) presented a model for prediction of mucking productivity which was defined as bank cubic metres loaded into trucks per hour. This production rate was estimated from the product of maximum

production rate and the efficiency of loading equipment. The efficiency of the loading equipment was defined as a function of rock strength, nominal bucket capacity and explosive energy concentration or energy powder factor.

Mechanical rock characteristics, blasting design parameters and loading equipment productivity data were collected from field measurements in 20 blasts at two open pit mines (iron and copper). Excavator productivity data includes excavator type (front-end-loader and rope shovel), nominal bucket payload, mass loaded into a truck, passes required to load the truck and truck loading time. All of these data were recorded manually. The gathered data in the field were used to obtain coefficients of the developed model. As a result, production rate was defined as:

$$Q = Q^{\circ} \mathrm{e}^{-kf_s / B_P} \left[\frac{\sigma^2}{(E - E^{\circ})^2 + \sigma^2} \right] \tag{7}$$

where

Q: production rate

Q^{o}: maximum production rate[2]

k: coefficient

f_s: rock strength factor

B_p: nominal payload of excavator

σ: scale parameter

E: energy concentration (energy powder factor)

E^{o}: energy concentration at which the excavator's efficiency is maximum

Q^{o}, k, σ and E^{o} were determined from data using non-linear least square regression technique. Rock strength factor was also given by:

$$f_s = 0.0015\rho_r - 3 + 0.264\, I_{s(50)} \tag{8}$$

where ρ_r is rock density (kg/m^3) and $I_{s(50)}$ is point load strength. Segarra et al. (2010) concluded that this model explains up to 90% of the variance of the production rates and is statistically significant though it is a site dependant equation.

In an attempt to improve the model presented in equation (7), Sanchidrian et al. (2011) suggested that Q^{o} depends on the dipper capacity and proposed a new model given below:

$$Q = c_1 B_M{}^{c_2} \mathrm{e}^{-kf_R} \mathrm{e}^{-\frac{(E_E - E_E^0)^2}{2\sigma^2}} \tag{9}$$

where

B_M: dipper payload

c_1, c_2, k: coefficient

f_s: rock strength factor[3]

σ: shape parameter

E_E: energy concentration (energy powder factor)

E_E^0: energy concentration at which the excavator's efficiency is maximum.

Compared to model presented in equation (7), it was concluded that the modified model explains 92% of the variance of the production rate.

Similarly, Koski and Giltner (2009) and Giltner and Koski (2010) reported the outcomes of an audit performed on blasting operations at an iron mine. The main goal of this study was to improve productivity through digging conditions improvement and oversize reduction.

According to this, to assess diggability, 17 measures of diggability such as photometric fragmentation analysis, digging rates, plugged mill chute frequency, secondary breakage, etc were identified. However, most of these measures were infeasible to use due to the high cost, inadequate records, safety issues and being too subjective. Hence, dig rate, crusher delay and incident reports were employed for electric shovels and front end loaders. Table 10 shows an example of their analysis which compares the cycle times to fill the shovel dipper for different digging conditions and different shovel models.

Table 10 Cycle time for shovels

		Digging conditions		
Loader type		*Easy*	*Normal*	*Hard*
P&H2100 electric shovels	Average (s)	38.7	55.9	
	Standard deviation (s)	10.8	17.0	
P&H2800 electric shovels	Average (s)	35.8		46.2
	Standard deviation (s)	8.3		11.5

Source: After Giltner and Koski (2010)

Table 10 shows that both cycle time average and standard deviation increases for each shovel type as the digging conditions become harder. Giltner and Koski (2010) concluded that in harder digging conditions not only cycle time increases, but also the variability in the equipment operation. Additionally, this table provides information on how different machine types may affect the cycle time values in the same digging conditions.

In this study shovel operators were also interviewed. According to operators' comments it was stated that the hardest digging conditions usually occur in the bottom of the muck-pile and it is easier around the areas correspond to the location of blastholes which agrees with Onederra et al.'s (2004) results.

Finally, it was concluded that through improved digging conditions and reduced oversize fragments in the muck-pile, achieved by blast design changes, a lower cost and higher productivity could be achieved. Also, the crusher operation could be improved and therefore cost of re-handling material in the surge pile decreases.

All of the studies that have been presented so far are based on one dimensional analysis of shovel performance data. However, Halatchev and Knights (2007) used geostatistical techniques to analyse the spatial variance of shovel digging performance in 2D space (bench width and height space). They used shovel payload, dig rate, payload frequency and shovel production as KPIs captured by available monitoring systems aboard the shovel. The method used in this study to process the mentioned KPIs was ordinary kriging. Halatchev and Knights (2007) defined dig rate as the ratio of payload to

the dig time, payload frequency as the number of payloads made within a cell of x and y (coordinates) locations which was used for meshing the data and implementing an interpolation approach, and shovel production as the amount of rock excavated by the shovel within a given time.

The case study undertaken used data from a P&H4100A shovel operating in a copper mine in North America. Using their proposed method, Halatchev and Knights (2007) produced contour maps of the shovel digging performance. They suggested that the contour maps can be used for assessing shovel operating context, operator proficiency and muck-pile characteristics.

3.2.3 Analytical and dynamic modelling of electric rope shovel

All the studies have been presented so far were either based on the shovel instrumentation or experimental and manual studies. Additionally, there are a few studies reported in the past decade based on the analytical and numerical modelling of electric rope shovels. Awuah-Offei and Frimpong (2007) employed electric rope shovel kinematics and dynamics, formation resistance model and dynamic payload to model the excavation process. In this case, hoist and crowd forces depend on the shovel kinematics and formation resistance model depends on the muck-pile properties. They asserted that based on the previously conducted research

> "the resistance to digging by a shovel dipper can be described completely by six forces and that the cutting resistance, the empty dipper weight and the payload are the most significant in mining applications." (Awuah-Offei and Frimpong, 2007, p.1000)

The case undertaken in this study was P&H 2100BL operating in typical surface mine overburden conditions. It was concluded that a lower dipper handle (crowd) speed and a higher hoist rope speed and therefore lower depth of cut gives better performance. Awuah-Offei and Frimpong (2007) introduced energy per unit loading rate, given by Equation (10), as a measure of diggability and shovel performance.

$$\hat{E} = \frac{\text{Digging energy (J)}}{\text{Payload (tonnes)}} \times \text{Digging time (h)} \tag{10}$$

Similarly, Rasuli (2012) as part of his PhD studies created a dynamic model of a P&H2100-XP cable shovel which could simulate DC motors and various parameters such as inertia, friction and forces. Using the kinematic and simplified dynamic equations, a dynamic payload monitoring system was built. To accomplish this, swing, crowd and hoist motor currents were measured and then actuator torques and forces required by the cable shovel were estimated. In addition to payload, cutting forces and loading time could be estimated which are useful in diggability assessment.

Stavropoulou et al. (2013) modelled the excavation process using a kinematic model, dynamic payload and cutting resistance models. In addition, an analytical estimation of specific energy consumed in the process of excavation was presented.

They introduced dipper trajectory and its capacity, the depth of cut, hoist and crowd speeds, geomaterials physical and mechanical properties and the repose angle of the bank as main parameters affecting the digging performance and energy consumed by the cable shovel. To calculate cutting forces, a theoretical model was considered. They also developed an analytical algorithm to estimate material weight in the dipper.

Finally, using the material weight algorithm and kinematic shovel model, crowd and hoist forces, the specific energy consumed by the crowd and hoist components were calculated. This specific energy was defined as the energy per unit volume of materials in the dipper which depends on the kinematics and material properties.

4 Summary and recommendations

A literature review highlighted that some studies have been reported in the past to assess diggability. Table 11 summarises the most relevant studies. As this table confirms, the results of most of past studies agree that a properly measured specific energy of digging could be an indicator of digging conditions, but other factors such as operator proficiency and skill as well as machine type and conditions should be taken into consideration.

Table 11 Diggability assessment studies

Researcher (s)	*Diggability index/indicator*	*Loader type*	*Operation*
Williamson et al. (1983)	Diggability index $= \dfrac{\sum\lvert\delta V\rvert}{\int_{t_1}^{t_2} V\,\mathrm{d}t}$ where V is crowd motor voltage and δV is change in voltage values	Electric shovels (P&H 1900, P&H 2100)	Iron ore mine
Mol et al. (1987)	Diggability index = *f*(Crowd current, crowd current, dig time)	Electric shovels (P&H2300)	Open cut coal mine
Hendricks (1990)	Hoist DI $= \dfrac{\sum_{i=1}^{n}\lvert\mathrm{HV}_{i+1}-\mathrm{HV}_i\rvert}{\sum_{i=1}^{n}\lvert\mathrm{SR}\times\mathrm{HV}_i\rvert}\times\dfrac{\sum_{i=1}^{n}\lvert\mathrm{HI}_{i+1}-\mathrm{HI}_i\rvert}{\sum_{i=1}^{n}\lvert\mathrm{SR}\times\mathrm{HI}_i\rvert}$ where n: number of readings taken during the dig cycle DI: diggability index HV: hoist armature voltage HI: hoist armature current SR: sampling rate	Electric shovel (P&H 2800XP)	Coal mine
Hunter et al. (1990)	Williamson et al.'s (1983) diggability index, boom vibration index	Electric shovel (P&H2100)	Uranium mine
Karpuz et al. (1992, 2001)	Specific digging energy	Electric shovels (P&H2100)	Coal mine
P&H MinePro Services (2003)	Fill factor $= \dfrac{\text{Loose volume per load}}{\text{Dipper rated volume}}$	Electric and hydraulic shovels	Open pit mines
Onederra et al. (2004)	Digging rate	Hydraulic shovels	Gold mine
Clark et al. (2004)	Dig energy, dig time and dipper payload	Electric shovel (Scaled model of P&H4100XPB)	Laboratory

Table 11 Diggability assessment studies (continued)

Researcher (s)	*Diggability index/indicator*	*Loader type*	*Operation*
Patnayak (2006)	Average hosit power $= \frac{\sum_{i=1}^{n} \text{Hoist energy for individual dig cycle}}{\sum_{i=1}^{n} \text{Dig time for individual dig cyle}}$ Hoist power $= \frac{0.5\sum_{i=1}^{n} \lvert \text{HV}_{i+1} \times \text{HI}_{i+1} + \text{HV}_i \times \text{HI}_i \rvert}{\text{Dig time}}$ where HV: hoist armature voltage HI: hoist armature current	Electric shovels (P&H4100 series: TS and BOSS)	Oil sand
Segarra et al. (2007, 2010) Sanchidrian et al. (2011)	Excavator efficiency	Front loaders and rope shovels	Iron and copper ore mines
Koski and Giltner (2009)	Dig rate, average dig time, crusher delay and incident reports	Electric shovels (P&H 2100 and 2800)	Iron ore mine
Giltner and Koski (2010)		Front end loaders (LeTourneau 1850)	
Halatchev and Knights (2007)	Shovel payload, dig rate and shovel production	Electric shovel (P&H 4100A)	Copper ore mine
Awuah-Offei and Frimpong (2007)	Energy per unit loading rate	Electric shovel (P&H 2100BL)	Typical surface mine operation (simulation)
Stavropoulou et al. (2013)	Specific energy (energy per unit volume of materials in the dipper)	Medium sized cable shovel	Simulation

On the basis of the literature, crowd motor responses are less sensitive to different digging conditions and the dipper is mainly filled through the hoist action, and the crowd action only helps to maintain a proper dipper depth of penetration into the muck-pile. Therefore, a diggability index could be developed based on the hoist motor responses. However, with advances in instrumentation and remote sensing technologies, mechanical crowd and hoist forces can be measured directly in the future using a set of strain gauges and accelerometers which allows estimation of the net digging force in the bank. The net digging force can be used to estimate the digging energy which could be used as a diggability index. As well, the ability to measure payload per pass and digging time could be used to calculate specific energy of digging (energy per unit loading rate) per pass. In addition to energy based diggability indices, fill factor, digging rate, excavator efficiency and dig time have been used to assess digging conditions. But some of these indicators like fill factor and dig time could be misleading if they are being used alone. For example, in hard digging conditions, the operator may take shallower paths to fill the bucket, so the dig time will be reduced.

In addition to aforementioned indices, it is believed that there are other indicators such as dipper linear and radial speeds in the bank during digging, vibration energy, etc. which might be considered in a diggability assessment study in the future. Few researchers have reported using vibrations for diggability assessment, despite the fact that most shovel operators classify digging conditions based on the amount of shaking (vibration) that they feel while filling the dipper.

Many researchers have reported the effect of operator practice on diggability assessment and shovel performance. However, there is a lack of a diggability index for the purpose of post-blast evaluation which considers the effect of operator practice to ascertain that variations in diggability index are only caused by variations in muck-pile digging conditions. To achieve this goal, it is believed that shovel performance data (motors response, payload, dig time, dipper position, etc.) should be gathered and then analysed for different operators under different digging conditions and different operating shifts (day and night) to establish an index which could reflect changes in muck-pile digging conditions independent of changes in operators. However, even a single operator could use varying approaches from cycle to cycle due to different digging height, depth of penetration and digging trajectory. To minimise the effect of equipment operating variability, a proposed index could be averaged over a number of cycles (e.g., 50 cycles) as adopted by a few researchers in the past.

Researchers in the past mainly analysed crowd and hoist motor responses to derive a diggability index, but there are other data such as joystick reference signals which might be collected and analysed. For example joystick reference signals provide information on how operators act during different shovel activities which it is believed that can help to interpret motor responses, isolate different shovel activities and finally establish a diggability index which is less sensitive to operator digging practice and style. Finally, in addition to operator proficiency and skills, the effect of machine type and conditions as well as weather conditions should also be taken into consideration.

Although a few metrics have been developed to assess diggability, no universally accepted and established method for digging assessment has been defined. Most of presented studies in the literature did not consider the effect of operator proficiency, machine type and condition and or operating shifts and suffer from the lack of a reliable technique to continuously and in a real-time or near real-time basis calculate a diggability index. A successful diggability index should be easily understandable and provide repeatable and reliable results on the muck-pile digging conditions. It is believed that it may be possible to develop a universal methodology to determine a diggability index which incorporates muck-pile digging conditions, operator practice and skill and machine type and condition. Advances in data acquisition systems, analysis approaches and new monitoring technologies will enable the development of a more reliable method which can provide feedback on actual muck-pile conditions. Ongoing research in this area will be the subject of a future paper.

References

Allen, F., Hawkes, P. and Noy, M. (1999) 'Bucket fill factors-a laboratory and field study with implications for blasting', *Kalgoorlle*, 7–11 November, WA, pp.43–46.

Andersson, T., Thurley, M. and Carlson, J.E. (2012) 'A machine vision system for estimation of size distributions by weight of limestone particles during ship loading', *Journal of Minerals Engineering*, Vol. 25, No. 1, pp.38–46.

Awuah-Offei, K and Summers, D. (2010) *Reducing Energy Consumption and Carbon Footprint through Improved Production Practices*, Technical report, Missouri University of Science and Technology.

Awuah-Offei, K. and Frimpong, S. (2007) 'Cable shovel digging optimization for energy efficiency', *Mechanism and Machine Theory*, Vol. 42, pp.995–1006.

Babaei Khorzoughi, M. (2013) *Improved Rock Mass Characterisation using Measurement While Drilling Techniques in Open Pit Mines*, Master Thesis, University of British Columbia, Canada.

Bergmann, O.R., Riggle, J.W. and Wu, F.C. (1973) 'Model rock blasting – effect of explosives properties and other variables on blasting results', *International Journal of Rock Mechanics and Mining Sciences & Geomechanics Abstracts*, Vol. 10, No. 6, pp.585–612, http://dx.doi.org/10.1016/0148-9062(73)90007-7.

Brandt, E.G. and Evans, W.C. (1998) *Shot-Rock Diggability Monitor*, US Patent, 5844800.

Brunton, I., Thornton, D., Hodson, R. and Sprott, D. (2003) 'Impact of blast fragmentation on hydraulic excavator dig time', *Proceedings of the Fifth Large Open Pit Conference*, The Äustralasian Institute of Mining and Metallurgy, Carlton, pp.39–48.

Chung, S. and Katsabanis, P.D. (2000) 'Fragmentation prediction using improved engineering formulae', *The International Journal for Blasting and Fragmentation*, Vol. 4, Nos. 3–4 (200), pp.198–207.

Chung, S.H. and Katsabanis, P.D. (2008) 'A discrete element code for diggability analysis', *Proceedings of the Annual Conference on Explosives and Blasting Technique*, Vol. 34, pp.235–244.

Chung, S.H. and Preece, D.S. (1999) 'Explosive energy and muck-pile diggability', *Proceeding of the 25th Annual Conference on Explosives and Blasting Technique*, Vol. 2, pp.241–248.

Clark, S., Lever, P. and Dean, R. (2004) 'Influence of muck-pile characteristics on rope shovel digging performance', *Proceeding of the CRC Mining Research and Effective Technology Transfer Conference*, 15–16 June, 2004, Noosa, Australia, pp.1–6.

Cunningham, C.V.B. (1983) 'The Kuz–Ram model for prediction of fragmentation from blasting', in Holmberg, R. and Rustan, A. (Eds.): *Proceedings of First International Symposium on Rock Fragmentation by Blasting*, Luleå, pp.439–454.

Cunningham, C.V.B. (1987) 'Fragmentation estimations and the Kuz–Ram model – four years on', in Fourney, W. (Ed.): *Proceedings of Second International Symposium on Rock Fragmentation by Blasting*, Keystone, Colorado, pp.475–487.

Cunningham, C.V.B. (2005) 'The Kuz-Ram fragmentation model – 20 years on', *Brighton Conference Proceedings*, European Federation of Explosives Engineers, UK, pp.201–210.

Doktan, M. (2001) 'Impact of blast fragmentation on truck shovel fleet performance', *17th International Mining Congress and Exhibition of Turkey – IMCET200*, Antalya, pp.375–379.

Franklin, J.A., Broch, E. and Walton, G. (1971) 'Logging the mechanical character of rock', *Trans. Inst. Min. Metall.*, Vol. 80, pp.A1–A9.

Giltner, S.G. and Koski, A.E. (2010) 'The application of a blast audit for production improvement', in Sanchidrián, J.A. (Ed.): *Rock Fragmentation by Blasting*, © Taylor & Francis Group, London, pp.723–230, ISBN 978-0-415-48296-7.

Hadjigeorgiou, J. and Poulin, R. (1998) 'Assessment of ease of excavation of surface mines', *Journal of Terramechanics*, Vol. 35, pp.137–153.

Haghir Chehreghani, S., Alipour, A. and Eskandarzade, M. (2011) 'Rock mass excavatability estimation using artificial neural network', *Journal of geological society of India*, Vol. 78, pp.271–277.

Halatchev, R.A. and Knights, P.F. (2007) 'Spatial variability of shovel dig performance', *International Journal of Mining, Reclamation and Environment*, Vol. 21, No. 4, pp.244–261, DOI:10.1080/17480930701352933.

Han, J.H. and Song, J.J. (2014) 'Statistical estimation of blast fragmentation by applying stereophotogrammetry to block piles', *International Journal of Rock Mechanics & Mining Sciences*, Vol. 68, pp.150–158.

Han, J.H., Song, J.J. and Jo, Y.D. (2011) 'Estimation of blast fragmentation using stereophotogrammetry', *Tunn. Under gr Space*, Vol. 21, No. 1, pp.82–92.

Hansen, J. (2000) 'Fragmentation: a vital link in the drill to mill process information system', *103rd Annual General Meeting of Canadian Institute of Mining, Metallurgy, and Petroleum*, 29 April–02 May, Quebec City, CA, pp.1–8.

Hawkes, P. (1998) 'Using simulation to assess the impact of improvements in drill and blast on down stream processes', *Proceedings Mine to Mill*, The Australasian Institute of Mining and Metallurgy, Melbourne, pp.209–217.

Hawkes, P.J., Spathis, A.T. and Sengstock, G.W. (1995) 'Monitoring equipment productivity improvements in coal mines', *EXPLO 95*, 4–7 September, Brisbane, Australia.

Hendricks, C. (1990) *Performance Monitoring of Electric Mining Shovels*, PhD Thesis., McGill University, Canada.

Hendricks, C., Peck, J. and Scoble, M. (1990) 'Integrated drill and shovel performance monitoring for improved fragmentation and productivity', *Proceeding 3rd International Symposium Rock Fragmentation by Blasting*, The Australian Institute of Mining and Metallurgy, Melbourne, pp.9–20.

Ho Cho, S., Nishi, M., Yamamoto, M. and Kaneko, K. (2003) 'Fragmentation size distribution', *Materials Transactions*, Vol. 44, No. 5, pp.951–956.

Hunter, G.C., Sandy, D.A. and Miles, N.J. (1990) 'Optimization of blasting in a large open pit mine', *Third International Symposium on Rock Fragmentation by Blasting-FlagBlast90*, August, Brisbane, Australia, pp.21–30.

Hustrulid, W.A. (1999) *Blasting Principles for Open Pit Mining*, Vol. 1, A.A. Balkema, Rotterdam.

Iphar, M. and Goktan, R.M. (2006) 'An application of fuzzy sets to the digability index rating method for surface mine equipment selection', *International Journal of Rock Mechanics and Mining Sciences*, Vol. 43, pp.253–266.

Jessett, A. (2001) *Tools for Performance Monitoring of Electric Rope Shovels*, Master Thesis, University of Queensland, Australia.

Jimeno, E.L., Jimino, C.L. and Careedo, A. (1995) *Drilling and Blasting of Rocks*, CRC Press, pp.290–298.

Joseph, T.G. and Hansen, G.W. (2002) 'Oil sands reaction to cable shovel motion', *CIM Bull.*, Vol. 95, pp.62–64.

Kanchibotla, S.S., Valery, W. and Morrell, S. (1999) 'Modelling fines in blast fragmentation and its impact on crushing and grinding', *Explo 99 – A Conference on Rock Breaking*, The Australasian Institute of Mining and Metallurgy, Kalgoorlie, Australia, pp.137–144.

Karpuz, C., Ceylanoglu, A. and Pasamehmetoglu, A.G. (1992) 'Investigation on the influence of depth of cut and blasting on shovel digging performance', *Int. J. Surf. Mining, Reclam. Environ.*, Vol. 6, pp.161–167.

Karpuz, C., Hindistan, M.A. and Bozdag, T. (2001) 'A new method for determining the depth of cut using power shovel monitoring', *Journal of Mining Science*, Vol. 37, No. 1, pp.85–94.

Kennedy, P. (1995) 'Dig index will put blast engineers on the path to profit', *Australia's Mining Monthly*, March, Paper 24.

Kirsten, H.A.D. (1982) 'A classification system for excavation in natural materials', *Civ. Eng. S. Afr.*, Vol. 24, pp.293–308.

Koski, A. and Giltner, S.G. (2009) 'Improvements in blasting technology at Cliffs Natural Resources', *Proceedings of the 35th Conference on Explosives and Blasting Technique*, Denver, CO, 8–11 February, International Society of Explosives Engineers, pp.1–9.

Kumar, K., Thakur, T. and Roy, O.P. (2000) 'Performance monitoring of electric mining shovel using microprocessor', *Modelling Measurement and Control a General Physics Electronics and Electrical Engineering*, Vol. 73, No. 3, pp.1–12.

Mol, O., Danell, R. and Leung, L. (1987) 'Studies of rock fragmentation by drilling and blasting in open cut mines', in Foumey, W.C. and Dick, R.D. (Ed.): *Rock Fragmentation by Blasting, Second International Symposium*, Keystone, Colorado (Society for Experimental Mechanics, Bethel, Connecticut), pp.381–392.

Onederra, I., Brunton, I., Battista, J. and Grace, J. (2004) 'Shot to shovel-understanding the impact of muck-pile conditions and operator proficiency on instantaneous shovel productivity', *EXPLO*, Perth, WA, pp.205–213.

Osanloo, M. and Hekmat, A. (2005) 'Prediction of shovel productivity in the Gol-E-Gohar iron mine', *Journal of Mining Science*, Vol. 41, No. 2, pp.177–184.

Oskouei, M.A. and Awuah-Offei, K. (2014) 'Statistical methods for evaluating the effect of operators on energy efficiency of mining machines', *Mining Technology*, Vol. 123, No. 4, pp.175–182, doi:10.1179/1743286314Y.0000000067.

Oskouei, M.A. and Awuah-Offei, K. (2015) 'A method for data-driven evaluation of operator impact on energy efficiency of digging machines', *Energy Efficiency*, Vol. 123, No. 4, pp.175–182, http://dx.doi.org/10.1007/s12053-015-9353-3.

Ouchterlony, F. (2005) 'The Swebrec function: linking fragmentation by blasting and crushing', *Mining Technology (Trans. Inst. Min. Metall. A)*, Vol. 114, pp.29–44.

P&H MinePro Services (2003) *Peak Performance Practicies-Excavator Selection*, pp.31–60.

Patnayak, S. (2006) *Key Performance Indicators for Electric Mining Shovels and Oil Sand Diggability*, PhD Thesis, University of Alberta, Canada.

Patnayak, S. and Tannant, D.D. (2005) 'Performance monitoring of electric cable shovels', *International Journal of Surface Mining, Reclamation and Environment*, Vol. 19, No. 9, pp.276–294.

Patnayak, S., Tannant, D.D., Parsons, I., Del Valle, V. and Wong, J. (2008) 'Operator and dipper tooth influence on electric shovel performance during oil sands mining', *International Journal of Mining, Reclamation and Environment*, Vol. 22, No. 2, pp.120–145, DOI:10.1080/17480930701482961.

Rasuli, A. (2012) *Dynamic Modeling, Parameter Identification, Payload Estimation, and Non-contact Arm Geometry Sensing of Cable Shovels*, PhD Thesis, University of British Columbia, Canada.

Rholl, S.A. (1993) 'Photographic assessment of the fragmentation distribution of rock quarry muck-piles', *Proceedings of the 4th Int. Symposium Rock Fragmentation by Blasting*, Vienna, Austria, pp.501–506.

Sanchidrian, J.A., Segarra, P. and Lopez, L.M. (2011) 'On loader productivity, rock strength and explosive energy in metal mining', *Sixth EFEE World Conference on Explosives and Blasting*, 18–20 September, Lisboa, Portugal, pp.461–468.

Sanchidrián, J.A., Segarra, P., Ouchterlony, F. and Lopez, L.M. (2009) 'On the accuracy of fragment size measurement by image analysis in combination with some distribution functions', *Rock Mechanics and Rock Engineering*, Vol. 42, No. 1, pp.95–116, DOI 10.1007/s00603-007-0161-8.

Sari, M. and Lever, P. (2007) 'Effect of blasted rock particle size on excavation machine loading performance', *20th International Mining Congress and Exhibition of Turkey – IMCET*, Ankara, Turkey, pp.375–379, ISBN 975-395-417-4.

Scoble, M.J. and Muftuoglu, Y.V. (1984) 'Derivation of a diggability index for surface mine equipment selection', *Mining Science and Technology*, Vol. 1, pp.305–322.

Scott, A. and McKee, D.J. (1994) 'The interdependence of mining and mineral beneficiation process on the performance of mining projects', *Proceeding AusIMM Annual Conference*, The Australian Institute of Mining and Metallurgy, Melbourne, pp.303–308.

Segarra, P., Sanchidrian, J.A., Lopez, L.M. and Querol, E. (2010) 'On the prediction of mucking rates in metal ore blasting', *Journal of Mining Science*, Vol. 46, No. 2, pp.167–176.

Segarra, P., Sanchidrián, J.A., Montoro, J.J. and López, L.M. (2007) 'Mucking efficiency in open pit blasting', *CIM Bulletin Technical Papers: Peer-Reviewed Technical Papers*, Canadian Institute of Mining, Metallurgy and Petroleum, Vol. P33, pp.1–11.

Singh, S.P. and Narendrula, R. (2006) 'Productivity indicators for loading equipment', *CIM Bulletin*, Vol. 99, No. 1094, pp.1–7, Paper 16.

Singh, S.P. and Narendrula, R. (2007) 'Factors affecting the productivity of loaders in surface mines', *International Journal of Mining, Reclamation and Environment*, Vol. 20, No. 01, pp.20–32, DOI:10.1080/13895260500261574.

Stavropoulou, M., Xiroudakis, G. and Exadaktylos, G. (2013) 'Analytical model for estimation of digging forces and specific energy of cable shovel', *Coupled Systems Mechanic*, Vol. 2, No. 1, pp.23–51.

Tafazoli, S. and Ziraknejad, N. (2009) 'An in-shovel camera-based technology for automatic rock size sensing and analysis in open pit mining', *ROCKENG09: Proceedings of the 3rd CANUS Rock Mechanics Symposium*, Toronto, May, pp.1–8.

Thurley, M.J. (2011) 'Automated online measurement of limestone particle size distributions using 3D range data', *Journal of Process Control*, Vol. 21, pp.254–262.

Torrance, A.C. and Baldwin, G. (1990) 'Blast performance assessment using a dragline monitor', *Fragblast'90*, 26–31 August, Brisbane, pp.219–223.

Tosun, A., Konak, G., Karakus, D., Onur, A.H. and Toprak, T. (2013) 'Investigation of the relationship between blasting pile density and loader productivity', *Rock Fragmentation by Blasting*, FragBlast10, pp.385–389.

Van Aswegen, H. and Cunningham, C.V.B. (1986) 'The estimation of fragmentation in blast muck-piles by means of standard photographs', *J.S.AF, Republic of South Africa: Institute of Mining and Metallurgy*, Vol. 86, No. 12, pp.469–474.

Venkatesh, H.S., Adhikari, G.R. and Raju, N.M. (1995) 'Application of high resolution video camera for blast evaluation', *Explo'95 Conference*, 4–7 September, Brisbane, pp.269–271.

Vukotic, I.M. (2013) *Evaluation of Rope Shovel Operators in Surface Coal Mining using a Multi-Attribute Decision-Making Model*, Master Thesis, West Virginia University, USA.

Williamson, S., McKenzie, C. and O'Loughlin, H. (1983) 'Electric shovel performance as a measure of blasting efficiency', *Rock Fragmentation by Blasting, First International Symposium*, Lulea University of Technology, Lulea, Sweden, Vol. 2, pp.625–636.

Notes

[1]The error associated with some of mentioned methods such as fragmentation measurement using image analysis has been quantified in the literature (Sanchidrián *et al.*, 2009).

[2]In the presented paper, Q^0 was calculated in a data-dependant manner while it could be related to factors such as machine type and conditions, dipper capacity and loading technique (single or double sided).

[3]In this work f_s was given by: $f_s = 0.025\rho_r - 50 + 4.4\,I_{s(50)}$.

A diesel particulate matter dispersion study inside a single dead end entry using dynamic mesh model

Magesh Thiruvengadam and Yi Zheng

Department of Mining & Nuclear Engineering,
Missouri University of Science and Technology,
226 McNutt Hall, Rolla, MO 65401, USA
Email: mtwv8@mst.edu
Email: yzz59@mst.edu

Hai Lan

Clean Air Power Inc.,
Poway, CA 92064, USA
Email: hlanphd@gmail.com

Jerry C. Tien*

Department of Civil Engineering,
Division of Mining and Resources Engineering,
Monash University,
Clayton Campus, Wellington Road,
Clayton, VIC 3800, Australia
Email: jerry.tien@monash.edu
*Corresponding author

Abstract: Three-dimensional simulations of diesel particulate matter (DPM) distribution inside a single dead end entry with a push-pull system for the load-haul-dump (LHD)-truck loading and truck hauling operations were carried out using ANSYS FLUENT computational fluid dynamics (CFD) software. The loading operation was performed for a fixed period of time. Then dynamic mesh technique in FLUENT was used to study the impact of truck motion on DPM distribution. The resultant DPM distributions are presented for the cases when the vehicles were fitted with and without diesel particulate filters (DPF). The results from the simulation can be used to determine if the areas inside the single dead end entry exceed the current U.S. regulatory requirement for DPM concentration (160 $\mu g/m^3$). This research can guide the selection of DPM reduction strategies and improve the working practices for the underground miners.

Keywords: computational fluid dynamics; CFD; dead end; diesel particulate matter; DPM; dynamic meshing; loading; hauling operation.

Reference to this paper should be made as follows: Thiruvengadam, M., Zheng, Y., Lan, H. and Tien, J.C. (2016) 'A diesel particulate matter dispersion study inside a single dead end entry using dynamic mesh model', *Int. J. Mining and Mineral Engineering*, Vol. 7, No. 3, pp.210–223.

Biographical notes: Magesh Thiruvengadam is currently working as a Research Assistant Professor in the Department of Mining and Nuclear Engineering at Missouri University of Science and Technology, Rolla. He obtained his Bachelor of Engineering (BE) in Mechanical Engineering from College of Engineering Guindy, Anna University in Chennai, India; MS in Mechanical Engineering from Indian Institute of Technology Madras in Chennai, India; and PhD in Mechanical Engineering from Missouri S&T, Rolla, USA. His research interests focuses on mining machine dynamics, finite element analysis (FEA), fatigue, fluid flow and heat transfer and computational fluid dynamics (CFD).

Yi Zheng is a PhD graduate from the Mining and Nuclear Engineering program at the Missouri University of Science and Technology studying ventilation. He is currently a Service Fellow for a research institute in Pittsburgh.

Hai Lan is a Research Scientist in Clean Air Power Inc. He got his PhD in Mechanical Engineering from Missouri S&T, Rolla, USA. His research interests focuses on fluid and thermal design of clean engines for on-road and off-road applications.

Jerry C. Tien is Chairman of Division of Mining and Mineral Resource Engineering, Department of Civil Engineering, Faculty of Engineering, Monash University, Melbourne, Australia. He has over 39 years of mining and academic experience. His main research interests/specialty areas including: mine ventilation; diesel particulate matter (DPM) emission, dissipation and control; mine fires, coal mining, short- and long-range mine planning, and mine feasibility study. He wrote two technical books and edited one symposium proceeding (mine ventilation), authored and co-authored over 135 journal and conference publications and internal reports.

1 Introduction

Diesel engine operated LHDs and Trucks are widely used in underground metal/nonmetal (M/NM) mines. Although they have better fuel efficiency and good manoeuvrability, emission from the tailpipes and the subsequent distribution in the underground mine are of growing concerns for miners. DPM is the particulate by-product of diesel exhaust and it can exist in different modes with different size distributions (5–10 μm). Nearly 90% of the DPM emitted from the diesel engines have size distributions in nanometre ranges. Owing to its very small size, it remains airborne for a long time after leaving the tailpipe and pollutes the entire mine environment downstream the diesel engine, causing health hazard to the miners. It is established that long time exposure to diesel exhaust can lead to cancer (ACGIH, 2001; NIOSH, 1988; US EPA, 2002), asthma (Kahn and Orris, 1988; Rundell et al., 1996; Wade III and Newman, 1993) and other health effects such as eye and nose irritation, headaches and nausea. For underground M/NM mines, the final DPM limit of 160 micrograms of total carbon (TC) per cubic metre of air (160_{TC} $\mu g/m^3$) set by US Mine Safety and Health Administration (MSHA) became effective on 20 May, 2008.

For underground M/NM mines to control DPM hazards, two types of strategies have been commonly used. One is DPM reduction and removal before it is released from the engine tailpipe, which includes proper diesel engine selection and maintenance

(Anyon, 2008; McGinn, 1999; McGinn et al., 2010), use of alternative fuels (Bugarski et al., 2010; Zannis et al., 2009), and exhaust gas treatment devices (Bugarski et al., 2009; Shah et al., 2007), e.g., diesel particulate filters (DPF). The other is through control measures after DPM is discharged into the environment – mine ventilation, an enclosed equipment cab with filtered breathing air (environmental cab), personal protective equipment, and administrative controls (Cecala et al., 2005; Noll et al., 2008; MSHA, 2013).

Experiences (Bugarski et al., 2011) showed that no single strategy can solve all DPM problems and a combination of several measures needs to be implemented in the field to attain compliance. Since none of the strategies are cost free, an effective, efficient, and economical control scheme for operations under different mining conditions is essential in order for a mining company to provide a safe working environment and to meet regulatory criteria. To achieve that, an understanding of DPM behaviour in mining environment can be very useful in selecting the control strategies and training the miners. Numerical simulations using CFD can be used for that purpose by visualising DPM distribution based on laboratory experiments and field studies.

CFD simulations have been successfully used in mining research to detect spontaneous combustion, explosion, and apply inertisation in gob areas (Ren et al., 2005; Wedding, 2014; Yuan and Smith, 2007), study airflow patterns and gas concentrations in continuous miner operations or heading development (Hargreaves and Lowndes, 2007; Kollipara et al., 2012; Petrov, 2014; Torno et al., 2013), investigate scrubber intake designs for longwall dust control (Ren and Balusu, 2008), and estimate a mine's damage status by tracer gas and simulation after a disaster (Xu et al., 2013). CFD modelling has been demonstrated as a powerful tool for understanding airflow movement and gas/dust behaviour in a complicated three dimensional environment. It can also provide useful information for initial concept testing of new ideas and equipment for environment control.

Simulation of DPM dispersion in underground M/NM mines was carried out by Zheng and Tien (2008), in which DPM was considered to behave like a gas. Subsequent study showed that it gave good agreement for the DPM distribution and successfully identified the DPM affected areas above the threshold limit (Zheng et al., 2011). In the present study, DPM emission was also treated as a gas to examine its diffusion inside the underground single dead end entry.

Since vehicles move around underground most of the time, it is essential that the motion and the effect of the motion on mine ventilation and DMP distribution to be considered. The mining operations chosen for the study were the LHD-truck loading and truck hauling operations in one of the face areas inside a dead end. The LHD was assumed to be loading for three minutes, and then ores were hauled away by the truck. During the truck motion, the LHD was assumed to be idling. The study consisted of two cases

1 the LHD and truck with DPF (resulting in low DPM emission)

2 the LHD and truck with no DPF (high DPM emission).

The dead end was ventilated using a push-pull system (Figure 1). This is the first underground DPM study considering vehicle motion using CFD.

Figure 1 Computational domain for a single dead end entry

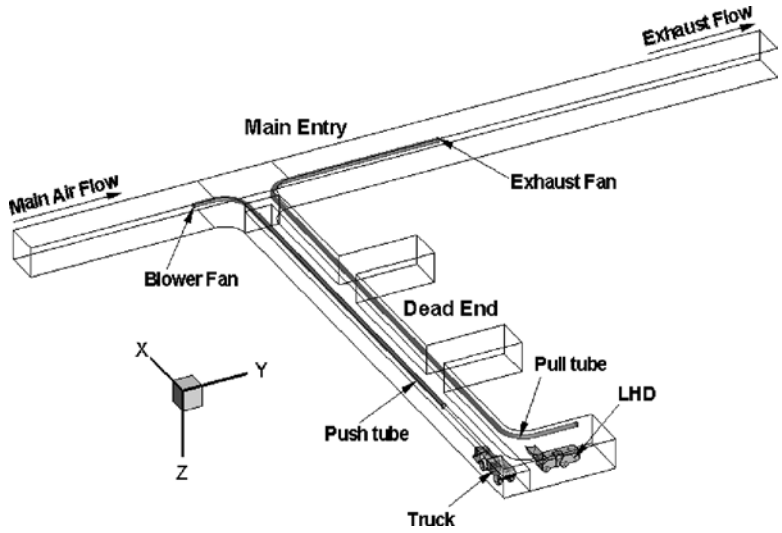

2 Problem statement and governing equations

The schematic of the single dead end entry with push-pull tubings was designed based on a typical entry in a M/NM operation in the US. It contained three face areas and the loading operation was taking place in the inner most one (Figure 1). The hauling operation of the truck started after the loading operation and completed once the frontal portion of the truck reached the main entry while the other two face areas remained inactive. The main entry inlet provided 19.5 m^3/s of fresh air flowing from left to right into the computational domain as shown in Figure 1. A push-pull system was considered for face ventilation. To reduce face recirculation, the blowing fan and tubing provided 8.0 m^3/s of fresh air, while the return fan and tubing pulled approximately 9.5 m^3/s of contaminated air in the face region.

The main entry measured 6 m × 5 m × 131 m, width × height × length, while the dead end measured 6 m × 5 m × 90 m. The push tubing extended into the dead end entry for about 67 m and about 3.4 m in the main entry while the pull tubing extended into the dead end entry for about 77 m, while 22 m remained in main entry as shown in Figure 1. The pull tubing also curved into the working face area of dead end for additional 12 m as shown in Figure 1. The diameter of both the push and pull tubings was 0.8 m.

The physical properties of fresh airflow treated as constants are listed as follows: inlet temperature, $T_0 = 27°C$; specific heat (C_p), 1006 J/(kg·k); dynamic viscosity (μ), 1.789×10^{-5} kg/(m·s), and thermal conductivity (κ), 0.0242 W/(m·k).

The density variation in the fluid owing to temperature gradient between the air and exhaust was calculated using incompressible ideal gas model within ANSYS FLUENT, one of the most popular CFD programs. In the presence of gravity, this density gradient resulted in buoyancy flow. The DPM concentration inside the single dead end entry was determined using species transport model within FLUENT where diesel particulates were treated as gas (continuous phase) and the material used as a surrogate for DPM was n-octane vapour (C_8H_{18}) with density ($\rho = 4.84$ kg/m^3), specific heat

(C_p = 2467 J/(kg·k)), thermal conductivity (κ = 0.0178 W/(m·k)) and dynamic viscosity ($\mu = 6.75 \times 10^{-5}$ kg/(m·s)). The species transport model allowed the two species, air and DPM, to diffuse and form a mixture. The mixture properties were derived using incompressible ideal gas law for density, mixing law for specific heat, thermal conductivity and viscosity. The mass diffusivity between air and DPM was assumed to be a constant with $D = 5 \times 10^{-6}$ m^2/s. The chemical reaction between the species was not considered in this study.

The airflow inside the computational domain was solved in Eulerian frame as continuous phase using time averaged three-dimensional turbulent transient Navier-Stokes, energy, and continuity equations using the finite volume method. An additional non-reacting two species transport equation (DPM and air) was solved in Eulerian reference frame (since both air and DPM were treated as continuous phase) to determine the mass fraction of DPM. The turbulence in the flow was modelled using standard k–ε turbulence model with standard wall functions for near wall treatment. Boundary conditions used to determine the DPM distribution inside the single dead end entry are listed in Table 1. The emission rates for truck and LHD were calculated from a diesel emission evaluation program (DEEP) field study (McGinn et al., 2004) and were reported in the DPM CFD research carried out by Zheng (2011). The pressure jump values in Table 1 for blower and exhaust fans were obtained after repeated calculations to yield designed flow rates as discussed previously.

Table 1 Boundary conditions used for DPM simulation

Boundaries		*Boundary conditions*
Main entry-inlet		Velocity (normal to boundary) = 0.65 m/s, T = 300 K, DPM Mass fraction = 0.0
Main entry-outlet		Outflow or fully developed boundary conditions
LHD-tailpipe		Velocity (normal to boundary) = 24.1 m/s, T = 594 K, DPM mass fraction: With DPF filter = 1.7×10^{-6} and W/O DPF filter = 7×10^{-6}
Truck-tailpipe		Velocity (normal to boundary) = 27.5 m/s, T = 644 K, DPM mass fraction: With DPF filter = 2×10^{-6} and W/O DPF filter = 7×10^{-6}
Push tubing	Inlet	Fan boundary condition (pressure Jump, ΔP = 491 Pa)
	Outlet	Interior boundary condition
Pull tubing	Inlet	Interior boundary condition
	Outlet	Fan boundary condition (pressure jump, ΔP = 800 Pa)
Walls		No slip boundary conditions
		Adiabatic walls (Heat flux = 0)
		Zero diffusive flux

3 Mesh generation and solution methodology

In this study, the truck was assumed to move with an average speed of 1 m/s. To account for the vehicle motion, a technology called ‘dynamic mesh simulation’ is available in FLUENT which permits the motion of some components in a domain, while the other components remain stationary. The dynamic mesh model in FLUENT is capable of

modelling flows where the shape of the domain is changing with time due to motion. In this study, the motion of the truck was prescribed by specifying the linear speed and the direction of motion using UDF (User Defined Function) option in FLUENT. The update of the volume mesh was handled automatically at each time step based on the new positions of the boundaries. To use the dynamic mesh model, a starting volume mesh needs to be provided and the description of the motion of any moving zones in the model needs to be specified. In this study, the starting volume mesh for the computational domain was obtained using FLUENT's pre-processor GAMBIT as shown in Figure 2. A total of 1.8 million cells (both hexahedral and tetrahedral) were generated for this initial dynamic mesh geometry. The mesh generation was made by ensuring high density near the truck and in the bounding wall regions where high gradients exist to ensure simulation accuracy. During mesh generation the equi-size skew was monitored and maintained at a value less than 0.8.

Figure 2 Starting computational mesh generated for the study (see online version for colours)

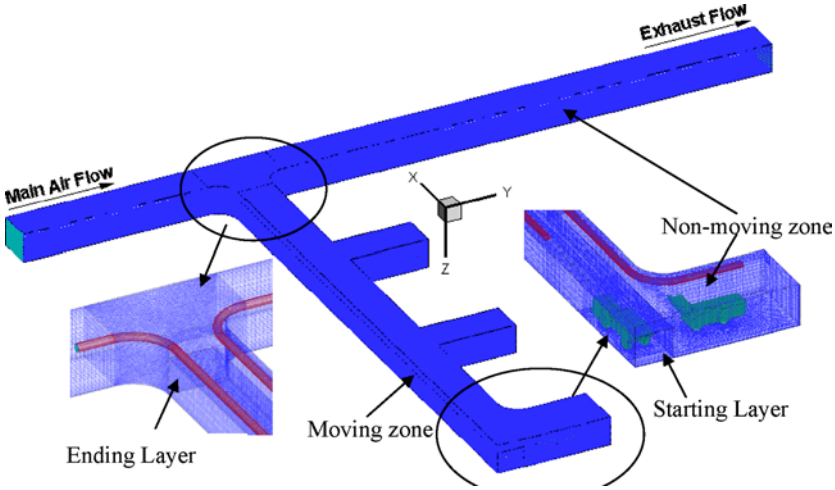

FLUENT expects the description of the motion to be specified on either face or cell zones. If the model contains moving and non-moving regions, these regions are identified by being grouped into their respective face or cell zones in the starting volume mesh (as shown in Figure 2). Furthermore, regions that are deforming owing to motion on their adjacent regions must also be grouped into separate zones in the starting volume mesh. As shown in Figure 3, the moving fluid zone was further grouped into mesh collapsing zone, moving truck zone and mesh regeneration zone.

In this study, the truck was defined as a separate zone and meshed with tetrahedral cells. The neighbouring zones were meshed with hexahedral cells to facilitate the new mesh generation. Whenever the zone moved to a new location, one layer ahead the zone collapsed while one layer behind it added. This method of meshing during the vehicle motion is called dynamic layering approach. In this process, the time step is very critical – too big a 'step' can result in a larger deformation in generated mesh that can cause a divergence in simulation. Mesh regeneration behind the truck and mesh collapse in front of the truck during the vehicle motion using the dynamic layering approach mentioned above can be seen in Figure 3. The time duration for this hauling operation was exactly

75.5 s with the hauling operation started immediately after the loading operation was completed and continued until the frontal layer of the moving truck zone reached the ending layer of the dynamic motion.

Figure 3 Mesh generation and collapse during the hauling operation in the dead end entry (see online version for colours)

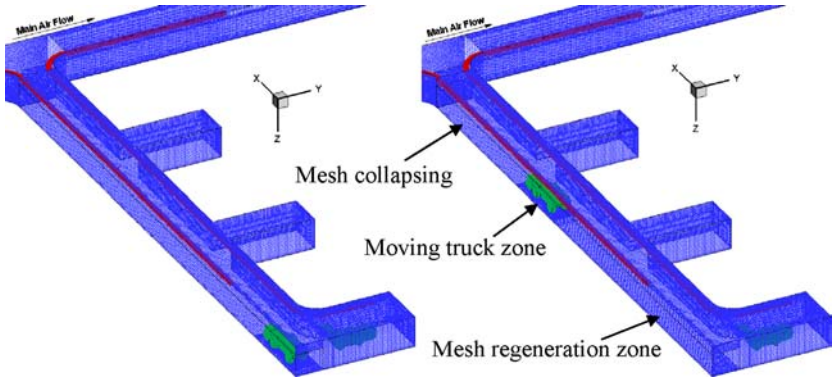

Numerical solution of the governing equations and boundary conditions were performed utilising FLUENT 12.0. The SIMPLE algorithm was used for the pressure velocity coupling. The momentum, scalar turbulence equations, energy equation, and species transport equations were discretised using the second order upwind scheme to improve the accuracy of the simulations. Second order discretisation scheme was used for the pressure interpolation. Detailed descriptions of the CFD code and the solution procedures can be found in the FLUENT 12.0 documentation (ANSYS, 2009). The unsteady flow was calculated using time step $\Delta t = 0.1$ s for both loading and hauling operations for the total time duration of 255.5 s (180 s for loading operation plus 75.5 s for hauling operation). The convergence criterion required that the scaled residuals be smaller than 10^{-4} for the mass, momentum, turbulent, and species transport equations and smaller than 10^{-9} for the energy equation. Calculations were performed on the numerical intensive computing (NIC)-cluster using 16 processors and the CPU time for converged solution was approximately 48 h to obtain the results for both loading and hauling operations.

4 Results and discussion

Numerical simulation of stationary loading and the subsequent dynamic hauling operation was carried out for the computational domain shown in Figure 1. The general flow features for diesel engines in this single dead end entry during loading operation are shown in Figure 4. It showed that the fresh air entered the main entry split into three parts. One part of the air current flowed directly downstream to the exhaust section and exited the domain, while the other turned and entered into the dead end entry. The third part entered into the blower fan and tubing and was delivered directly to the face region.

Figure 4 Pathlines coloured by velocity showing general flow features during loading operation (see online version for colours)

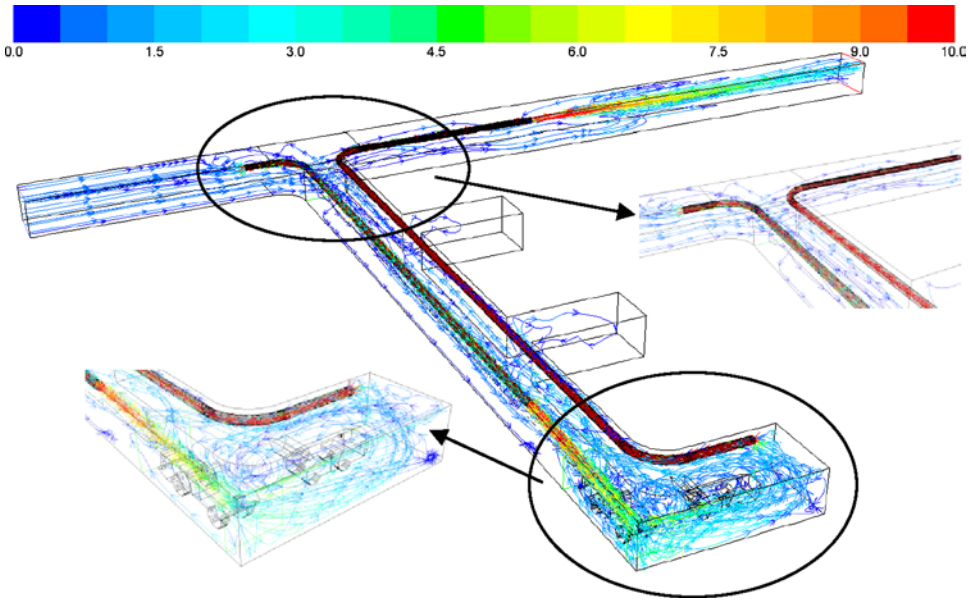

Figure 5 Pathlines coloured by velocity showing general flow features during hauling operation (see online version for colours)

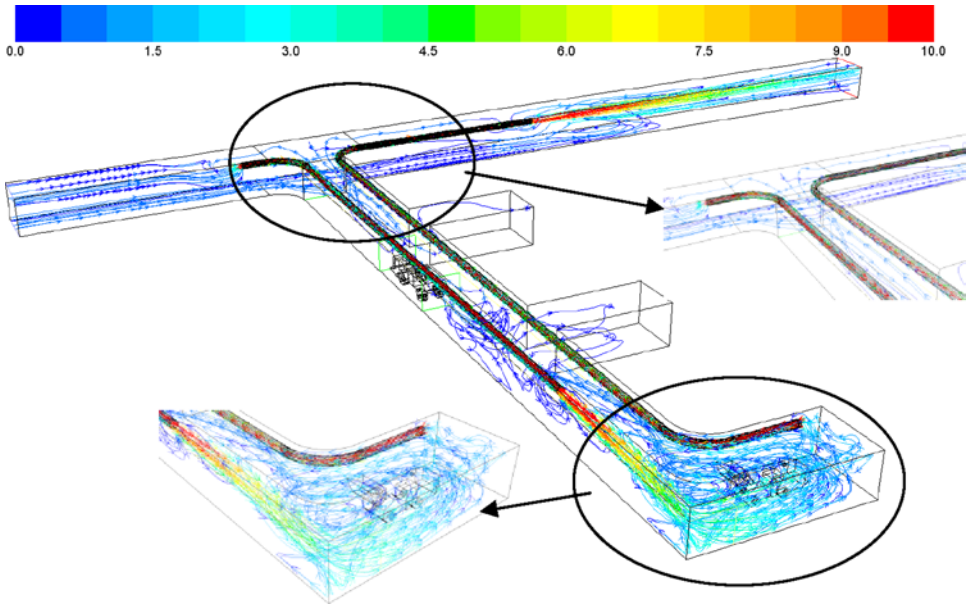

In the face region, fresh air coming out of the blowing tube with a velocity of 15.24 m/s mixed with the high temperature DPM emissions from the tailpipe of LHD and truck. Owing to the high velocity from the blowing tube combined with buoyancy effect, part of the diffused mixture hit the wall at the back of the truck and flowed back toward the main

entry, while some part swept across the face region and was sucked by the exhaust fan and discharged directly into the main entry. The remaining part recirculated in the face area, but kept on being diluted by the incoming fresh air (Figure 4).

Figure 5 shows the general flow pattern (pathlines) developed during the hauling operation with the truck more than halfway through the dead end. The flow pattern was similar to the loading operation in the face area, except that as the vehicle moved toward the main entry a majority of the air flowing towards the dead end face (not the airflow inside the tubings) was blocked by the truck, reversed direction, and flowed back into the main entry. The flow pattern at the back of the truck was caused by piston effect and continuously diluted DPM from the truck tailpipe. Since the amount of DPM from equipment tailpipes can be much reduced if filters were used, the following sessions compared a LHD and a truck with and without DPFs.

4.1 Case (a): with DPF filter

4.1.1 Loading operation

The loading operation took place for exactly three minutes. The DPM distribution (≥160 μg/m^3) in the dead end entry at the beginning (0 s) and at the end of the loading operation (3 min) is shown in Figure 6(a)–(b). It can be clearly seen that the push-pull arrangement worked well for diesel engines fitted with DPFs. Fresh air with low temperature coming into the mining area mixed and diluted the emissions from the tailpipes while lowering the high-temperature exhausts from tailpipes. This diluted mixture was then removed by the exhaust fan through the exhaust tubing and discharged into the main stream. As it is shown that, except in the immediate tailpipe area, all other places were in compliance (<160 μg/m^3). This push-pull auxiliary ventilation worked adequately because of the low DPM emission as a result of the DPF. However, protective devices had to be used when miners were constantly working in the immediate areas of the tailpipes.

Figure 6 DPM distribution in the dead end during loading operation (a) 0 s and (b) 180 s (see online version for colours)

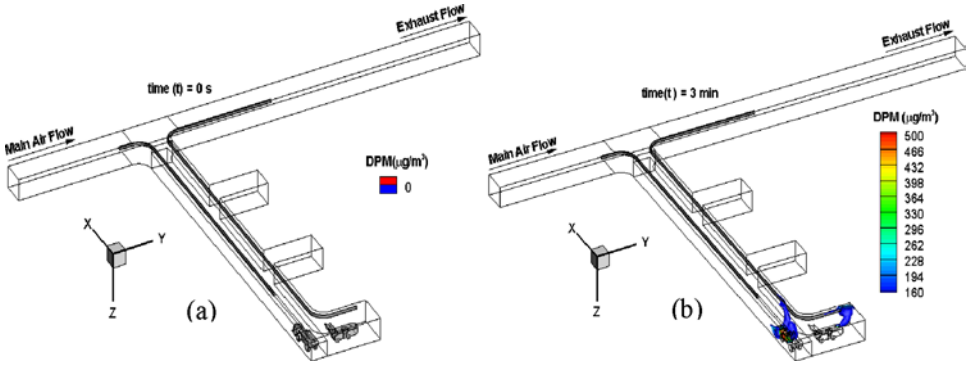

4.1.2 Hauling operation

Hauling started as soon as ore loading was completed. The haulage truck (2.7 m × 2.5 m × 10 m, width × height × length) started driving towards the main entry with a uniform

speed of 1 m/s discharging DPM at a constant rate along the way. Meanwhile the LHD remained stationary in the face area, but its engine was still operating, as shown in a series of time-lapsed simulated results showing truck in four different locations in Figure 7(a)–(d). As shown in Figure 7(a), diesel exhaust that was gathered in the front part of the truck before hauling operation starts to move toward back of the vehicle as the truck started hauling toward the main entry (Figure 7(b)–(d)). This was owing to the piston effect caused by the motion of vehicle inside the dead end entry. This piston effect also contributed to the decreased DPM occupied area near the truck region when compared with the truck position at the end of the ore loading. With continuing intake air from the blowing tubing diluting the diesel exhaust, the face area continued to remain in compliance.

Figure 7 DPM distribution in the dead end with the truck at four positions after the start of the hauling simulation: (a) 180 s; (b) 210 s; (c) 240 s and (d) 255 s (see online version for colours)

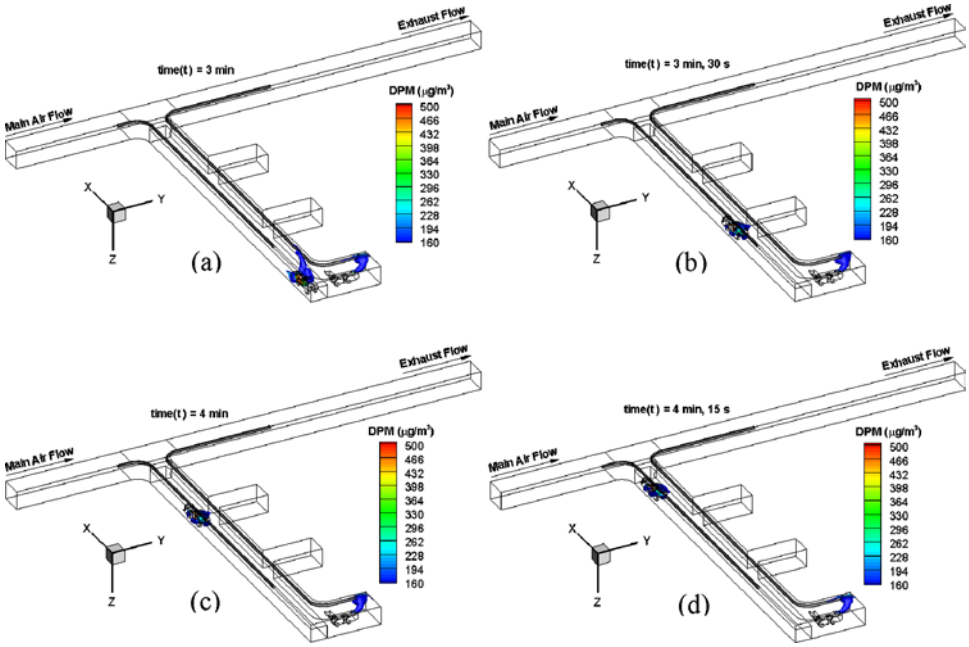

4.2 Case (b): Without DPF filter

4.2.1 Loading operation

The results of the DPM dispersion without DPF are shown in the four time-lapsed drawings in Figure 8(a)–(d). The impact of a DPF is clearly shown by the increasingly larger areas out of compliance as time went on, and the entire face region was engulfed by diesel fumes at the end of the loading operation (180 s). The entry of the dead end and part of the '*T*' junction of the main entry were also filled with diesel fumes near the roof region due to the buoyancy effect. Although the DPM mixture in the entry was continuously diluted by incoming fresh air and swept out of the dead end area through

exhaust fan and tubing, they were inadequate. Simulation clearly demonstrated the effect of a DPF.

Figure 8 DPM distribution in the dead end during loading operation (a) 0 s; (b) 60 s; (c) 120 s and (d) 180 s (see online version for colours)

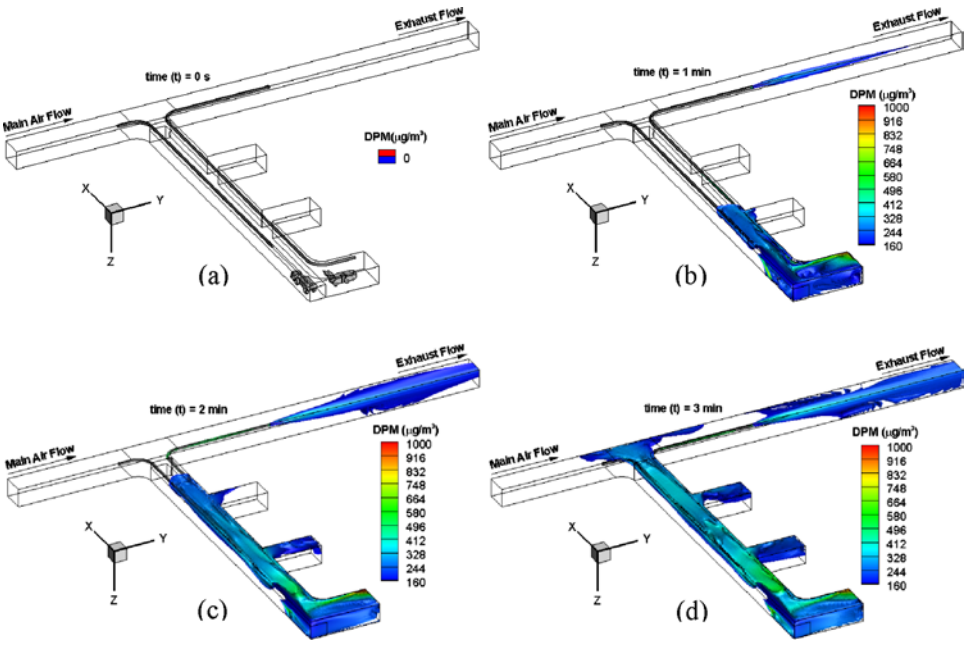

Figure 9 DPM distribution in the dead end with the truck at four positions after the start of the hauling simulation: (a) 180 s; (b) 210 s; (c) 240 s and (d) 255 s (see online version for colours)

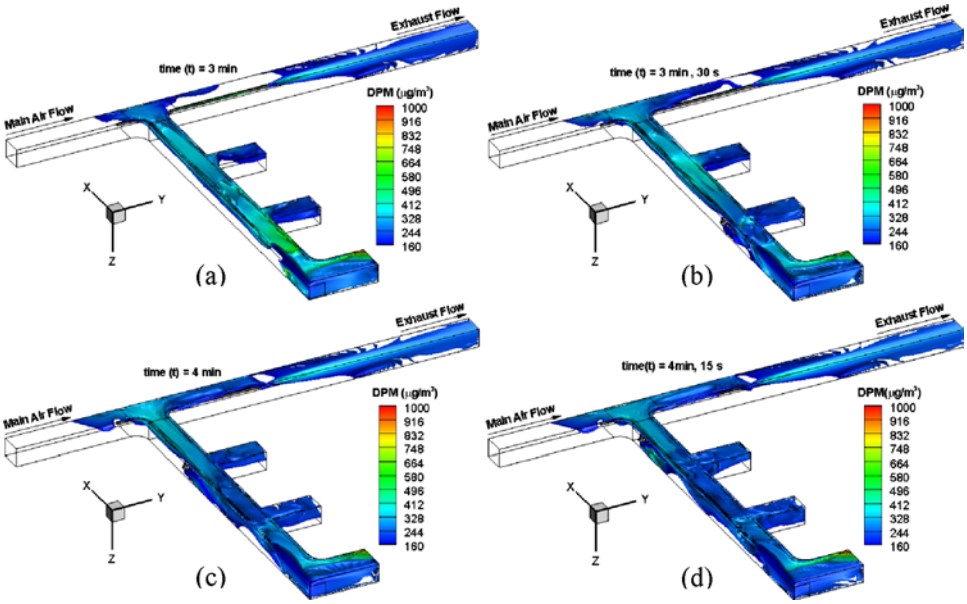

4.2.2 Hauling operation

During the hauling operation (Figure 9(a)–(d)), the truck started moving towards the main entry. The roofing effect continued to grow in the 'T' junction region of main entry owing to the continuous emission from the tailpipe of diesel vehicles. The main problem here was that it began to interfere with push tubing ventilation. Since the push tubing blower fan was located close to the roof area upstream of main entry as shown in Figure 1, it drew high concentration DPM into the push tubing. Owing to this, the outlet end of the push tubing was not able to supply fresh air into the working face in the dead end. The miners in the face and downstream of the main entry were totally unsafe in this configuration as the previous loading operation and had to use environmental cabs or personal protective equipment.

5 Conclusions

Numerical simulation of DPM distribution inside the dead end entry was carried out for LHD-truck loading and truck hauling operation. The push-pull auxiliary ventilation system was used inside the dead end entry. The simulation included cases of diesel engines fitted with and without DPF. The general flow features showed the development of complicated three-dimensional flow inside the dead end. The motion of the vehicle inside the dead end continuously altered this three-dimensional flow which in turn affected the DPM distribution. For each case during the hauling operation, the LHD was assumed to be operating. The results showed that for diesel engines fitted with DPF, the DPM distribution pattern inside the dead end remained almost constant for the entire time duration of loading operation. The LHD can continue to operate during hauling operation and miners working inside the dead end were generally safe and may need to wear personal protective instruments when they were constantly working near the tailpipe region. The push-pull tubing auxiliary ventilation effectively diluted the DPM emission from the tailpipe when the engines were fitted with DPF.

When the diesel engines were not fitted with DPF, the designed main ventilation and auxiliary ventilation fans failed to dilute the high concentration DPM emission from the tailpipe. The DPM concentration higher than the permissible limit of 160 $\mu g/m^3$ occupied the entire face area. The miners have to use personal protective instruments and environmental cabs to work inside and downstream of the face areas.

Acknowledgements

The authors wish to thank National Institute for Occupational Safety and Health (NIOSH) for its financial support.

References

ACGIH (2001) *Threshold Limit Values for Chemical Substances and Physical Agents and Biological Exposure Indices*, American Conference of Governmental Industrial Hygienists, Cincinnati.

ANSYS (2009) *ANSYS FLUENT 12.0 User's Guide*, Available at https://www.sharcnet.ca/Software/Fluent12/html/ug/main_pre.htm

Anyon, P. (2008) 'Managing diesel particle emissions through engine maintenance - an Australian perspective', *Proceedings of the 12th U.S./North American Mine Venti-lation Symposium*, 9–12 June, Reno, NV, USA, pp.521–526.

Bugarski, A.D., Cauda, E.G. and Janisko, S.J. (2010) 'Aerosols emitted in underground mine air by diesel engine fueled with biodiesel', *J. Air Waste Manage Assoc.*, Vol. 60, pp.237–244.

Bugarski, A.D., Janisko, S.J. and Cauda, E.G. (2011) *Diesel Aerosols and Gases in Underground Mines: Guide to Exposure Assessment and Control*, Department of Health and Human Services, Centers for Disease Control and Prevention, National Institute for Occupational Safety and Health, Office of Mine Safety and Health Research, Pittsburgh, PA and Spokane, WA.

Bugarski, A.D., Schnakenberg Jr., G.H. and Hummer, J.A. (2009) 'Effects of diesel exhaust after treatment devices on concentrations and size distribution of aerosols in underground mine air', *Env. Sci. Tech.*, Vol. 43, pp.6737–6743.

Cecala, A.B., Organiscak, J.A. and Zimmer, J.A. (2005) 'Reducing enclosed cab drill operator's respirable dust exposure with effective filtration and pressurization techniques', *J. Occup. Environ. Hyg.*, Vol. 2, pp.54–63.

Hargreaves, D.M. and Lowndes, I.S. (2007) 'The computational modeling of the ventilation flows within a rapid development drivage', *Tunn. Undergr. Sp. Tech.*, Vol. 22, pp.150–160.

Kahn, G. and Orris, P. (1988) 'Acute overexposure to diesel exhaust: report of 13 cases', *Am. J. Ind. Med.*, Vol. 13, pp.405–406.

Kollipara, V.K., Chugh, Y.P. and Relangi, D.D. (2012) 'A CFD analysis of airflow patterns in face area for continuous miner making a right turn cut', *Proceedings of the Society for Mining, Metallurgy & Exploration Annual Conference*, 19–22 February, 2012, Seattle, WA, Preprint 12-132.

McGinn, S. (1999) *Maintenance Guidelines and Best Practices for Diesel Engines*, Final Rept., Diesel Emissions Evaluation Program (DEEP), Available at http://www.camiro.org/DEEP/Project%20Reports/mtce_report.pdf

McGinn, S., Ellington, R. and Penney, J. (2010) *Diesel Emissions: Mechanics' Maintenance Manual*, Diesel Emissions Evaluation Program (DEEP), Available at http://www.camiro.org/DEEP/Technology%20Sum%20And%20Reports/mechanicsman.pdf

McGinn, S., Grenier, M., Gangal, M., Rubeli, B., Bugarski, A., Schnakenberg, G., Johnson, R., Petrie, D., Crowther, G. and Penney, J. (2004) *Noranda INC. – Brunswick Mine Diesel Particulate Filter Field Study*, Final Rep., the Diesel Emissions Evaluation Program (DEEP), Available at http://www.camiro.org/DEEP/Project%20Reports/nordpf_final.pdf

MSHA (2013) *Practical Ways to Reduce Exposure to Diesel Exhaust in Mining – A Toolbox*, U.S. Department of Labor, Mine Safety and Health Administration, Available at http://www.msha.gov/S&HINFO/TOOLBOX/DTBFINAL.htm

NIOSH (1988) *Carcinogenic Effects of Exposure to Diesel Exhaust*, National Institute for Occupational Safety and Health, Department of Health and Human Services, Available at http://www.cdc.gov/niosh/docs/88-116

Noll, J.D., Patts, L. and Grau, R. (2008) 'The effects of ventilation controls and environmental cabs on diesel particulate matter concentrations in some limestone mine', *Proceedings of the 12th US/North American Mine Ventilation Symposium*, 9–12 June, Reno, NV, USA, pp.463–468.

Petrov, T.P. (2014) *Development of Industry Oriented CFD Code for Analysis/Design of Face Ventilation Systems*, PhD Diss., University of Kentucky, http://uknowledge.uky.edu/mng_etds/12

Ren, T.X. and Balusu, R. (2008) 'Innovative CFD modeling to improve dust control in longwalls', *Coal 2008: Coal Operators' Conference*, 14–15 February, Wollongong, NSW, AU, pp.137–142.

Ren, T.X., Balusu, R. and Humphries, P. (2005) 'Development of innovative goad inertisation practices to improve coal mine safety', *COAL2005: Coal Operators' Conference*, 26–28 April, Brisbane, QLD, AU, pp.315–322.

Rundell, B., Ledin, M.C. and Hammarström, U. (1996) 'Effects on symptoms and lung function in humans experimentally exposed to diesel exhaust', *Occup. Environ. Med.*, Vol. 53, pp.658–662.

Shah, S.D., Cocker III, D.R. and Johnson, K.C. (2007) 'Reduction of particulate matter emissions from diesel backup generators equipped with four different after treatment devices', *Env. Sci. Tech.*, Vol. 41, pp.5070–5076.

Torno, S., Torańo, J. and Ulecia, M. (2013) 'Conventional and numerical models of blasting gas behavior in auxiliary ventilation of mining headings', *Tunn. Undergr. Sp. Tech.*, Vol. 34, pp.73–81.

US EPA (2002) *Health Assessment Document for Diesel Engine Exhaust (Final 2002)*, U.S. Environmental Protection Agency, Office of Research and Development, National Center for Environmental Assessment, Washington Office, Washington DC.

Wade III, J.F. and Newman, L.S. (1993) 'Diesel asthma: reactive airways disease following overexposure to locomotive exhaust', *J. Occup. Med.*, Vol. 35, pp.149–154.

Wedding, W.C. (2014) *Multiscale Modeling of the Mine Ventilation System and Flow through the Gob*, PhD Diss., University of Kentucky, http://uknowledge.uky.edu/mng_etds/11

Xu, G., Luxbacher, K.D. and Ragab, S. (2013) 'Development of a remote analysis method for underground ventilation systems using tracer gas and CFD in a simplified laboratory apparatus', *Tunn. Undergr. Sp. Tech.*, Vol. 33, pp.1–11.

Yuan, L. and Smith, A.C. (2007) 'Computational fluid dynamics modeling of spontaneous heating in longwall gob areas', *Trans. Soc. Min. Metall. Explor.*, Vol. 322, pp.37–44.

Zannis, T.C., Hountalas, D.T., Papagiannakis, R.G. and Levendis, Y.A. (2009) 'Effect of fuel chemical structure and properties on diesel engine performance and pollutant emissions: review of the results of four European research programs', *SAE Int. J. Fuels Lubr.*, Vol. 1, No. 1, pp.384–419, doi:10.4271/2008-01-0838.

Zheng, Y. (2011) *Diesel Particulate Matter Dispersion Analysis in Underground Metal/Non-Metal Mines using Computational Fluid Dynamics*, PhD Diss., Missouri University of Science and Technology, http://scholarsmine.mst.edu/doctoral_dissertations/2016

Zheng, Y. and Tien, J.C. (2008) 'DPM dispersion study using CFD for underground metal/nonmetal mines', *Proceedings of the 12th U.S./North America Mine ventilation Symposium*, 9–11 June, Reno, NV, USA, pp.487–493.

Zheng, Y., Lan, H. and Thiruvengadam, M. (2011) 'DPM dissipation at MST's experimental mine and comparison with simulation', *J. Coal Sci. Eng. (China)*, Vol. 17, No. 3, pp.285–289.

Identification of mining steel rope broken wires based on improved EEMD

Tie-Zhu Qiao, Zhao-Xing Li* and Bao-Quan Jin

Key Laboratory of Advanced Transducers and Intelligent Control System, Ministry of Education, Taiyuan University of Technology, Taiyuan 030024, China
Email: qtz2007@126.com
Email: krauselee@qq.com
Email: 2410729789@qq.com
*Corresponding author

Abstract: Metal magnetic memory (3M), which is used to evaluate the stress concentration and fatigue damage of ferromagnetic materials, belongs to a weak magnetic detection. When 3M technology is used to detect working steel rope, the detected signal contains lots of interfering signals to distort real signal. To improve signal to noise ratio (SNR), ensemble empirical mode decomposition (EEMD) is used to denoise the original signal. A new method of confirming white noise standard deviation (WNSD) added to EEMD has been proposed, which has a higher accuracy. Besides, a self-adaptive method of selecting intrinsic mode functions (IMFs) has been proposed. The method is used to denoise magnetic memory signal of steel rope metal and the result is better than other common denoising methods. After denoising the tested signal of steel rope, the broken wires field of the rope can be recognised by the normal component of 3M crossing zero point.

Keywords: broken wires; EEMD denoise; 3M signal; SNR; signal to noise ratio.

Reference to this paper should be made as follows: Qiao, T-Z., Li, Z-X. and Jin, B-Q. (2016) 'Identification of mining steel rope broken wires based on improved EEMD', *Int. J. Mining and Mineral Engineering*, Vol. 7, No. 3, pp.224–236.

Biographical notes: Tie-Zhu Qiao is an Associate Professor at the Institute of Measurement and Control Technology, Taiyuan University of Technology, Taiyuan. His research areas include a major coal mine disaster prediction theory of intelligent detection, intelligent intrinsically safe sensors, limited space wireless signal transmission mechanism and coal networking technology.

Zhao-Xing Li is a Graduate student at the Institute of Measurement and Control Technology, Taiyuan University of Technology, Taiyuan. His research areas include a major coal mine disaster prediction theory of intelligent detection, intelligent intrinsically safe sensors, limited space wireless signal transmission mechanism and coal networking technology.

Bao-Quan Jin is an Associate Professor at the Institute of Measurement and Control Technology, Taiyuan University of Technology, Taiyuan. His research areas include a major coal mine disaster prediction theory of intelligent detection, intelligent intrinsically safe sensors, limited space wireless signal transmission mechanism and coal networking technology.

1 Introduction

Nowadays, the mining steel rope broken wires detection is still a worldwide problem (Wang and Tian, 2013). Steel rope testing methods include Electromagnetic detection, Ultrasonic detection, Acoustic Emission detection, Ray detection and Optical test. Electromagnetic detection is the most effective method at present. The advantages of Electromagnetic detection are:

- there is a flexibility to assemble the equipment for various sizes of wire rope
- there is a highly output signal which detects the leakage field from the external and internal discontinuities (Jomdecha and Prateepasen, 2009).

3M, a new magnetic detection technology and is always used to evaluate the stress concentration (Doubov, 1999; Mingxiu, 2008; Chongchong et al., 2016; Roskosz et al., 2013; Roskosz and Bieniek, 2012) and fatigue damage (Jilin et al., 2012; Changliang et al., 2010; En et al., 2007) of ferromagnetic materials, belongs to the weak magnetic inspection field. In the process of wire rope working, the detected signal contains 3M signal and interference signals. The interference signals include the shake of steel rope itself, magnetic field from mutual effect of steel wires (Yangsheng et al., 1989) and external magnetic field. Generally using of magnetic memory signal maximum gradient value can quickly judge the stress concentration zone, but the magnetic memory signal is susceptible to effected by environmental and noise (Qiao et al., 2013). In the broken wires field of steel rope, the normal component of 3M crosses zero point; the amplitude of the normal component goes up with the increase of the number of broken wires. Therefore, the signal characteristic of 3M should be extracted accurately to identify the flaw field of the rope. The paper employs ensemble empirical mode decomposition (EEMD) to denoise the detected signal and then extracts the real 3M signal. A new method has been proposed to determine the white noise standard deviation (WNSD) added to original signal for EEMD. After the decomposition of original signal, we also have proposed an effective method, a self-adaptive selection method, to select IMFs component for the 3M signal. The results of data tests reveal that employing the proposed method to denoise the detected data shows a higher signal to noise ratio (SNR) compared with other methods.

2 EEMD denoising

2.1 A brief introduction of EEMD

Empirical mode decomposition (EMD) is a kind of self-adaptive and unsupervised method and its base functions derive from the data itself (Cao et al., 2015). Compared

with wavelet transform, it is difficult to determine the suitable wavelet base functions and decomposition levels, which has a significant influence on the analysis results (Cao et al., 2015). It decomposes the data into a set of IMFs after a sifting process and the original signal of interest is reconstructed as a sum of selected IMFs. An IMF must satisfy the following conditions:

- the number of extrema and the number of zero crossings must be equal or can differ at most by one
- the mean value of the envelope defined by local maxima and local minima, at any location, must be zero, i.e., envelopes should be symmetric with respect to zero.

Huang et al. (1998), Wang et al. (2015) and Flandrin et al. (2004) introduce the detailed decomposition process of EMD. EMD equals to second order filter of multi-types noises which include Gaussian white noise and fractional Gaussian noise (Flandrin et al., 2004; Wu and Huang, 2004; Flandrin et al., 2005). However, when the extreme values of signal distributed unevenly, EMD is prone to mode mixing (Wu and Huang, 2009).

To solve the problem of mode mixing inherent of EMD, an effective EEMD analysis was proposed by Wu and Huang (2009). In EEMD, white noise, having the amplitude of a fraction of the standard deviation of the signal, is added before executing (EMD) to decompose the signal into intrinsic mode functions (IMFs), in each trial, and the ensemble average of each IMF is taken over all the trials to represent the true IMFs. The noise added in each trial to prevent the mode mixing effect, tends to cancel when ensemble averaged since no correlation exists among the noise introduced at different trials. EEMD makes the EMD algorithm a real binary filter. The flow chart of EEMD denoising is shown in Figure 1.

2.2 White noise added for EEMD

In EEMD algorithm, a finite amplitude of identically distributed white noise $n_i(t)$ is added to the original signal or input data $S(t)$ and then the mixed data is decomposed into IMFs using EMD. The equals can be represented as:

$$S_i(t) = S(t) + \varepsilon n_i(t), \tag{1}$$

where

$S_i(t)$: signal during the ith trial

ε: scaling factor for the white noise at each trial.

The scaling factor should be neither too small nor too large (Zhang et al., 2010) and Wu and Huang (2009) reported that the optimum amplitude of the noise to be added is in the range 0.1–0.4 times the standard deviation of the signal. However, when the noise amplitude is larger than the amplitude of the signal to be denoised or decomposed, this prescription fails to achieve the prevention of mode mixing with a relatively small number of trials. Therefore, the white noise amplitude added to the tested data should not affect extremum point distribution of high frequency components of the data and should affect extremum point distribution of low frequency components. As a result in equation (1):

$$\varepsilon = \frac{\sigma_n}{\sigma_0};\ \varepsilon < k \cdot \frac{\sigma_h}{\sigma_0}, \tag{2}$$

where

σ_n: WNSD

σ_h: high frequency components standard deviation of original signal

σ_0: standard deviation of the original signal

K: control coefficient to control the value range of σ_n.

In statistics, treating measurement value as samples, in confidence interval CI, the probability of the emergence of true value is confidence level, generally set $1 - 0.05 = 0.95$, according to the normal distribution function, namely: $P\{\mu - 2\sigma < x < \mu + 2\sigma\} < 0.95$, so we can obtain that when $\sigma_n = \sigma_h / 2$, it indicates 95% of the white noise amplitude won't affect extremum point distribution of high frequency components of the data. Hence, in order to restrain effectively mode mixing, the best k should satisfy $k \leq 0.5$. The range of the WNSD added to original signal is too large determined by this method and it makes no difference to paper (Wu and Huang, 2009). We have summarised a more precise selection range of WNSD and proposed a self-adaptive method to filtrate IMFs after denoising dozens of sets of data.

Figure 1 Flow chart of EEMD denoising (see online version for colours)

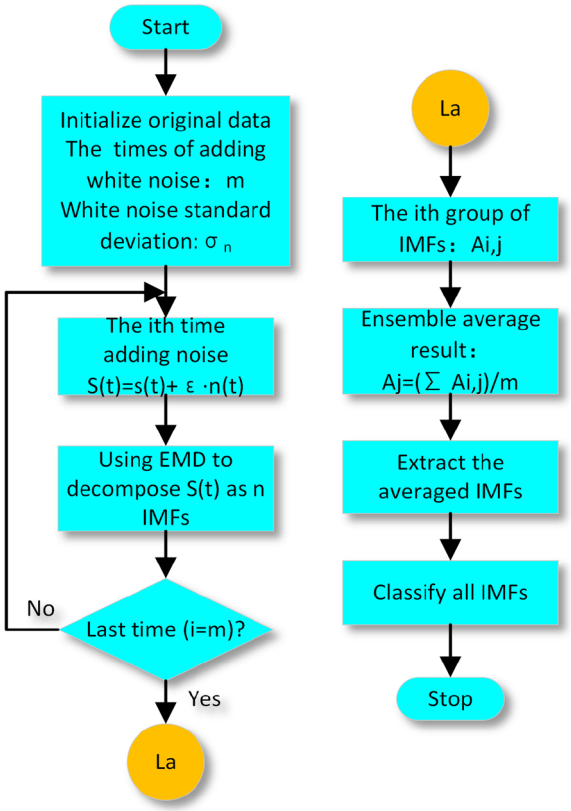

2.3 Determination of the WNSD

Mariyappa et al. (2014) introduced empirical equation for ε after denoising all kinds of original signal:

$$\varepsilon = \frac{F}{f_s^n} \times \sigma\left(\frac{\mathrm{d}^n S(t)}{\mathrm{d}t^n}\right), \tag{3}$$

where

F: scale factor

f_s: sampling frequency, used for normalising the unit bandwidth of the signal

n: order of the derivative

$\sigma(x)$: the standard deviation of x.

When set $n = 2$, the denoising results reveal well for almost all sets of data after EEMD. In equation (3),

$$F = \frac{\| S(t) \|_2}{\sqrt{S(t)_{\min}^2 + S(t)_{\max}^2}} \times \sqrt{\frac{\sqrt{2}}{N}}, \tag{4}$$

where

$S(t)_{\min}$: the minimum value of the input data

$S(t)_{\max}$: the maximum value of the input data

N: the length of the data.

Based on the above empirical model, we have extracted the more precise range of WNSD after denoising dozens of sets of data (3M signal). The inequation can be represented as:

$$\frac{F}{f_s} \times \sigma\left(\frac{\mathrm{d}S_l(t)}{\mathrm{d}t}\right) < \sigma_n < \frac{F}{f_s^n} \times \sigma\left(\frac{d^n S_h(t)}{\mathrm{d}t^n}\right). \tag{5}$$

where

$S_l(t)$: low frequency component of original signal

$S_h(t)$: high frequency component of original signal.

Experiments with practical data show that the range narrows down compared with the method of statistics. The conventionally used WNSD can be obtained from equation (6) when $n = 0$ indirectly. Flandrin et al. (2004) studied the relationship between the amplitude ratio coefficient of white noise added to original signal and the times of the added white noise,

$$e \approx \alpha / \sqrt{m}, \tag{6}$$

where

e: expectation of the relative error minimum of signal decomposition

m: total number of times of the added white noise, $\alpha = \sigma_n / \sigma_0$.

All *m* is worked out from equation (6) in this paper.

2.4 IMFs component selection

In the process of employing EEMD to denoise the original signal, it will cause error due to decomposition and interpolation. The accumulation of error generates pseudo components for decomposition results. In order to get rid of the pseudo components effectively, we proposed a self-adaptive method based on correlation coefficient difference to select the IMFs.

From probability and statistics, correlation coefficient may be represented as:

$$r = \frac{\sum_{i=1}^{N}(x_i - \overline{x})(y_i - \overline{y})}{\sqrt{\sum_{i=1}^{N}(x_i - \overline{x})^2 \bullet \sum_{i=1}^{N}(y_i - \overline{y})^2}}. \tag{7}$$

where

x_i: *i*th sample point of $x(t)$

$\overline{x}$: mean value of $x(t)$

y_i: *i*th sample point of $y(t)$, $\overline{y}$ -the mean value of $y(t)$.

According to equation (7), the steps of IMFs component selection may be represented as:

- Work out the EEMD of original signal, a series of IMFs *imf*1, *imf*2 … *imfn* can be obtained from the EEMD.
- Work out every IMF component correlation coefficients *r*1, *r*2 … *rn* with original signal.
- Work out every IMF component correlation coefficients *r*1, *r*2 … *rn* with defect-free signal of the same steel rope.
- Work out the two sets correlation coefficients difference $\lambda i = ri – r1i$.
- Sort λ_i on the basis of progressive increase as λ_j, *n*–1 differences can be obtained from $D_j = \lambda_{j+1} - \lambda_j$, if the maximum of the differences is D_{js}. According to the signal we need to extract, 3M signal is low-frequency signal, so *j*sth~(*n* – 1)th IMFs and res should be considered as the real component to rebuild the signal which reflects the broken field of the rope.

The above method, depending on the IMFs and input data, avoids the threshold value selection in some method and improve the efficiency of the program execution. IMFs selection is selecting the real component of original signal or input data. The size of correlation coefficient difference λ_i reflects the degree of relationship between IMF and original signal, IMF and defect-free signal.

3 The denoising of noised signal

In order to distinguish the common method of EEMD (according to the empirical value 0.2 of WNSD, and selecting IMFs by setting threshold), here we name our method as IEEMD. Firstly, add a set of defect-free signal (noise signal) obtained from a non-defective rope to another set of defected signal obtained from a smooth-faced ferromagnetic materials (to get a smooth 3M signal) as the original signal. Here we choose one set of the tested data (3M signal) to talk about. So the original SNR can be worked out and the SNR of the original signal is 40.35. Then, the signal is denoised by IEEMD ($n = 0$, $n = 1$, $n = 2$), EEMD and wavelet analysis. The better denoising method will be verified from the mentioned ways for rope magnetic signal. The acquisition of signal is same with the next section.

Figure 2 shows the noise signal and original signal (noised signal). Set the expectation of the relative error minimum of signal decomposition $e = 0.1\%$, Table 1 shows the correlation coefficients using IEEMD ($n = 2$) to denoise the original signal.

Figure 2 Noise and original signal (see online version for colours)

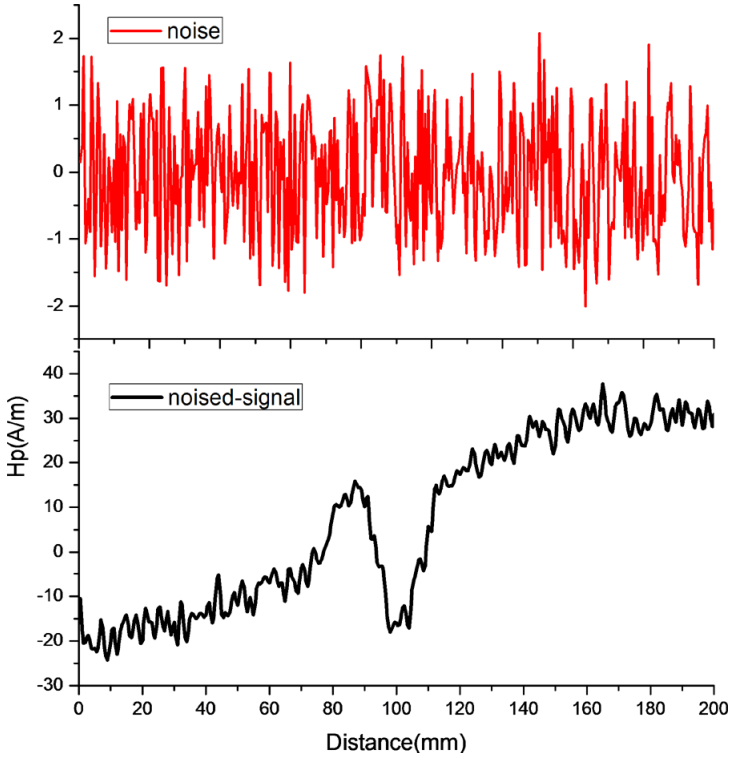

Table 1 Correlation coefficient

Category IMFs	*imf1*	*imf2*	*imf3*	*imf4*	*imf5*	*imf6*	*imf7*	*res*
Noise signal	–0.016	0.020	0.032	–0.099	–0.006	–0.032	0.241	0.505
Original signal	0.073	0.101	0.095	0.273	0.312	0.165	0.775	0.933
Difference	0.089	0.081	0.063	0.372	0.318	0.197	0.534	0.428

The denoised signal can be represented as $S_{dn} = imf4 + \cdots + imf7 + \text{res}$ after the IMFs selection. Table 2 shows the parameters of different de-noising methods. The paper selects 'db4' as the wavelet basis function and employs six-layers decomposition for wavelet denoising. The hardware configuration of the used computer is i5 CPU and 4GB RAM.

Compared the above method, the larger the n is, the smaller the range of WNSD is; the IEEMD ($n = 2$) is better than other method for original signal denoising after taking the program running time and stability of the denoising into consideration. From the process of the denoising, we have drawn a conclusion that the larger the WNSD is, the less steady the SNR will be (the difference of the results of each calculation of SNR). So the WNSD should not be too large.

Table 2 Parameters and SNR

Method parameter	*Upper limit*	*Lower limit*	*Selection value*	*Addition times*	*Run time* (s)	*SNR*
$N = 0$	2.50	0.103	0.4	200	15.77	45.62
$N = 1$	1.05	0.103	0.3	150	12.73	45.61
$N = 2$	0.46	0.103	0.25	100	7.85	45.52
EEMD	0.4	0.1	0.2	50	3.92	43.13
Wavelet	×	×	×	×	0.7	42.27

Figure 3 shows the obtained IMFs after using IEEMD ($n = 2$) to denoise the original signal, the first three IMFs cannot reflect the characteristic of 3M signal (normal component crossing zero point), so they should be treated as spurious signal and be abandoned. The last four IMFs may be treated as the real signal.

Figure 4 shows the denoising comparison for the mentioned methods above. The partial enlarged figures show the difference between the different denoising methods clearly. From the above conclusion, so we will use IEEMD ($n = 2$) to denoise the rope 3M signals next section.

4 Experiment data processing

In this section, we will denoise three sets of original signal. Here, we should declare the first set of data comes from a 6 × 37 specification cracked mining steel rope whose diameter is 39 mm and so does the second set of data. The third set of data comes from a 6 × 37 specification cracked rope whose diameter is 24 mm. Figure 5 shows the detection equipment for signal acquisition and a 39 mm-diameter cracked steel rope.

4.1 The steps of signal processing

For the sake of safety, the signals are acquired in the laboratory. Here, we introduce the steps of signal processing below:

- get original signal by Eddysun EMS–2003 intelligent magnetic memory/eddy current detector, adding random shake to the rope in the process of signal acquisition to simulate the online working rope
- process the data by MATLAB, including smoothing and intercept the data into five sets of data and the data includes three sets of defect data (original signal) and two sets of defect-free data (noise signal)
- filter every set of original signal as a set of high-frequency component and a set of low-frequency component by Parks-McClellan high pass filter and low pass filter
- work out the WNSD added to the original signal and the times of the addition by the proposed method in the paper for IEEMD
- select the IMFs after IEEMD as the reconstitution component of 3M signal who can reflects the broken wires field of the experimental rope.

Figure 3 IMF component when $n = 2$ (see online version for colours)

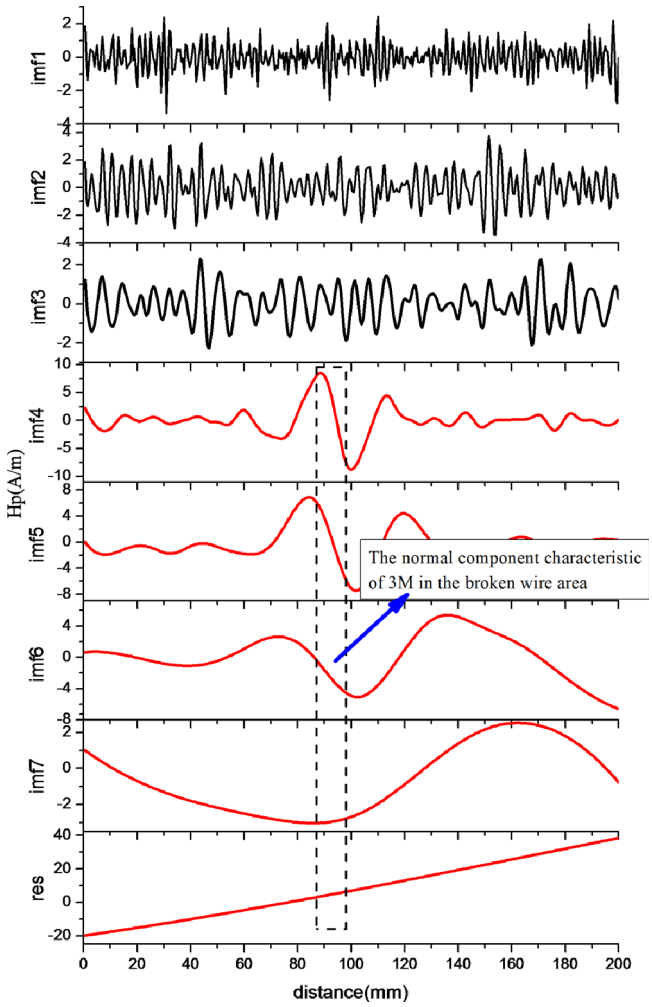

Figure 4 Denoising comparison (see online version for colours)

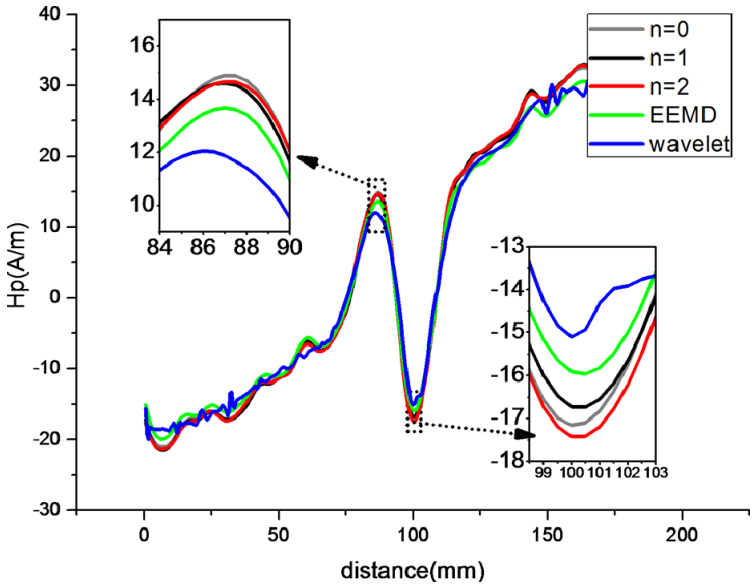

Figure 5 Detection platform (see online version for colours)

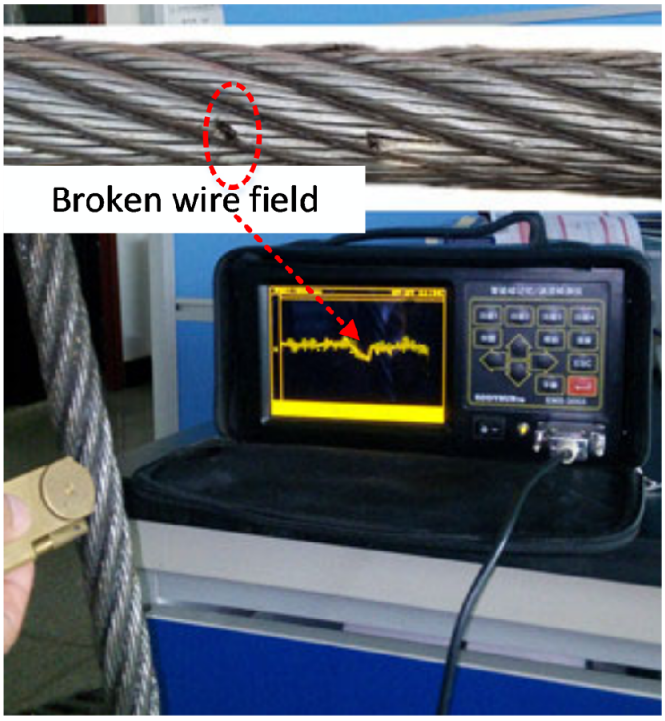

4.2 Signal processing

Set the expectation of the relative error minimum of signal decomposition $e = 0.1\%$, using IEEMD ($n = 2$) to denoise the original signal. The parameters of EEMD: WNSD is 0.2 and the times of the addition is 100. The parameters result and SNR of every set of data denoised by IEEMD are shown in Table 3. The number of broken wires of the three sets of data measured is 4, 2 and 4 approximately.

Table 3 The results of denoising

Group parameter	*Upper limit*	*Lower limit*	*Selection*	*Addition times*	*IEEMD SNR*	*EEMD SNR*	*Wavelet SNR*
First	0.54	0.18	0.40	160	24.49	23.05	22.65
Second	0.25	0.13	0.25	120	15.38	14.21	13.85
Third	0.37	0.04	0.35	100	17.93	17.03	15.74

The SNR of IEEMD ($n = 2$) is larger than other denoising methods and the SNR of wavelet analysis is less than EEMD. The reason for this is the unsuitable wavelet base functions and decomposition levels for wavelet denoising. The larger the number of the broken wires is, the larger the SNR is.

Figure 6 shows the comparison of the mentioned denoising methods. The green curve is the denoising result of IEEMD, the red curve is the denoising result of EEMD and the blue curve is the denoising result of wavelet analysis. The grey is the original signal. Overall, the amplitude of IEEMD denoising is larger than the other two methods.

Figure 6 Denoising comparison: (a) different denoise methods of group 1 data compared with the original signal; (b) different denoise methods of group 2 data compared with the original signal and (c) different denoise methods of group 3 data compared with the original signal (see online version for colours)

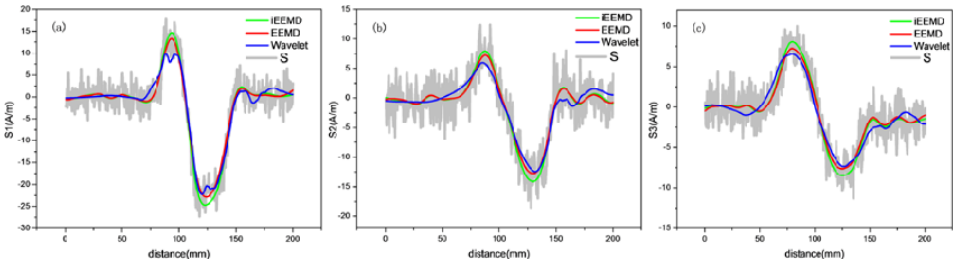

Figure 7 shows the peak-to-valley value of the denoised signal, the value may reflect the strength of 3M signal. No matter in the theoretical analysis or in the experimental analysis, the value can be a method to evaluate injury degree of ferromagnetic materials. Obviously, the value of IEEMD denoising is larger than others.

Figure 7 Peak-to-valley value comparison (see online version for colours)

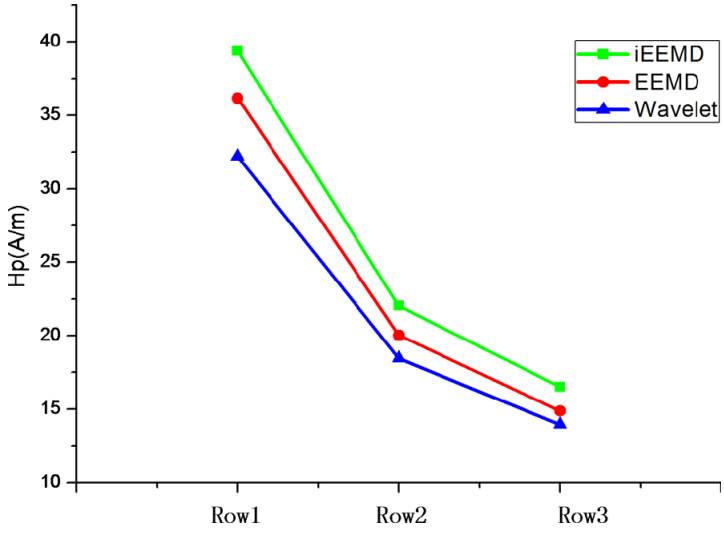

5 Conclusion

A lot of interference, existing in the operation process of mining steel rope, has a great impact on broken wires identification accuracy for rope flaw detection. The paper has proposed an improved EEMD method to denoise rope 3M signal, namely, selecting WNSD by threshold value and a new self-adaptive way to select IMFs after EEMD. The method narrows the threshold of WNSD down compares with previous related papers and IMFs selection depends on the input data itself which improve the time of program execution compares some paper which use wavelet analysis or set threshold for the selection. Therefore, the proposed method can get a high SNR and amplitude relatively for rope 3M signal which is propitious to identify the flaw field of mining rope.

References

Cao, H., Zhou, K. and Chen, X. (2015) 'Chatter identification in end milling process based on EEMD and nonlinear dimensionless indicators', *International Journal of Machine Tools and Manufacture*, Vol. 92, pp.52–59.

Changliang, S., Shiyun, D., Binshi, X. and Peng, H. (2010) 'Stress concentration degree affects spontaneous magnetic signals of ferromagnetic steel under dynamic tension load', *NDT&E International*, Vol. 43, No. 1, pp.8–12.

Chongchong, L., Lihong, D., Haidou, W., Guolu, L. and Binshi, X. (2016) 'Metal magnetic memory technique used to predict the fatigue crack propagation behavior of 0.45%C steel', *Journal of Magnetism and Magnetic Materials*, Vol. 405, pp.150–157.

Doubov, A.A. (1999) 'Diagnostics of metal items and equipment by means of metal magnetic memory', *Proceeding of CHSNDT 7th Conference on NDT and International Research Symposium*, Shantou, China, pp.181–186.

En, Y., Luming, L. and Xing, C. (2007) 'Magnetic field aberration induced by cycle stress', *Journal of Magnetism and Magnetic Materials*, Vol. 312, No. 1, pp.72–77.

Flandrin, P., Goncalvás, P. and Rilling, G. (2005) 'EMD equivalent filter banks, from interpretation to applications', in Huang, N.E. and Shen, S.S.P. (Eds.): *Hilbert–Huang Transform: Introduction and Applications*, World Scientific, Singapore, pp.57–74.

Flandrin, P., Rilling, G. and Goncalvés, P. (2004) 'Empirical mode decomposition as a filter bank', *IEEE Sig Process Lett*., Vol. 11, pp.112–116.

Huang, N.E., Shen, Z., Long, S.R., Wu, M.C., Shih, H.H., Zheng, Q., Yen, N.C., Tung, C.C. and Liu, H.H. (1998) 'The empirical mode decomposition and the Hilbert spectrum for nonlinear and non-stationary time series analysis', *Proc Roy Soc Lond A*, Vol. 454, pp.903–995.

Jilin, R., Junming, L. and Wenjian, R. (2012) 'Metal magnetic memory testing technology development status and prospects', *NDT*, Vol. 34, No. 4, pp.3–12.

Jomdecha, C. and Prateepasen. A. (2009) 'Design of modified electromagnetic main-flux for steel wire rope inspection', *NDT & E International*, Vol. 42, No. 1, pp.77–83.

Mariyappa, N., Sengottuvel, S., Parasakthi, C., Gireesan, K., Janawadkar, M.P., Radhakrishnan, T.S. and Sundar, C.S. (2014) 'Baseline drift removal and denoising of MCG data using EEMD: Role of noise amplitude and the thresholding effect', *Medical Engineering and Physics*, Vol. 36, No. 10, pp.1266–1276.

Mingxiu, X. (2008) *Research on the Damage Diagnosis of Ferromagnetic Materials Rotating Bending Fatigue using Magnetic Memory Technology*, Harbin Institute of Technology.

Qiao, T., Li, X. and Zhang, X. (2013) 'Singularity detection of magnetic memory signal of steel-cord conveyor belt', *Telkomnika Indonesian Journal of Electrical Engineering*, Vol. 11, No. 9, pp.4904–4910.

Roskosz, M. and Bieniek, M. (2012) 'Analysis of the similarity between residual magnetic field distribution and the stress and strain state for 7CrMoVTiB10–10 (T/P24) steel', *International Journal of Applied Electromagnetics and Mechanics*, Vol. 30, No. 5, pp.521–527.

Roskosz, M., Rusin, A. and Bieniek, M. (2013) 'Analysis of relationships between residual magnetic field and residual stress', *Meccanica*, Vol. 48, No. 1, pp.45–55.

Wang, H-y. and Tian, J. (2013) 'Method of magnetic collect detection for coal mine wire rope base on finite element analysis', *Journal of China Coal Society*, Vol. 38, No. S1, pp.256–260.

Wang, Y., Wub, X., Lia, W., Lia, Z., Zhang, Y. and Zhou, J. (2015) 'Analysis of micro-Doppler signatures of vibration targets using EMD and SPWVD', *Neurocomputing*, Vol. 171, No. C, pp.1–9.

Wu, Z. and Huang, N.E. (2004) 'A study of the characteristics of white noise using the empirical mode decomposition method', *Proc Roy Soc Lond A*, Vol. 460, No. 2046, pp.1597–1611.

Wu, Z. and Huang, N.E. (2009) 'Ensemble empirical mode decomposition: a noise-assisted data analysis method', *Advances in Adaptive Data Analysis*, Vol. 1, No. 1, pp.1–41.

Yangsheng, W., Hanmin, S. and Shuzi, Y. (1989) 'The principle and the implementation of quantitative test of steel wire rope broken wires', *China Science*, Vol. 9, pp.993–1000.

Zhang, J., Yan, R., Gao, R.X. and Feng, Z. (2010) 'Performance enhancement of ensemble empirical mode decomposition', *Mech. Syst. Sig. Process*, Vol. 24, pp.2104–2127.

Simultaneous prediction of blast-induced flyrock and fragmentation in opencast limestone mines using back propagation neural network

Ratnesh Trivedi*

CSIR-Central Institute of Mining and Fuel Research,
Regional Centre,
Nagpur, 440006, India
Email: ratneshtrivedicimfr@gmail.com
*Corresponding author

T.N. Singh

Department of Earth Sciences,
Indian Institute of Technology Bombay,
Powai, Mumbai, 400 076, India
Fax.: 022 25767253
Email: tnsingh@iitb.ac.in

A.K. Raina

CSIR-Central Institute of Mining and Fuel Research,
Regional Centre,
Nagpur, 440006, India
Email: rainaji@gmail.com

Abstract: Goal of blasting operations is to achieve desired fragment size to operate the mine and plant economically while maintaining safety that includes prevention of flyrock accidents. This paper focuses on the simultaneous prediction of flyrock distance and fragmentation using back propagation neural network techniques. Thus, linear charge concentration, burden, spacing, stemming length, specific charge, unconfined compressive strength and rock quality designation are taken as input. Flyrock distance and fragment size are chosen as output. The predicted outputs by back propagation neural network (BPNN), multi variate regression analysis (MVRA) have been compared. The quite lower root mean square error (RMSE) and mean absolute error (MAE) in BPNN than MVRA prove that BPNN is a better prediction method. Also, the predicted output in BPNN correlates better with the observed output than MVRA. Sensitivity analysis for both independent variables for BPNN and MVRA is also included in this paper.

Keywords: opencast mining; blasting; BPNNs; back propagation neural networks; multiple regression; flyrock; fragmentation.

Reference to this paper should be made as follows: Trivedi, R., Singh, T.N. and Raina, A.K. (2016) 'Simultaneous prediction of blast-induced flyrock and fragmentation in opencast limestone mines using back propagation neural network', *Int. J. Mining and Mineral Engineering*, Vol. 7, No. 3, pp.237–252.

Biographical notes: Ratnesh Trivedi has 15 years of research and teaching experience in the field of rock blasting, rock mechanics, mine planning and environment management of mining industry.

T.N. Singh has more than 30 years of teaching and research experience in the field of rock mechanics, rock blasting and engineering geology.

A.K. Raina has around 25 years of research and teaching experience in the field of rock engineering and rock blasting.

1 Introduction

Growing demand of limestone with sprawl of urbanisation along with the increased environmental constrains have compelled opencast mines to conduct blasting operations with higher factor of safety. In order to cope up with higher production capacity, size of equipment and blast sizes have also increased considerably. This has enforced a blasting regime, wherein flyrock is controlled or eliminated simultaneously, while achieving optimum fragmentation and thus ensuring safe and productive blasting. The rock is broken into small fragments that are suitable for crushing (Lawrence et al., 2002). Only a small proportion of the total energy is utilised for actual breakage and displacement of rock mass, and the rest of the energy is partitioned into undesirable effects like ground vibrations, air blast, noise, back break, flyrock, and dust (Bajpayee et al., 2002; Hagan, 1973, 1983; Singh et al., 1994; Wiss and Linehan, 1978). Flyrock is defined as the rock propelled beyond the blast area by the force of an explosion (IME, 1997). A flyrock that travels beyond the desired or allowable distances has a potential to damage nearby structures, equipment and injure men. These flying fragments are the main reason of many fatal and non-fatal blasting accidents in opencast mines (Lundborg, et al., 1975; Verakis and Lobb, 2003). Despite of the destructive nature of flyrock the problem has received less attention from researchers in comparison to ground vibration prediction (Raina et al., 2012).

A large volume of gases and fumes gets liberated after initiation of explosive in a blast hole. These gases and fumes exert pressure on side wall of the blast hole in which strain waves get generated (Wharton et al., 2000). These strain waves are responsible for the fragmentation of the rock mass by means of breakage mechanism such as crushing, radial cracking and reflection breakage in the presence of a free face. The excessive gas pressure after fragmentation results in flyrock projectiles in opencast mines. Cratering, riffling and face burst are the prominent mode of flyrock occurrences (Richards and Moore, 2004). Due to excessive crushing of the rock mass surrounding the blast hole, a large portion of the explosive energy is wasted. Once the compressive waves pass through medium, the movement is virtually discontinued and the medium attains a quasi-static equilibrium state (Chiappetta and Mammele, 1987; Moxon et al., 1993). Several studies have been conducted on the prediction of rock fragmentation by blasting accounting for controllable blast design, explosive related parameters as well as uncontrollable physical and geo-mechanical parameters of rock mass (Kulatilake et al., 2010; Singh and Sastry, 1986). A relationship between mean fragment size and specific charge was developed by Kuznetsov (1973). On the basis of equation developed by

Kuznetsov and the Rosin and Rammler distribution, Cunningham (1983) proposed Kuz–Ram fragmentation model, which was further modified by Cunningham (1987).

Prediction of flyrock distance has been recognised as an effective way of reducing accidents due to blasting. The major causes of flyrock in opencast mines are reduced burden, inadequate stemming length, faulty drilling, back-break due to poor previous blast, very high explosive concentration, inaccuracy of delays and unfavourable geological conditions such as open joints, weak seam and presence of cavities in rock mass (Bhandari, 1997; Fletcher and Andrea, 1986; Persson et al., 1984; Rehak et al., 2001; Shea and Clark, 1998; Siskind and Kopp, 1995; Workman and Calder, 1994). Any imbalance between the distribution of the explosive energy, geo-mechanical strength of the surrounding rock mass, and confinement creates a potential hazardous condition by channelling the energy through the path of least resistance. Such imbalance can propel flyrock beyond the protected blast area (Bajpayee et al., 2004). The review and analysis of past data can improve blast design, execution and help in the achievement of desired blasting outcomes (Parihar and Bhandari, 2012).

The development of empirical relationship within the parameters for a given system can be useful for prediction. However, the laws underlying the behaviour of a system are not easily understood and the empirical regularities are not always evident and can often be masked by hidden variables. That is why, nowadays, more precise techniques such as artificial neural networks (ANNs), adaptive neuro-fuzzy inference system (ANFIS), maximum likelihood classification (MLC), genetic algorithm (GA), technique for order preference similarity to ideal solution (TOPSIS), are frequently applied to solve blasting and several rock engineering problems (Monjezi et al., 2010, 2011; Tawadrous, 2006; Tawadrous and Katsabanis, 2005, 2007; Trivedi and Singh, 2014). Tang et al. (2007) have adopted the back-propagation neural network model to predict the peak particle velocity of blast vibration. Khandelwal and Singh (2007) have underlined the significance of neural network in the prediction of ground vibration and frequency. Remennikov and Mendis (2006) have stressed the importance of neural network-based model in predicting air overpressure in complex environmental configurations. Tawadrous and Katsabanis (2005) have stressed the importance of ANNs in the prediction of the geometry of surface blast patterns in limestone quarries. Trivedi et al. (2015) have predicted blast-induced flyrock in opencast mines using ANN and ANFIS. Sharma and Rai (2015) have investigated the impact of crushed aggregate as a stemming material used in bench blasting at an opencast lead zinc mine for flyrock control.

The present paper attempts to predict flyrock distance and oversize fragmentation, i.e., (+)300 mm size, simultaneously using back propagation neural network technique (BPNN). Since, rock fragmentation and flyrock occurrence are the outcome of detonation of explosive in the blast hole during bench blasting operations, it is imperative to predict fragmentation and flyrock simultaneously. Neural Network has been trained and tested using 120 datasets and validated using 20 datasets generated from blasting in four limestone mines in India. In order to know the relationship with output variables and input variables, multi-variate regression (MVRA) was carried out for both the output variables separately. Results of BPNN and MVRA have thus been compared. Blast design and geotechnical parameters, such as linear charge concentration, burden, spacing, stemming length, specific charge, depth of blast hole, unconfined compressive strength and rock quality designation (RQD), have been taken as input. Flyrock distance and percentage of fragmentation above 300 mm have been chosen as output. The input variables, i.e., independent variables have been selected on the basis of nature of

dependent variables. In order to ascertain the relative influence of independent variables on output variables, sensitivity analysis has been performed using Cosine Aptitude Method.

2 Materials and methods

2.1 Field study at opencast limestone mines

The study site namely mining lease of Bamangaon and Mehgaon Mines is located at Kymore village, Vijayraghavgarh Block, Katni District, Madhya Pradesh. This Aditya Birla Limestone mine is located in Tehsils Chittorgarhand Nimbahera, District Chittorgarh, Rajasthan. The site is located 18 km South West of Chittorgarh town. Sheopura–Kesarpura (S-K) mine of Shree Cement is located near Beawar city. The Kotputli Limestone mine of Grasim Cement is located at Mohapura Jodhapura near Kotputli Town of District Jaipur, Rajasthan. A brief description of the mines is given in Table 1 and their approximate locations are provided in Figure 1.

Table 1 Brief description of the study sites

S. No.	*Name of mine*	*Latitudes*	*Longitudes*	*Annual production capacity*	*General strike*	*General true dip*
1	Bamangaon and Mehgaon mines, Kymore	N 23º48′ to N 24º8′	E 80º29′ to E80º57′	6 million tons	NE-SW	10º to 20º, NW to W
2	Sheopura Kesarpura mine, Beawar	N 26º 01′ to N 26º05′	E 74º22′ to E 74º26′	2.0 million tons	N30ºE	45º to 60º, W to NW
3	Aditya Limestone Mine	N 24º43′ and 24º45′	E 74º35′ and 74º37′	6.6 million tons	N-S°	0° to 20º , due to folding W or E
4	Kotputli Limestone Mine	N27º39′ to N 27º42′	E76º 06′ to E 76º 09′	6 million tons	NE-SW	38^{Q} to 80^{Q}E

2.2 Data generation

The problem of blast-induced flyrock is dominating in opencast mines under investigation since blasting sites in these mines have proximity to villages.

Blast design variables like burden, spacing, stemming, average depth of blast holes, blast hole diameter, charge per hole, linear charge concentration, specific charge, i.e., ratio of explosive consumed to tonnage of rock broken per blast (kg/ton). Geotechnical parameters such as volumetric joint count, joint spacing, dip and strike of major joint set, joint condition were generated and at exposed rock near blast face before blasting operation took place. RQD has been estimated using volumetric joint count (*Jv*) method (Palmstrom, 1982). Density and unconfined compressive strength were evaluated by testing cubes of inch samples. Bench faces before and after blasting have been

shown in Figure 2. Blast-induced flying fragments having a diameter ~10 cm or more were considered as flyrock as such flying fragments may cause fatal injuries or damage. A hand-held GPS was used to measure the distance of flyrock from the blasting face in the mines. Figure 3 depicts the flyrock generation during bench blasting.

Figure 1 Index of map showing location of limestone mines

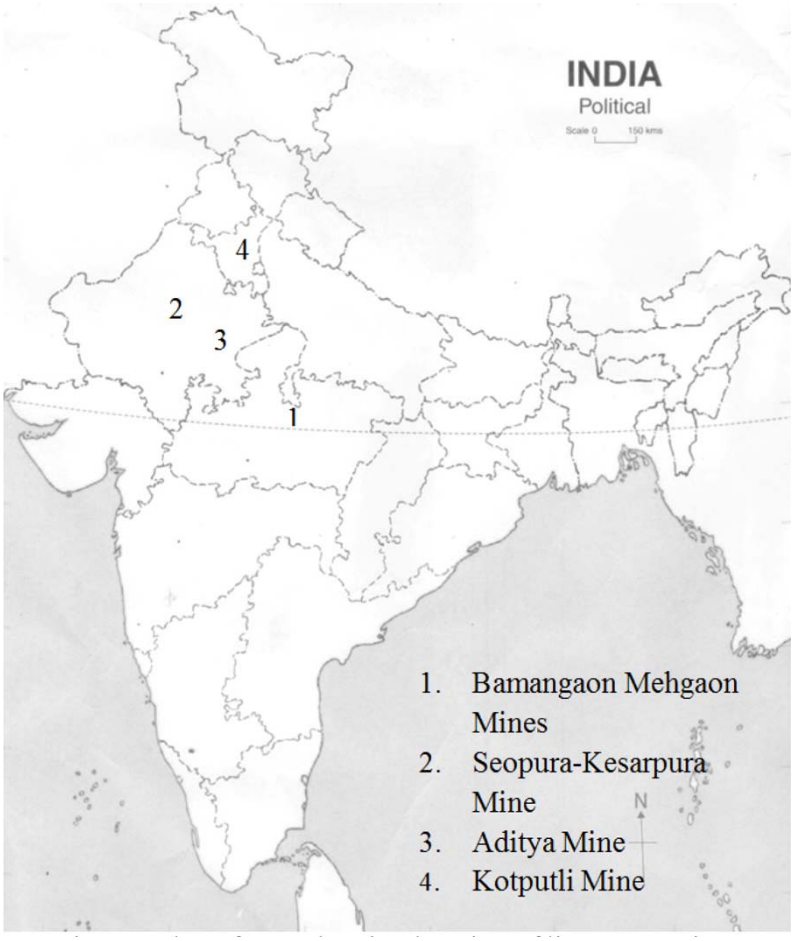

Figure 2 Photographs of bench faces before and after blasting (see online version for colours)

Figure 3 Flyrock generated during bench blasting in limestone a mine (see online version for colours)

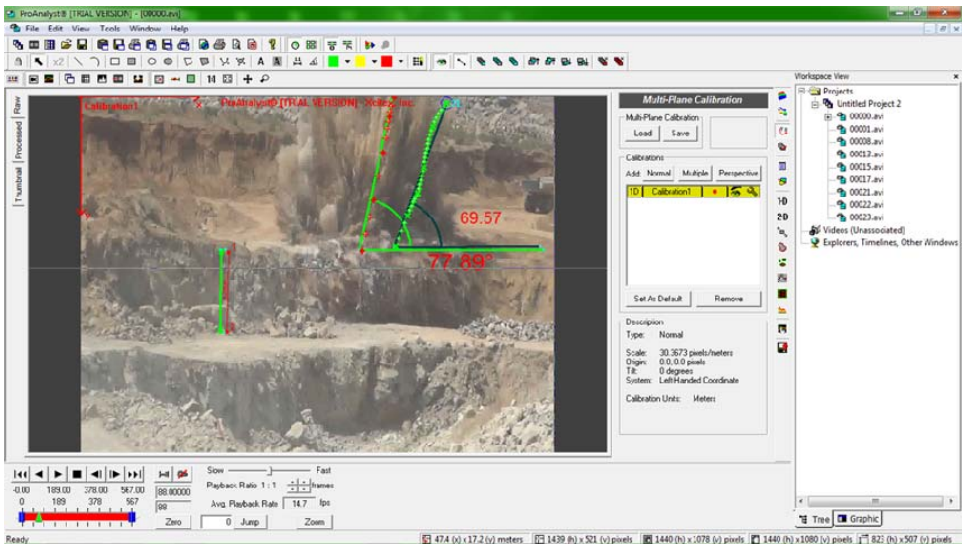

Adequate calibrated photographs of rock fragmentation by blasts were taken and analysed using 'Fragalyst© Software' to assess blasted fragmentation size distribution at different intervals during mucking (Figure 4). The automatic edge detection method and range technique was used to trace the size distribution of fragments in all the blasts (Figure 5). The oversize percentage in the muck was derived from the R-R distributions of the fragmentation provided by the software in all the blasts monitored as shown in Figure 6.

Figure 4 Images of blasted muck at different stages of loading (see online version for colours)

Since limestone mines covered under the present study are cement-grade limestone ones the efficiency of the crusher decreases and energy consumption increases sharply if blasted fragments of the size (+)300 mm are fed to the crusher. Thus, blasted fragments of (–)300 mm in size are considered as ideal fragmentation for the crusher. The fragmentation (+)300 mm are considered here as 'Oversize Fragmentation' and chosen as a performance variable which can be calculated as shown in equation (1).

$$\%\ \text{of fragmentation}\ (+)300\ \text{mm} = 100 - \%\ \text{of fragmentation up to 300 mm.} \quad (1)$$

The Blast as well as geotechnical data of the blast sites, type of variables with symbols used in text and data range have been summarised in Tables 2 and 3.

Figure 5 'Edge detection' of image of blasted muck in 'Fragalyst software' (see online version for colours)

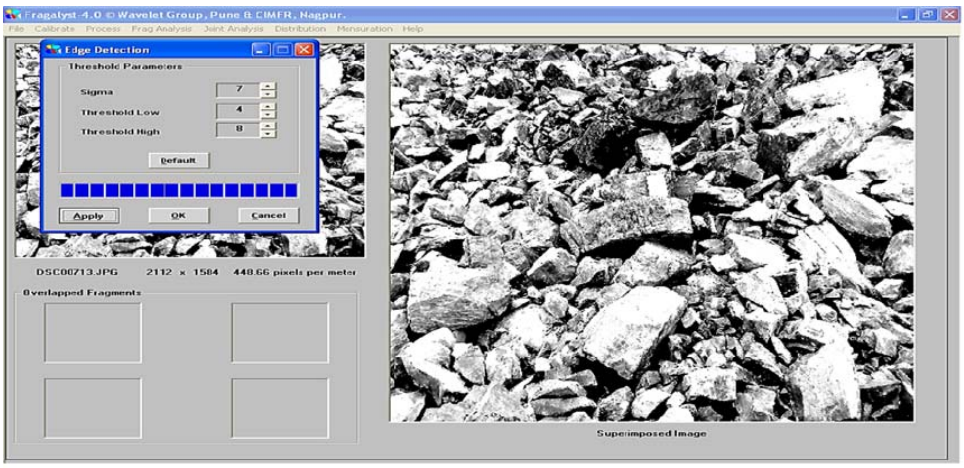

Figure 6 Cumulative size distribution of blasted muck in 'Fragalyst software' (see online version for colours)

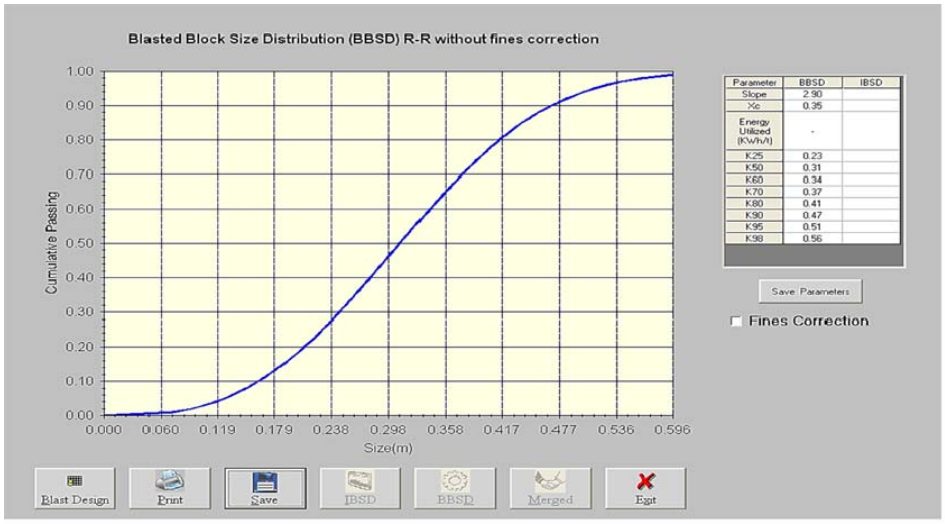

2.3 ANN-based approach to predict flyrock distance and over size fragmentation

Neural network-based technique has been considered to be one of the widely used intelligent tools for simulating complex blasting engineering problems. In this study prediction of flyrock distance and oversize fragmentation, i.e., (+)300 mm fragment size

been attempted simultaneously, using neural network technique. Linear charge concentration, burden, spacing, stemming length or depth of charge burial, depth of blast holes, specific charge, unconfined compressive strength, RQD have been used as input variables. The network has eight input variables and two output variables as shown in Table 2. The neural network has been trained and tested using 120 datasets and validated using 20 datasets generated from blasting in four limestone mines in India (Table 3). Different structures of BPNNs have been attempted with different types of transfer function as shown in Figure 7. Various structures of BPNNs have been evaluated using the performance indices namely root mean square error (RMSE), mean absolute error (MAE) and coefficient of determination (R^2) as discussed in Table 4.

Table 2 Symbols used for blast design and geotechnical data

Parameters used	*Unit*	*Symbol*	*Data range*	*Type of variable*
Charge per hole	kg	Q	17.5–103.2	
Linear charge concentration	kg/m	q_l	8.5–16.7	Input
Depth of blasthole	m	l_{bh}	5–10.5	Input
Burden	m	B	3–4.6	Input
Spacing	m	S_b	4–6.8	Input
Stemming	m	l_s	3–3.6	Input
Specific charge	kg/ton	q	0.07–0.18	Input
Blast hole diameter	mm	d	115–165	
Unconfined compressive strength	MPa	σ_c	58–68	Input
Rock quality designation	%	RQD	55–79	Input
Maximum distance or throw of flyrocks, observed	m	R_f	20–56	Output
Oversize fragmentation (+) 300 mm assessed by Fraglyst	m	$d_{0.3}$	15–31	Output

Table 3 Blast design and geotechnical parameters at various mines

Blast no.	*Name of the mine*	d	Q	q_l	l_{bh}	B	S_b	l_s	q	σ_c	RQD	R_f	$d_{0.3}$
b1	Mehgaon	115	47.22	8.7	8.4	3	5	2.9	0.15	61	60	49	20
b2	Mehgaon	115	47.26	8.7	8.7	3	5	3.1	0.14	61	64	45	21
b3	Mehgaon	115	50.04	8.7	8.9	3	5.2	3	0.14	62	62	45	20
b4	Bamangaon	115	49.37	8.7	9	*3.1*	5.5	3.2	0.12	63	64	42	22
b5	Bamangaon	115	47.26	8.5	9.1	3.5	5.5	3.6	0.11	67	70	30	24
b6	S-K Mine	165	65	16.4	8.3	4.3	6	3.4	0.12	66	62	37	23
b7	S-K Mine	165	67.5	16.4	8.5	4.3	6	3.4	0.12	65	62	38	23
b8	S-K Mine	165	85	16.7	9	4	5.8	3	0.16	60	61	51	20
b9	S-K Mine	165	31.2	16.3	5.5	4.5	5.7	3.7	0.09	67	70	28	29
b10	S-K Mine	165	65.38	16.6	8	4.1	6.1	3.2	0.13	62	60	46	23

Table 3 Blast design and geotechnical parameters at various mines (continued)

Blast no.	*Name of the mine*	*d*	*Q*	q_l	l_{bh}	*B*	S_b	l_s	*q*	σ_c	*RQD*	R_f	$d_{0.3}$
b11	S-K Mine	165	92.07	16.7	9.5	4	6	3	0.16	60	60	49	19
b12	S-K Mine	165	85.14	16.5	9.5	4.2	6.4	3.2	0.13	65	65	41	23
b13	S-K Mine	165	88.76	16.6	9.5	4.1	6.3	3.3	0.14	63	62	43	21
b14	Aditya	115	53.33	8.6	9.7	*4.2*	6.5	3.3	0.08	61	60	29	23
b15	Aditya	115	53.33	8.6	9.5	4	6.4	3.3	0.09	60	62	33	23
b16	Aditya	115	36.16	8.5	8	4.5	6.2	3.5	0.07	61	65	22	26
b17	Aditya	115	55	8.5	10	4.4	6.8	3.5	0.07	62	64	25	25
b18	Kotputli	115	47.72	9	9	3	4.1	3	0.17	62	62	50	18
b19	Kotputli	115	51.04	9	*9.5*	*3*	*4.2*	*3.1*	*0.17*	*62*	*62*	*50*	20
b20	Kotputli	115	51.36	9	*9.5*	*3*	*4.2*	*3.1*	*0.17*	*62*	*63*	*49*	17

2.4 Prediction of blast-induced flyrock and oversize fragmentation by multiple regressions

In order to determine relation between eight input variables with the output variables, MVRA, which performs least squares fit, to solve the dataset.

Figure 7 Transfer functions used in back propagation neural network: (a) Log-Sigmoid function (b) Tan-sigmoid function and (c) Purelin function

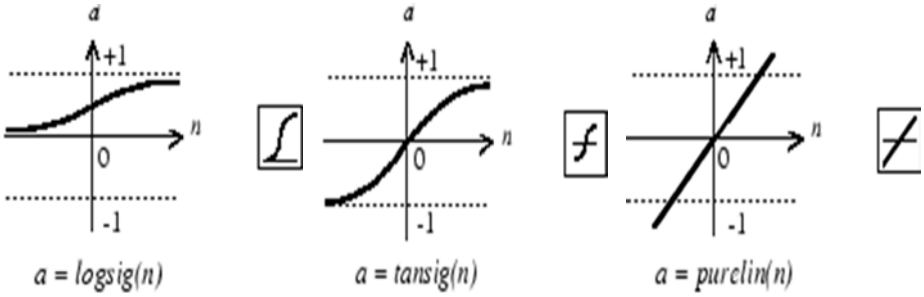

(a) (b) (c)

The MVRA-based equations have been developed separately for flyrock distances and oversize fragmentation. Regression matrix solves the simultaneous equations thus created. MVRA has been done by the same datasets and the same input variables which were used in ANN. Equations (2) and (3) for prediction of flyrock and oversize fragmentation, i.e., fragmentation of (+)300 mm size are as follows:

$$R_f = \frac{10^{4.7} q_l^{0.78} q^{0.24} l_b^{0.18}}{S_b^{0.08} B^{1.3} l_s^{0.3} \sigma_c^{0.91} RQD^{0.78}}, \tag{2}$$

and

$$d_{0.3} = \frac{q_l^{0.04} S_b^{0.2} B^{0.13} l_s^{0.26} \sigma_c^{0.4} RQD^{0.3}}{10^{0.2} l_b^{0.12} q^{0.2}}. \quad (3)$$

Flyrock distances and oversize fragmentation have been predicted by MVRA. The predicted values have been compared with the observed values. The performance indices, namely RMSE, MAE and R^2 of MVRA have been listed in Table 5.

Table 4 Performance indices for various combinations of back propagation neural network

S. No.	Transfer function	ANN structure	R^2 (%)		RMSE (m)		MAE	
			R_f	$d_{0.3}$	R_f, m	$d_{0.3,\%}$	R_f, m	$d_{0.3,\%}$
1	Logsig	6-8-2	82.5	78.8	2.53	1.40	2.35	1.27
2	Logsig	6-10-2	93.6	90.7	2.41	1.42	2.2	1.28
3	Pureline	6-10-2	77.4	78.8	3.3	1.7	2.9	1.54
4	Tansig	6-10-2	85.5	81.7	2.44	1.3	2.3	1.22
5	Logsig	6-8-8-2	94.8	91.8	1.99	1.05	1.67	0.94
6	*Logsig*	*6-10-10-2*	*98.5*	*96.2*	*1.58*	*0.85*	1.47	*0.8*
7	Tansig	6-10-10-2	95.1	92.8	2	1.1	1.88	0.94
8	Logsig	6-12-12-2	94.2	90.1	1.95	1	1.74	0.91

Table 5 Performance indices of multiple regression

S. No	Performance index	R_f	$d_{0.3}$
1	RMSE	2.21 m	1.3%
2	MAE	2.03 m	1.22%
3	R^2	0.81	0.77

RMSE is root mean square error; MAE is mean absolute error; R^2 is coefficient of determination; R_f is flyrock distance and $d_{0.3}$ is weight percent passing greater than 300 mm size.

3 Results and discussion

A comparative assessment of different types of structures of BPNN has been shown in Table 4 which indicates the BPNN with two hidden layers, 10 neurons in each of the hidden layers and log-sigmoidal transfer function has been found excellent combination for simultaneous prediction of flyrock distance and over size fragmentation (Figure 8). The predictions have also been made using MVRA. The performance indices of MVRA have been listed in Table 5. The Predictability of BPNN and MVRA has been assessed which conforms the superiority of BPNN. Using the best combination of BPNN, RMSE was as low as 1.58 m for flyrock distance and 0.85% for prediction of oversize fragmentation, i.e., (+)300 mm fragment size. Similarly, MAE was as low as 1.47 m for prediction of flyrock distance and 0.80% for prediction of (+)300 mm fragmentation.

Blast wise deviations of observed and predicted flyrock distance as well as observed and predicted oversize fragmentation have been shown in Figures 9 and 10. The Coefficient of determination (R^2) is as high as 0.985 in case of prediction of flyrock distance and 0.962 in case of prediction of oversized fragmentation. It is evident that there is a very good correlation between observed data and predicted values of flyrock distances and oversize fragmentation.

Figure 8 Structure of back propagation neural network with two hidden layers (see online version for colours)

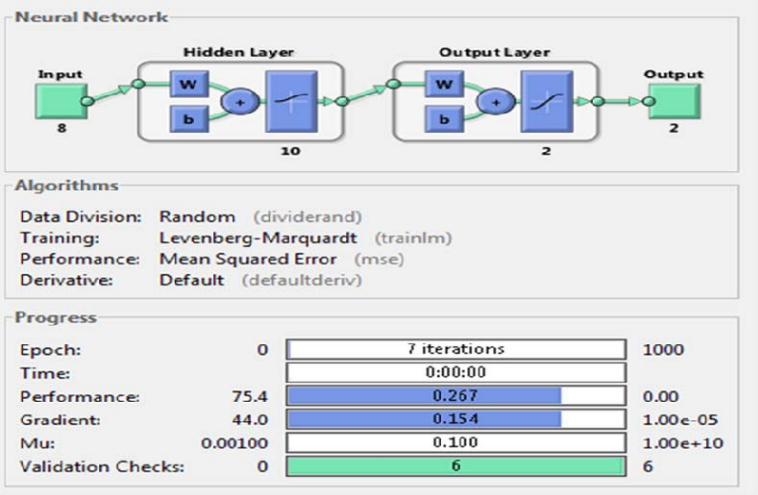

Figure 9 Observed and predicted flyrock distances for various blasts in mines

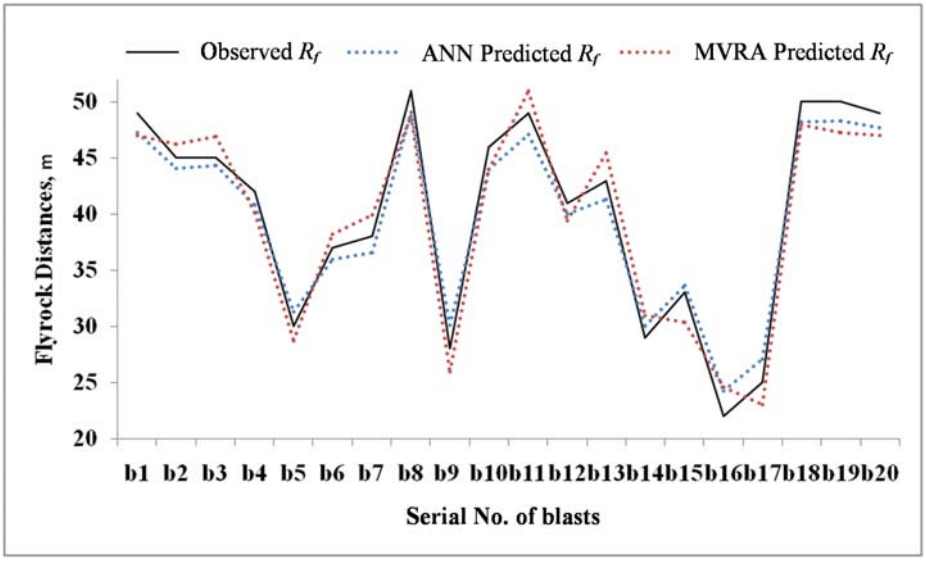

Figure 10 Observed and predicted oversize fragmentation for various blasts in mines (see online version for colours)

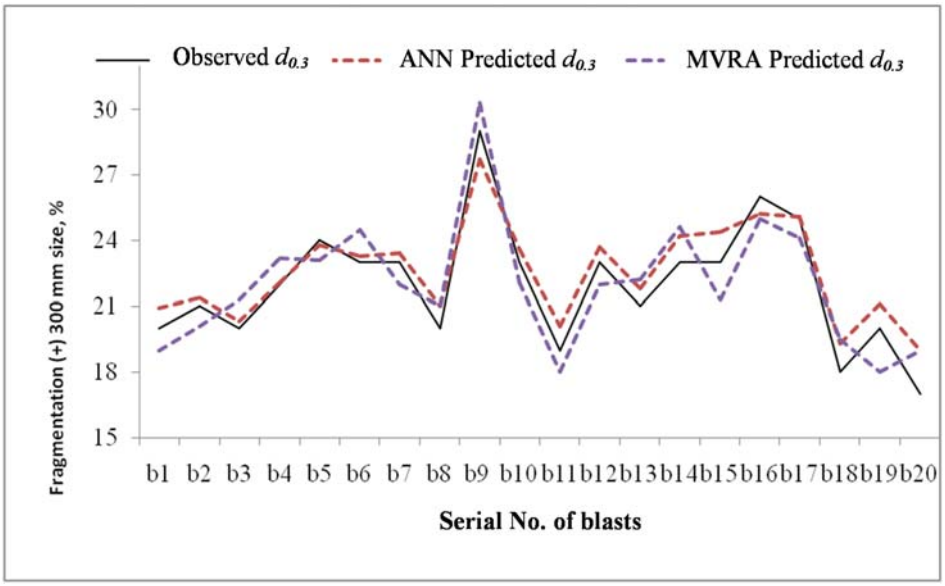

3.1 Sensitivity analysis using cosine amplitude method

In order to know the relative importance of an input variable on flyrock distance or oversize fragmentation, sensitivity analysis has been performed. Cosine amplitude method (CAM) was used for sensitivity analysis of each of the eight input variables with respect to flyrock distance and oversize fragmentation. In this method, the magnitude of sensitivity of each eight input variables is assigned by establishing the strength of the relationship (r_{ij}) between an input variable with respect to an output variable and input variable. The larger the value of r_{ij} the greater is the effect of corresponding input variable on output variable. The value of r_{ij} varies from (–1) to (1). The sign positive or negative indicates the nature of correlation between the input variable and output variable. The sensitivity analysis was performed for flyrock distance and oversize fragmentation, i.e., (+)300 mm fragmentation separately for all the eight input variables namely linear charge concentration, burden, spacing, depth of blast holes, stemming, specific charge, unconfined compressive strength and RQD. The results have been shown in Figures 11 and 12. Linear charge concentration and specific charge have positive correlation with flyrock distance, whereas burden, spacing, depth of blast hole, stemming, unconfined compressive strength and RQD have negative correlation with the flyrock distance Similarly, linear charge concentration and specific charge have negative correlation with oversize fragmentation, whereas burden, spacing, depth of blast hole, stemming, unconfined compressive strength and RQD have positive correlation with the oversize fragmentation.

Figure 11 Relative impact of input variables on flyrock distance (see online version for colours)

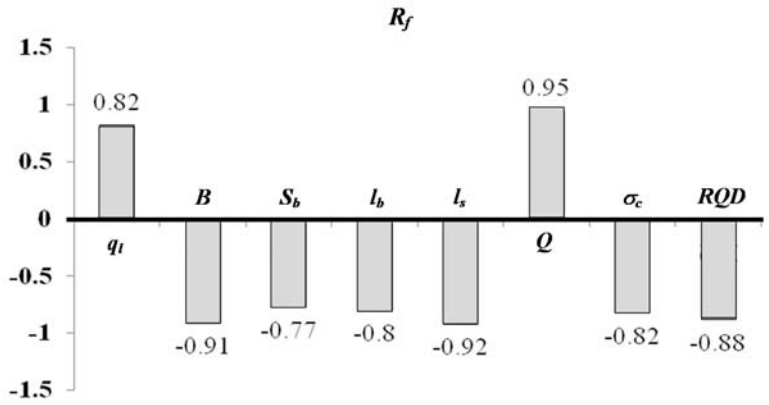

Figure 12 Relative impact of input variables on fragment size of (+)300 mm size (see online version for colours)

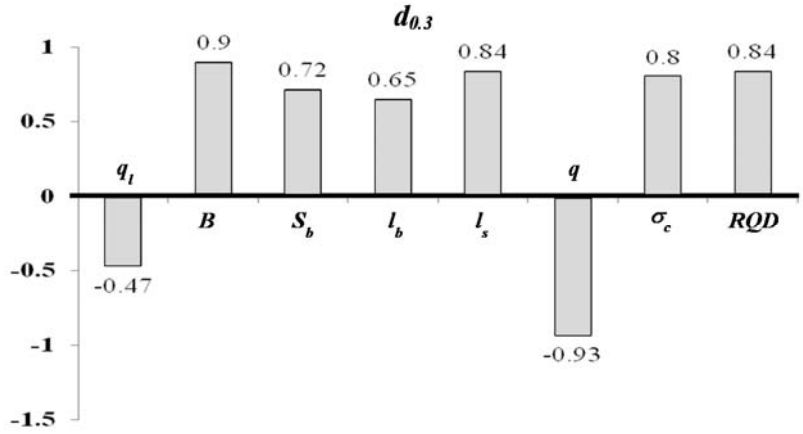

4 Conclusions

Back propagation neural network with two hidden layers has been found most suitable data fitting tool in simultaneous prediction of flyrock distance and oversize fragmentation when compared with multiple regression analysis. Low RMSE and MAE values with better correlation between observed and predicted data as seen in case of BPNN prove the excellence of neural network in prediction of engineering blasting problems in mines. Among the various blast design and geotechnical variables, eight variables namely linear charge concentration, burden, spacing, depth of blast holes, stemming, specific charge, unconfined compressive strength, RQD have been selected as the critically significant variables in predictive problem under the study. Linear charge concentration and specific charge bear positive correlation with flyrock distance and negative correlation

with oversize fragmentation, whereas burden, spacing, depth of blast hole, stemming, unconfined compressive strength and RQD have negative correlation with the flyrock distance and positive correlation with the oversize fragmentation.

References

Bajpayee, T.S., Rehak, T.R., Mowrey, G.L. and Ingram, D.K. (2002) 'A summary of fatal accidents due to flyrock and lack of blast area security in surface mining, 1989–1999', *Proceedings of the* 28*th Annual Conference on Explosives and Blasting Technique*, Las Vegas, pp.105–118.

Bajpayee, T.S., Rehak, T.R., Mowrey, G.L. and Ingram, D.K. (2004) 'Blasting injuries in surface mining with emphasis on flyrock and blast area security', *J. Safety Res.*, Vol. 35, pp.47–57.

Bhandari, S. (1997) *Engineering Rock Blasting Operations*, Balkema, Rotterdam, pp.315–322.

Chiappetta, R.F. and Mammele, M.E. (1987) 'Analytical high-speed photography to evaluate air-decks, stemming retention and gas confinement in pre-splitting reclamation and grossmotion studies', *Proceedings of the Second International Symposium on Rock Fragmentation by Blasting*, Society for Experimental Mechanics, Bethel, CT, USA, pp.257–301.

Cunningham, C.V.B. (1983) 'The Kuz–Ram model for prediction of fragmentation from blasting', *Proceedings of the 1st International Symposium on Rock Fragmentation by Blasting*, Lulea, Sweden, pp.439–453.

Cunningham, C.V.B. (1987) 'Fragmentation estimations and Kuz–Ram model-four years on', *Proceedings of the* 2*nd International Symposium on Rock Fragmentation by Blasting*, Keystone, Colo, pp.475–487.

Fletcher, L.R. and Andrea, D.V. (1986) 'Control of flyrock in blasting', *Proceedings of the* 12*th Annual Conference on Explosives and Blasting Technique*, International Society of Explosives Engineers, Cleveland, pp.167–177.

Hagan, T.N. (1973) 'Rock breakage by explosives', *Proceedings of the National Symposium on Rock Fragmentation*, Adelaide, pp.1–17.

Hagan, T.N. (1983) 'The influence of controllable blast parameters on fragmentation and mining cost', *Proc. 1st Int. Symp. Rock Fragmentation by Blasting, Lulea*, Sweden, pp.31–33.

IME (1997) *Glossary of Commercial Explosives Industry Terms*, Safety Publication, No. 12, Institute of Makers of Explosives, Washington DC, p.16.

Khandelwal, M. and Singh, T.N. (2007) 'Evaluation of blast-induced ground vibration predictors', *Soil Dynam. Earthq. Engg.*, Vol. 27, pp.116–125.

Kulatilake, P.H.S.W., Qiong, W., Hudaverdi, T. and Kuzu, C. (2010) 'Mean particle size prediction in rock blast fragmentation using neural networks', *Eng. Geol.*, Vol. 114, Nos. 3–4, pp.298–311.

Kuznetsov, V.M. (1973)'The mean diameter of fragments formed by blasting rock', *J. Min. Sci.*, Vol. 9, pp.144–148.

Lawrence, J.D., William, H.L. and Janet, S.S. (2002) 'Environmentalism and natural aggregate mining', *Nat. Resour. Res.*, Vol. 11, No. 1, pp.19–28.

Lundborg, N., Persson, A., Ladegaard-Pedersen, A.and Holmberg, R. (1975) 'Keeping the lid on flyrock in open-pit blasting', *Eng. Min. J.*, Vol. 176, pp.95–100.

Monjezi, M., Khoshalan, H.A. and Varjani, A.Y. (2011) 'Optimization of open pit blast parameters using genetic algorithm', *International Journal of Rock Mechanics and Mining Sciences*, Vol. 48, No. 5, pp.864–869.

Monjezi, M., Bahrami, A. and Yazdian, V. (2010) 'A simultaneous prediction of fragmentation and flyrock in blasting operation using artificial neural networks', *Int. J. Rock Mech. Min. Sci.*, Vol. 47, pp.476–80.

Moxon, N.T., Mead, D. and Richardson, S.B. (1993) 'Air-decked blasting techniques: some collaborative experiments', *Trans Inst. Min. Metall*, *(Sec. A: Mining Industry)*, Vol. 102, pp.A25–A30.

Parihar, C.P. and Bhandari, S. (2012) 'Improving blasting operations using data management and analysis', in Singh, P.K. and Sinha, A. (Eds.): *Proceedings of International Conference on Rock Fragmentation by Blasting, Fragblast 10*, Delhi, India, pp.405–409.

Persson, P., Holmberg, R. and Lee, J. (1984) *Rock Blasting and Explosives Engineering*, CRC Press, New York.

Raina, A.K., Soni, A.K. and Murthy, V.M.S.R. (2012) 'Spatial distribution of flyrock using EDA: an insight from concrete model tests', *Proceedings of the 10th Intl. Symp. Rock Fragmentation by Blasting*, 26–29, November, New Delhi, India, pp.563–570.

Rehak, T.R., Bajpayee, T.S., Mowrey, G.L. and Ingram, D.K. (2001) 'Flyrock issues in blasting', *Proceedings of the 27th Annual Conference on Explosives and Blasting Technique, Vol. I, International Society of Explosives Engineers*, Cleveland, pp.165–175.

Remennikov, A.M. and Mendis, P.A. (2006) 'Prediction of airblast loads in complex environments using artificial neural networks', *WIT Trans. on the Built Environ.*, Vol. 87, pp.269–278.

Richards, A.B. and Moore, A.J. (2004) 'Flyrock control: by chance or design', *Proceedings of 30th ISEE Conference on Explosives and Blasting Technique*, New Orleans, Vol. I, pp.335–348.

Sharma, S.K. and Rai, P. (2015) 'Investigation of crushed aggregate as stemming material in bench blasting: a case study', *Geotechnical and Geological Engineering*, Vol. 33, No. 6, pp.1449–1463.

Shea, C.W. and Clark, D. (1998) 'Avoiding tragedy: lessons to be learned from a flyrock fatality', *Coal Age*, Vol. 103, No. 2, pp.51–54.

Singh, D.P. and Sastry, V.R. (1986) 'Rock fragmentation by blasting influence of joint filling material', *Journal of Explosive Engineering*, pp.18–27.

Singh, D.P., Singh, T.N. and Goyal, M. (1994) 'Ground vibration due to blasting and its effect', in Pradhan, G.K. and Hota, J.K. (Eds.): *Enviromin.*, Bhubaneshwar, India, pp.287–293.

Siskind, D.E. and Kopp, J.W. (1995) 'Blasting accidents in mines: a 16 year summary', *Proceedings of the 21st Annual Conference on Explosives and Blasting Technique, International Society of Explosives Engineers*, Cleveland, pp.224–239.

Tang, H., Shi, Y., Li, H., Li, J., Wang, X. and Jiang, P. (2007) 'Prediction of peak velocity of blasting vibration based on neural network', *Chinese J. Rock Mech and Engg.*, Vol. 26, Suppl. 1, pp.3533–3539.

Tawadrous, A.S. and Katsabanis, P.D. (2007) 'Prediction of surface crown pillar stability using artificial neural networks', *International J. Numerical Analytical Methods Geomech*., Vol. 31, No. 7, pp.917–931.

Tawadrous, A.S. (2006) 'Evaluation of artificial neural networks as a reliable tool in blast design', *Int. Soc. Explos. Engg.*, Vol. 1, pp.1–12.

Tawadrous, A.S. and. Katsabanis, P.D. (2005) 'Prediction of surface blast patterns in limestone quarries using artificial neural networks', *Fragblast*, Vol. 9, No. 4, pp.233–242.

Trivedi, R. and Singh, T.N. (2014) 'Impact of blast design parameters on blast induced flyrocks–A case study', *Proceedings of Int. Conf. on Environmental Management and Practices in Mining and Allied Industries*', IIT-BHU, Varanasi, pp.607–622.

Trivedi, R., Singh, T.N. and Gupta, N. (2015) 'Prediction of blast-induced flyrock in opencast mines using ANN and ANFIS', *Geotechnical and Geological Engineering*, Vol. 33, No. 4, pp.875–891.

Verakis, H.C. and Lobb, T.E. (2003) 'An analysis of blasting accidents in mining operations', *Proceedings of 29th Annual Conference Explosives and Blasting Technique, International Society of Explosives Engineers*, Cleveland, Vol. 2, pp.119–129.

Wharton, R.K., Formby, S.A. and Merrifield, R. (2000) 'Airblast TNT equivalence for a range of commercial blasting explosives', *J. Hazard Mater.*, Vol. A79, pp.31–39.

Wiss, J.F. and Linehan, P.W. (1978) *Control of Vibration and Air Noise from Surface Coal Mines–III*', Report No. OFR 103(3) – 79, Bureau of Mines, US, pp.623.

Workman, J.L. and Calder, P.N. (1994) 'Flyrock prediction and control in surface mine blasting', *Proceedings of 20th Conf.* on *Explosives and Blasting Technique*, Austin, Texas, pp.59–74.

Reclamation and rehabilitation of waste dump by eco-restoration techniques at Thakurani iron ore mines in Odisha

Vibhash Ranjan*

Thakurani Iron Ore Mines of M/s Sarda Mines (P) Limited,
Soyabali, Barbil,
Keonjhar, Odisha, 758035, India
Email: vibhash.ranjan@sardamines.net
Email: yes_raj2001@yahoo.com
*Corresponding author

Phalguni Sen and Dheeraj Kumar

Department of Mining Engineering,
Indian School of mines,
Dhanbad, 826004, India
Email: dheeraj@dkumar.org
Email: phalgunisen@yahoo.co.in

Brijbir Singh

BSc (Agriculture)-Meerut University,
Thakurani Iron Ore Mines of M/s Sarda Mines (P) Limited,
Soyabali, Barbil,
Keonjhar, Odisha, 758035, India
Email: brijbir@sardamines.net

Abstract: Excavation of minerals by way of mining activities escalates generation of waste dumps in iron ore mines. For benefit of the society and generations to come, the ecological services of the denuded areas need to be established by eco-restoration technology. Based on the Miyawaki application, a field experiment was taken in the Thakurani iron ore mines in Odisha. The results obtained after 1 and 3 years were very impressive and plant biodiversity appeared to be very high when compared with the traditional reforestation techniques. The aim of Miyawaki plantation technique is 'survival at fittest' based on the area undergone such plantation have an ecology of their own. The local species are more preferable to other species because they are most likely to fit into an ecosystem and are quickly climatically adapted. The survival rate of local species has been improved from 72% to 87% when compared with traditional reforestation techniques.

Keywords: ecological restoration; local species; Miyawaki method of plantation; rehabilitation; waste dump.

Reference to this paper should be made as follows: Ranjan, V., Sen, P., Kumar, D. and Singh, B. (2016) 'Reclamation and rehabilitation of waste dump by eco-restoration techniques at Thakurani iron ore mines in Odisha', *Int. J. Mining and Mineral Engineering*, Vol. 7, No. 3, pp.253–264.

Biographical notes: Vibhash Ranjan is a Mining Engineer, PhD candidate at the Department of Mining Engineering, Indian School of Mines, Dhanbad, India.

Phalguni Sen is a Mining Engineering Professor and HOD at the Department of Mining Engineering, Indian School of Mines, Dhanbad, India.

Dheeraj Kumar is a Mining Engineering Professor at the Department of Mining Engineering, Indian School of Mines, Dhanbad, India.

Brijbir Singh is working as Manager, Horticulture at Thakurani Iron Ore Mines of M/s Sarda Mines (P) Limited, Barbil (Odisha), India.

1 Introduction

Mining has a significant negative impact upon the environment due to its nature; especially, opencast mining inevitably leads to degradation on ecological as well as aesthetic values of the landscape. The topography, drainage, air, soil and water quality, vegetation including forest ecosystems, noise levels and ground vibrations, human health and habitation have been listed as the typical parameters that are mainly affected due to opencast mining activities. When the extraction of iron ore reserve is over, the altered landscape due to mining has to be reclaimed scientifically in order to relieve the environmental effects of opencast mining and restore the landscape by rehabilitation (Kuter, 2011).

The issues relating to the reclamation and rehabilitation of waste dump is drawing attention world over. In India, the government bodies such as State Pollution Control Boards, Ministry of Environment and Forest (MoEF), Department of Mines and Geology, etc. have raised their concern by way of framing of specified rules and regulations and making it mandatory for all mines (Ranjan and Kumar, 2015).

The global climatic changes, together with recent rapid industrialisation, have been the main anthropogenic effects worldwide in destroying the natural environments and subsequently increasing the risk of desertification. Miyawaki (1981) suggests for performing more environmental conservation activity by the scientific manner of reclamation and rehabilitation as well as using innovative environmental recovery activities. During the last two decades, scientists have developed new insights both in theoretical as well as in practical actions for restoration along with reconstruction of natural ecosystems (Clewell and Aronson, 2007; Falk et al., 2006; Jordan et al., 1987; Perrow and Davy, 2002a, 2002b).

The eastern region of the country is rich in minerals. Open pit mining is comparatively safe, easy and economically, the environmental implications are much more significant in cluster area as these operations generate high level of cumulative impact on land and affect environmental settings. The Ministry of Environment and Forests imposes stipulations for reclamation and re-vegetation of area degraded due to mining operations such as

- proper stacking and protection of top soil for use in reclamation and rehabilitation of mined out areas
- back filling of the mined out areas and reclamation by plantation/afforestation
- plantation in external over burden (OB) and backfilled areas by local (host) species (Upadhyay, 2012).

Eco-restoration of mine OB or abandoned mine sites is a major environment concern (Dowarah et al., 2009).

Clements (1916) observed that, in a natural forest cycle, the annual plants on degraded land like waste dump area were succeeded by perennial grass, shrubs, light-demanding, fast-growing trees and finally natural forests. The climax vegetation could be formed after two centuries or more (Connell and Slatyer, 1977; Figure 1(a)). In the current scenario, most forest reforestation programs adopt a scheme of planting one or more early successional species after complete successful establishment. They are gradually replaced by intermediate species (either naturally or by planting), until late successional species arise.

Figure 1 Successional stages as would follow in natural conditions. (a) and (b) adopting traditional reforestation methods and (c) the Miyawaki method

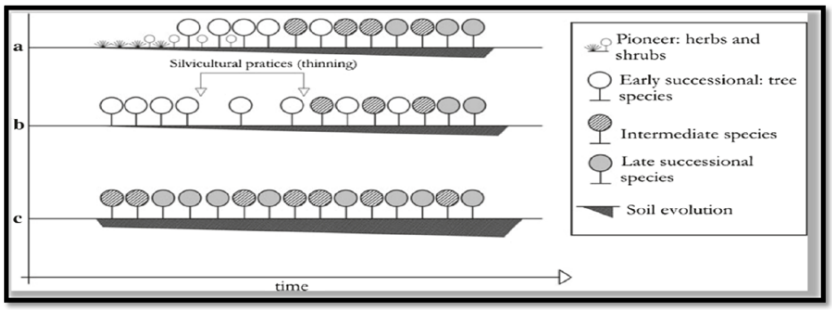

Source: Schirone et al. (2011)

There exists a reliable forest restoration method (native forests by native species) based on the vegetation – ecological theories as proposed by Prof. Akira Miyawaki and applied first in Japan (Miyawaki, 1993a, 1993b, 1996, 1998a, 1998b, 1999; Padilla and Pugnaire, 2006). According to Miyawaki method, restoring native green environments, multilayer forests and natural biocoenosis is possible, and well-developed ecosystems can be quickly established because of the simultaneous use of intermediate and late successional species in plantations (Figure 1(c)).

The Miyawaki method involves surveying of the potential natural vegetation of the area to be reforested and recovering topsoil to a depth of 20–30 cm by mixing the soil and compost from organic materials, such as leaves and mowed grass etc. In this way, the time of the natural process of soil evolution will be reduced by established the vegetational succession itself.

Based on the application of Eco-restoration technology like – Miyawaki method of plantation, a field experiment was taken in Thakurani Iron Ore Mines of M/s Sarda Mines (P) Limited within the Odisha State in India.

2 Material and methodology

2.1 Study area

The Thakurani Iron Ore Mines of M/s Sarda Mines (P) Limited is a large capacity mine within the Odisha state in India and carrying out mining activity since 2001. The mine is located in parts of Sayabali and Balita villages and adjoining reserve forest of Champua Range, Keonjhar Forest Division. Figures 2 and 3 depict the topographic view of the Thakurani Iron ore Mines and location for implementation of Miyawaki method of plantation.

Figure 2 Topographic view of Thakurani Iron Ore Mines, Block-B of Sarda Mines (P) Ltd., Barbil (see online version for colours)

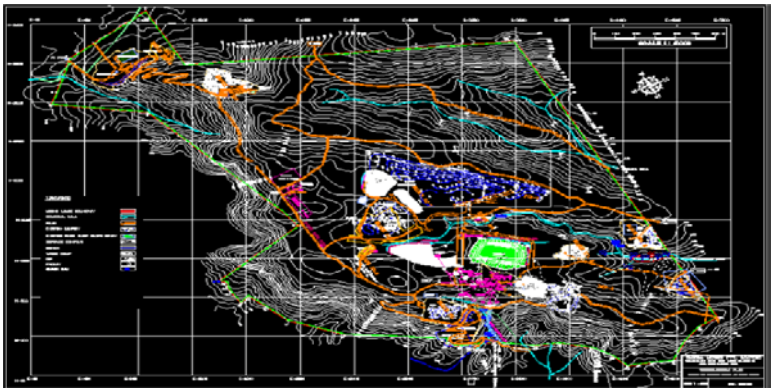

Figure 3 Site location for implementation of Miyawaki method of plantation (see online version for colours)

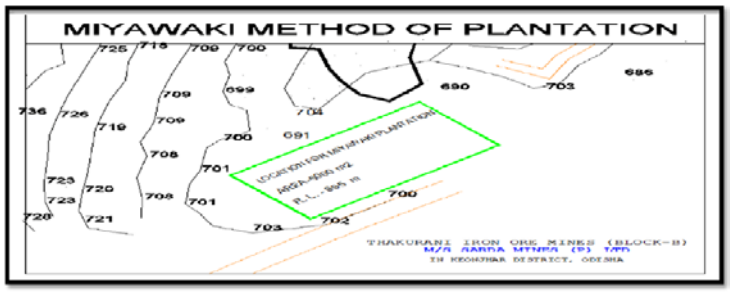

To test the Miyawaki method of plantation, an experimental plot area of 5000 m^2 was established during the month of July 2011 at the Thakurani iron ore mines of M/s Sarda mines (P) Limited closed to active OB dump at 695 RL. This has been shown in Figure 3.

2.2 Selection of local (host) species for Miyawaki method

Before selecting the species for plantation on selected site, an assessment was carried out to find out the potential natural species of the area and within the region of Odisha state. Across the site, local (host) species on the basis of examination of environmental Impact

Assessment report of projects were screened for plantation. The list of the recommended species is given in Table 1 (Upadhyay, 2012).

Table 1 Recommended local (host) species for Miyawaki plantation

S. No.	*Botanical name*	*Common name*
1	Acacia	Babul
2	Acacia Catechu	Khaira
3	HaldiniaCordifolia	Kurum
4	AegleMarmelas	Bei
5	AlbiziaLebbeck	Siriso
6	AlbiziaProcera	Garkhair/Tentra
7	AnogeissusLatifolia	Dohu
8	AnthocephalusChinensis	Kadamba
9	ArtocarpusHeterophyllus	Panasa
10	AzadirachtaIndica	Neem
11	Bauhinia Veriegata	Kanchana
12	BombaxCeiba	Simuli
13	BambusaTulda	Bamboo/Baunsha
14	BrideliaRetusa	Kasi
15	BuchananiaLanzan	Char
16	ButeaMonosperma	Palas/Palash
17	CareyaArborea	Kumbhi
18	Cassia Fistula	Sumari
19	ChloroxylonSwietiana	Bheru
20	CleistanthusCollinus	Karada
21	Crateva Magna	Baruna
22	DalbergiaSissoo	Sissoo
23	FicusRacemosa	Dimiri
24	DendrocalamusStrictus	Banso
25	DiospyrosMelanoxylon	Tendo/Kendu
26	PhyllanthusEmblica	Anola
27	ErythrinaVariegata	Paladhua
28	FicusBenghalensis	Banyan/Baro
29	FicusReligiosa	Pipal/Aswatta
30	CeriscoidesTurgida	Kurdu
31	GmelinaArborea	Gambari
32	GrewiaTiliifolia	Dhamuro/Dharman
33	HolarrhenaPubescens	Kurei/Kurchi
34	Lagerstroemia Parviflora	Sidha
35	LanneaCoromandelica	Moi/Mai
36	MadhucaIndica	Mhua/Mahula

Table 1 Recommended local (host) species for Miyawaki plantation (continued)

S. No.	*Botanical name*	*Common name*
37	MangiferaIndica	Aam/Amba
38	MitragynaParvifolia	GuriKoima/GudiKaima
39	Phoenix Sylvestris	Khajuri
40	PonganuaPinnata	Karanjo/Karanj
41	PlerocarpusMarsupium	Piasai
42	PlerospermumAcerifolium	Muchukund/Kanaka Chmpa
43	SaracaAsoca	Ashok
44	SchleicheraOleosa	Kusuma/Kusum
45	Anacardium	Bhalia
46	Shorea Robusta	Sal
47	SyzgiumCumini	Jamu
48	TectonaGrandis	Teak/Sagwan
49	TerminaliaArjuna	Arjuna
50	TerminaliaBellirica	Bahada
51	TerminaliaChebula	Harida
52	TerminaliaAlata	Asan
53	WoodfordiaFruticosa	Dhatki/Dhatuki

Source: Upadhyay (2012)

2.3 Methodology adopted for Miyawaki plantation

Excavation of minerals by way of mining activities escalates generation of degraded land. For benefit of the society and generations to come, the ecological services of the denuded areas need to be established at a faster rate. Twenty-five types of local (host) species from the recommended list of species have been planted over the degraded land (waste dumps area in opencast mining). The details are represented in Figure 4.

Figure 4 Number of local (host) species planted over the degraded land in the month of July'2011 (see online version for colours)

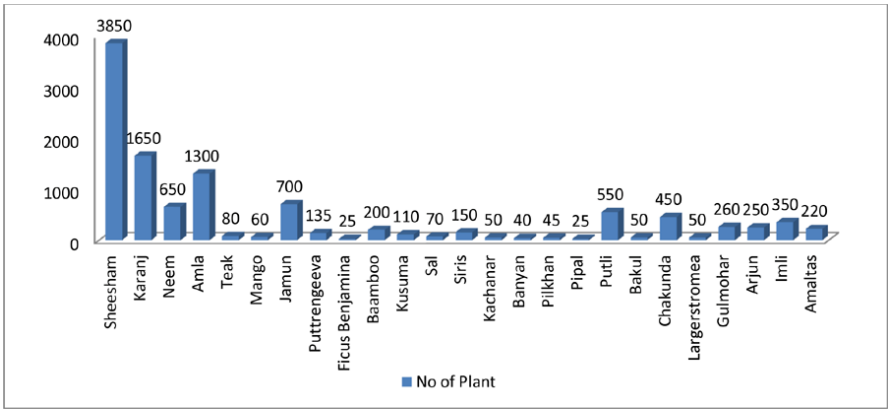

The following procedure was adopted during the Miyawaki plantation at the selected site.

1 After the complete extraction of iron ore, the same area was backfilled with waste for the purpose of reclamation as per guideline of Indian Bureau of Mines. Figure 5 shows the back filling with waste material.

2 After reclamation of selected site, the top soil up to 30–50 cm was spread over the degraded land for maintaining proper slope to avoid waster logging problems.

3 The selected site was kept for proper exposure of sunlight for 2 months.

4 One layer of ~2 inch cow dung was spread over the top soil of degraded land.

5 Selection of species was done by keeping in mind matching with the surrounding eco-system and fulfilling the need of wild life and local human population.

6 The species was selected from the list of the recommended species in above-mentioned table.

7 In this Miyawaki Plantation, there was no need of digging or trench/pit for planting the seedling. The seedlings were planted within 60 cm of the surface of the soil and the size of the pit was just little more than size of the seedling pot.

8 A small water container/pool was used for submerging the seedling pot into the water before removing the seedling from the pot and planted in the selected site.

9 After the plantation, the paddy straw was spread thickly and tied by jute rope from one corner to the other diagonally to ensure that the paddy straw was not windblown.

10 The seedling density was maintained 2–3 seedling per square metre area for the selected site.

11 Regular watering arrangement was ensured for first 6 months after the plantation.

Figure 5 Back filling with waste generated during mining and are being table topped with top soil before rainy season (see online version for colours)

3 Analysis and results

11,320 numbers of local (host) species were planted over the degraded land. Figure 6 shows the Miyawaki plantation at Thakurani iron ore mines of M/s Sarda Mines (P) Limited. To know the effectiveness of Miyawaki method, it was required to find out the growth and survival rate of different selected local (host) species over the degraded lend during the span of three years. Five numbers of each 11 types of local (host) species were selected as random samples and tagged by red tape to measure the growth of species with

respect to height and periphery (diameter of stem at height of 1 feet from the ground) as well as their survival rate. Figures 7 and 8 show the growth of local species with respect to height and periphery. Figure 9 presents the survival rate of Miyawaki plantation after 1 and 3 years as well as Figure11 shows the succession stage of Miyawaki method of plantation of waste dump during the year 2011–2014.

Past 3 years data (shown in Table 2) were collected as samples to study the survival rate of Conventional method of plantation Miyawaki method of plantation implemented at Thakurani iron Ore Mines of M/s Sarda Mines (P).

A comparison of conventional method of plantation and Miyawaki method of plantation (survival rate) is shown in Figure 10.

Figure 6 Miyawaki plantation at Thakurani iron ore mines of M/s Sarda Mines (P) Limited

Figure 7 Growth of local (host) species with respect to height (see online version for colours)

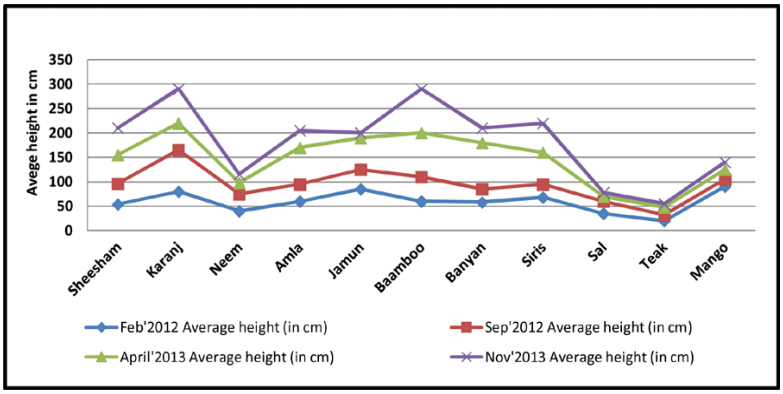

Figure 8 Growth of local (host) species with respect to Periphery (see online version for colours)

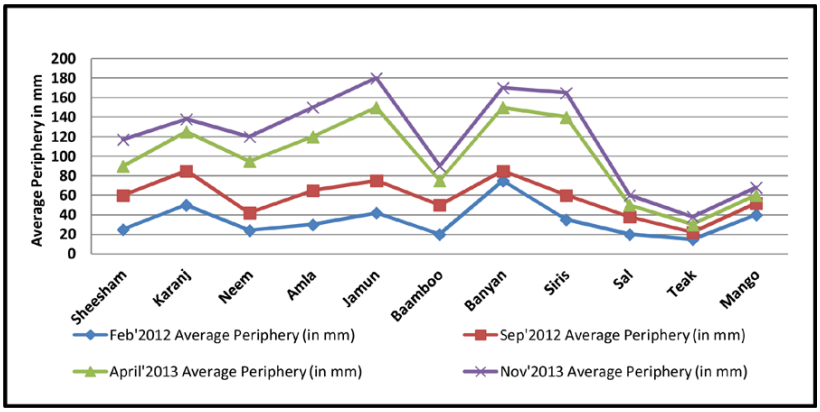

Figure 9 Survival rate of Miyawaki plantation after 1 and 3 years (see online version for colours)

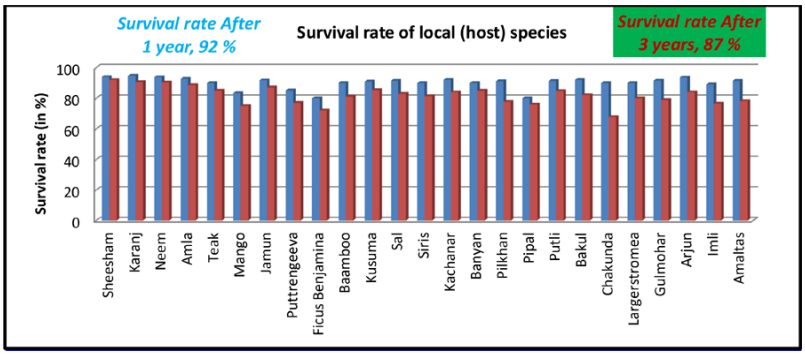

Figure 10 Comparison of survival rate of conventional method of plantation by Miyawaki method (see online version for colours)

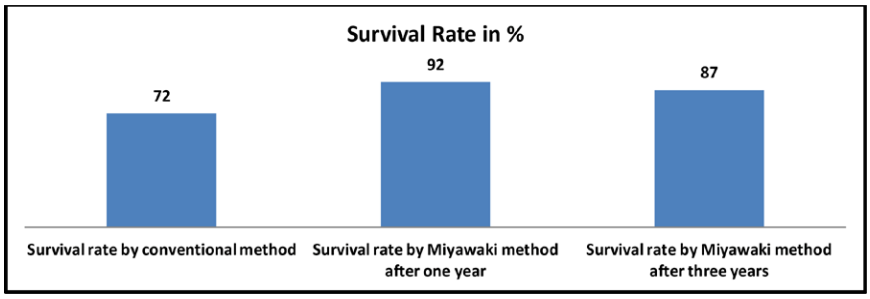

Table 2 Survival rate of plantation by conventional method (%)

2012–2013	73
2013–2014	71
2014–2015	72
Average rate	72

Figure 11 Shows the succession stage of Miyawaki Method of plantation of waste dump during the year 2011–2014

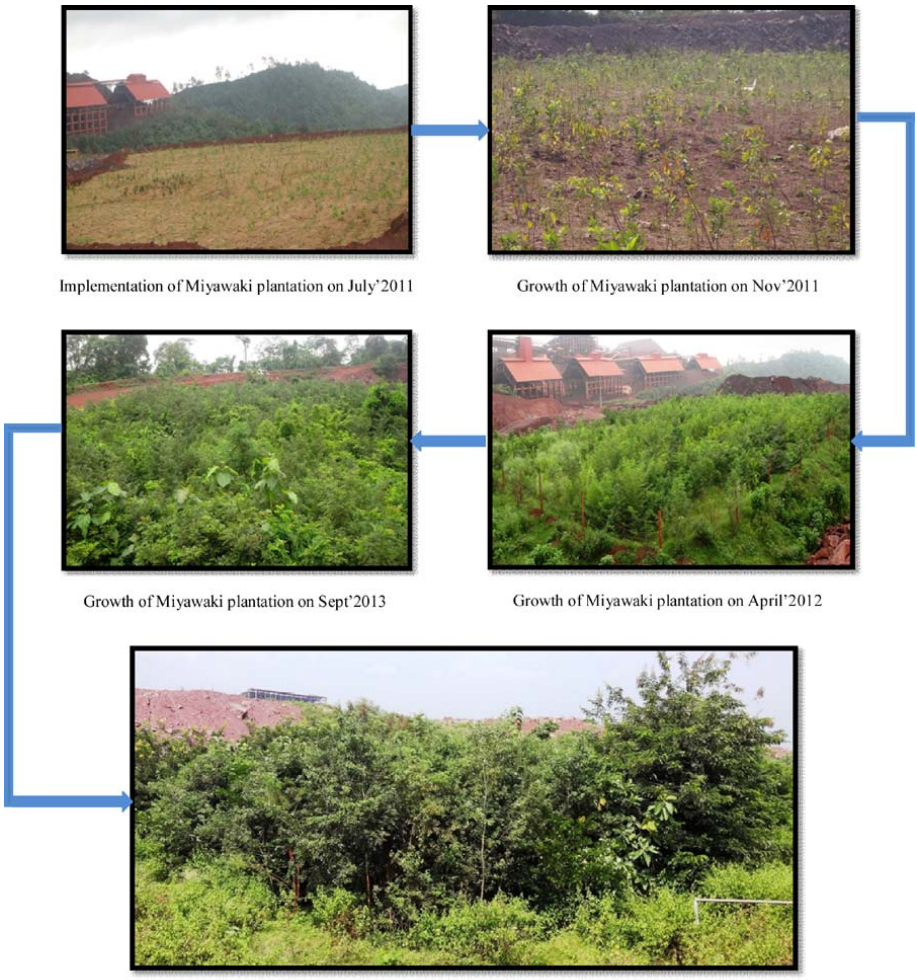

4 Conclusion

Reclamation and rehabilitation of waste dump area using eco-restoration technology is very critical and sensitive issue for any mining project. Mining industry has social responsibility and obligations to all people living in the region. Rehabilitation of any degraded land and waste dumps should aim at a self-sustaining ecosystem and as a social asset and sustainable livelihood source for the local community.

A unique technique in ecology-based reforestation, i.e., Miyawaki method has resulted into more effective reforestation approach adopting naturalistic theoretical principles in reclamation and rehabilitation of waste dumps in an Iron ore mines in Odisha, India. The results obtained after 1st and 3rd years were impressive with increased plant biodiversity when compared with the traditional reforestation techniques. It was

further observed that the survival rate of local (host) species by Miyawaki method of plantation was near about 87% after 3rd year of plantation when compared with traditional method of plantation where the survival rate was around 72%. The analytical results showed a more rapid development of trees in the Miyawaki plots, in particular, early successional species. The benefits over the traditional method of plantation methods are remarkable and comparable with those obtained by a specific unique technique, i.e., Miyawaki in Thakurani Iron Ore Mines of M/s Sarda Mines (P) Limited.

References

Clements, F.E. (1916) *Plant Succession: An Analysis of the Development of Vegetation, Vol. 242*, Carnegie Institution of Washington, Washington, pp.1–512.

Clewell, A.F. and Aronson, J. (2007) *Ecological Restoration: Principles, Values, and Structure of an Emerging Profession*, Island Press, Washington DC.

Connell, J.H. and Slatyer, R.O. (1977) 'Mechanisms of succession in natural communities and their role in community stability and organization', *The American Naturalist*, Vol. 111, No. 982. November–December, pp.1119–1144.

Dowarah, J., Deka Boruah, H.P., Gogoi, J., Pathak, N., Saikia, N. and Handique, A.K. (2009) 'Eco-restoration of a high-sulphur coal mine overburden dumping site in Northeast India: a case study', *J. Earth Syst. Sci.*, Vol. 118, No. 5, October, pp.597–608.

Falk, D.A., Palmer, M.A. and Zedier, I.B. (2006) *Foundations of Restoration Ecology*, Island Press, Washington DC.

Jordan, W.R., Gilpin, M.E. and Aber, J.D. (1987) *Restoration Ecology*, Cambridge University Press, Cambridge.

Kuter, N. (2011) *Reclamation of Degraded Landscapes Due to Opencast Mining, Advances in Landscape Architecture*, Dr. Murat Ozyavuz (Ed.), InTech, DOI: 10.5772/55796, Available from: http://www.intechopen.com/books/advances-in-landscape-architecture/reclamation-of-degraded-landscapes-due-to-opencast-mining

Miyawaki A (1996) 'Restoration of biodiversity in urban and periurban environments with native forest', in de Castri, F. and Younes, T. (Eds.): *Biodiversity, Science and Development*, CAB International, Wallingford, pp.558–565.

Miyawaki, A. (1981) 'Energy policy and green environment on the base of ecology', in Fazzolage, R.A. and Smith, C.B. (Eds.): *Beyond the Energy Crisis Opportunity and Challenge*, Oxford University Press, Oxford, pp.581–587.

Miyawaki, A. (1993a) 'Restoration of native forest from Japan to Malaysia', in Lieth, H. and Lohmann, M. (Eds.): *Restoration of Tropical Forest Ecosystems*, Kluwer Academic, Dordrecht, pp.5–24.

Miyawaki, A. (1993b) 'Global perspective of green environment-restoration of native forests from Japan to Malaysia and south America', *Based on an Ecological Scenario, IGRASS'93. Better Underst Earth Environ*., Vol. 1, pp.6–18.

Miyawaki, A. (1998a) 'Restoration of urban green environments based on the theories of vegetation ecology', *Ecol. Eng*., Vol. 11, pp.157–165.

Miyawaki, A. (1998b) 'Vegetation ecological study for restoration of forest ecosystems', in Fujiwara, K.A. (Eds.): *Vegetation Ecological Study for the Restoration and Rehabilitation of Green Environment based on the Creation of Environmental Protection Forests in Japanese Archipelago*, Inst. Veget. Sci., Inst. Environ. Sci. Technol., Yokohama Natl. Univ., pp.267–298.

Miyawaki, A. (1999) 'Creative ecology: restoration of native forests by native trees', *Plant Biotechnol*., Vol. 16, No. 1, pp.15–25.

Padilla, F.M. and Pugnaire, F.I. (2006) 'The role of nurse plants in the restoration of degraded environments', *Frontiers in Ecology and the Environment*, Vol. 4, pp.196–202, doi:10.1890/1540- 9295(2006)004[0196:TRONPI]2.0.CO;2.

Perrow, M.R. and Davy, A.J. (2002a) *Handbook of Ecological Restoration.1: Principles of Restoration*, Cambridge University Press, Cambridge.

Perrow, M.R. and Davy, A.J. (2002b) *Handbook of Ecological Restoration.2: Restoration in Practice*, Cambridge University Press, Cambridge.

Ranjan, V. and Kumar, D. (2015) 'A review on dump slope stabilization by re-vegetation with reference to indigenous plants', *Ecological Processes*, Vol. 4, p.14.

Schirone, B., Salis, A. and Vessella, F. (2011) 'Effectiveness of the Miyawaki method in Mediterranean forest restoration programs', *Landscape and Ecological Engineering*, Vol. 7, January, pp.81–92.

Upadhyay, V.P. (2012) 'Eco-restoration technology for lands degraded due to opencast Chromite and iron ore mining in Odisha', *4th Ramdeo Mishra Memorial Centenary Lecture*, National Institute of Ecology and Orissa Environment Society, Bhubaneswar, pp.28–42.

Website

Annual return in form H1 for the Year (2012, 2013 and 2014) with respect to Thakurani Iron Ore Mines, Block-B, www.orissaminerals.gov.in

Mineral sand handling: Kwale mineral sand equipment selection

Sammy Ombiro*

Department of Mining,
Materials and Petroleum Engineering,
Jomo Kenyatta University of Agriculture and Technology,
P.O. Box 62000-00200, Nairobi, Kenya
Email: sombiro@jkuat.ac.ke
*Corresponding author

Joseph Komu

Akili Mineral Services,
P.O. Box 25492-00603,
Nairobi, Kenya
Email: joseph.komu87@gmail.com

Abstract: In mining industry, the cost of material handling accounts for significant portion of the total capital investment cost. This is due to the fact that equipment used in material handling is capital intensive and expensive to operate and maintain. Therefore, a sufficient prior equipment analysis is usually undertaken. Equipment selection is done with the view of achieving maximum efficiency and reliability with minimum capital and operational costs. Achieving this huge challenge cannot be avoided since you will need equipment for material handling. Overcoming these challenges means that one understands the real costs of owning a mining equipment which include purchasing cost, operation cost and maintenance cost. This is not straight forward. In this research therefore, the most appropriate equipment for handling titanium mineral at Kwale Mineral Sand Project were selected. The results of this selection were then compared with the results of Base Titanium equipment selection.

Keywords: mine equipment selection; mineral sand; equipment sizing; material handling; Kwale mineral sand.

Reference to this paper should be made as follows: Ombiro, S. and Komu, J. (2016) 'Mineral sand handling: Kwale mineral sand equipment selection', *Int. J. Mining and Mineral Engineering*, Vol. 7, No. 3, pp.265–280.

Biographical notes: Sammy Ombiro is an Assistant Lecturer in the Department of Mining, Materials and Petroleum Engineering in Jomo Kenyatta University of Agriculture and Technology. He is a holder of Masters of Engineering in Mining Engineering from Wuhan University of Technology, and Bachelors in Mining and Mineral Processing Engineering from Jomo Kenyatta University of Agriculture and Technology (JKUAT).

Joseph Komu is a Senior Mining Engineer at Akili Mineral Services Limited. A Bachelor holder in Mining and Mineral Processing Engineering from Jomo Kenyatta University of Agriculture and Technology.

1 Introduction

One of major problems facing a mining engineer during mine planning and design is material handling which is done by mine equipment. These equipments must be selected and matched to the purpose they are intended for; otherwise money invested in them may not be recouped. The process of selecting and matching this machinery is not straight forward; it is a complex task that requires sufficient background in equipment productivity for mining purposes they are intended for. In addition, the capital investment in mine machinery may greatly affect the viability of mining project and therefore, sufficient prior analysis is usually undertaken (Wills, 2008).

There are a number of factors which affect productivity of mine equipment and subsequently affect selection of these mine machinery. These factors may include: equipment cycle time, capacity and site conditions (Topal and Kuruppu, 2010). The site conditions that may affect equipment productivity (equipment performance) include: ore grade, space limitations and characteristics of material to be handled (Topal and Kuruppu, 2010).

The engineers at Base Titanium (the developers of Kwale Mineral Sand Project) were at one stage in planning of the above-mentioned project, faced with problem of selecting the most suitable equipment for various purposes in the proposed mine. This research paper, therefore, aims at selecting equipment for various purposes in Kwale Mineral Sand Project by employing various numerical models and comparing the results of these models with results of Base Titanium.

2 Project background information

2.1 Location

The Kwale Mineral Sand Project located in the East African nation, Kenya at an approximate distance of 50 km south of the coastal city of Mombasa, and around 10 km from the Indian Ocean (Ausenco Limited, 2006). Figure 1 shows the location of this project.

2.2 Kwale mineral sand resource

Kwale mineral sand deposit is hosted in Migarini Sands which is of Aeolian origin and was deposited as coastal dunes as a result of intense erosion (Ausenco Limited, 2006). The deposit is poorly stratified and contains silt and clay of approximately 24%. The heavy minerals (HM) in this deposit include: zircon, ilmenite and rutile. This ore deposit is mainly composed of brown sand at the top which is underlain by reddish or orange sand. As the depth increases, this sand becomes pinkish or beige. The base of the deposit is composed of weathered sandstone (Ausenco Limited, 2006).

Figure 1 Location of Kwale mineral sand project (see online version for colours)

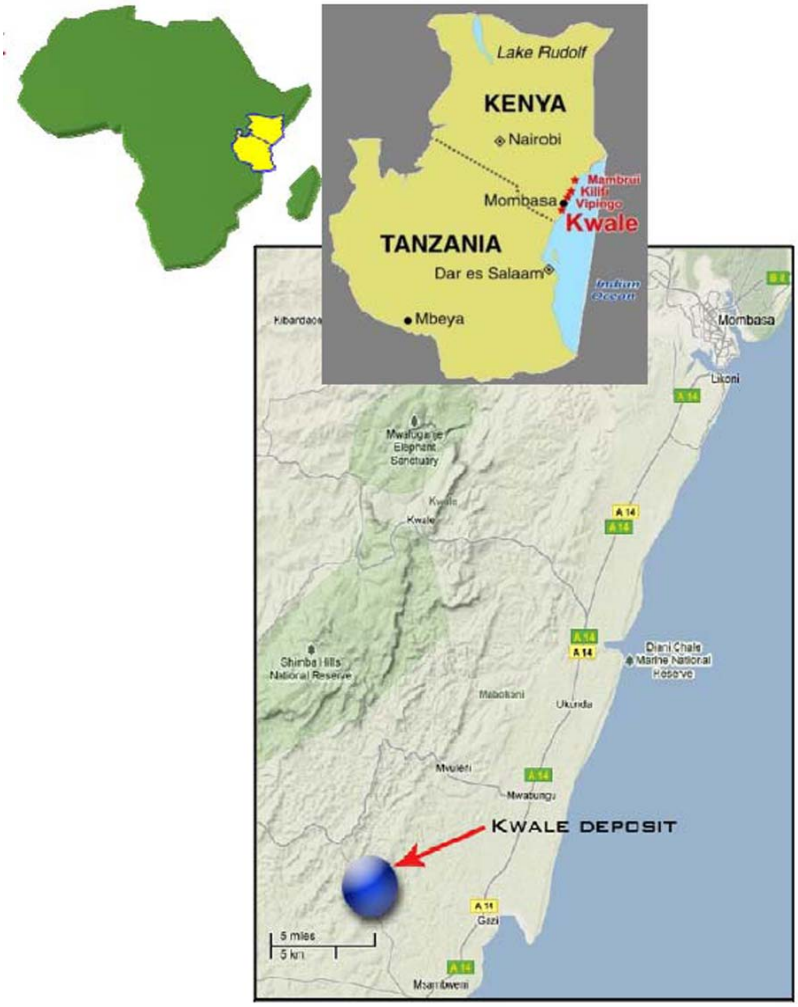

Source: Ausenco Limited (2006)

3 Research objectives

- Select the most appropriate equipment for mining Kwale mineral sand.
- Compare the results of this equipment selection with that of Base Titanium.

4 Research methods and materials

This research involved collection and analysis of data that were obtained from Base Titanium enhanced-definitive-feasibility study report. Equipments selected were then selected, sized and matched with the most appropriate mining activity. The data were

obtained from enhanced definitive feasibility study report obtained from Base Titanium are shown in Table 1.

Table 1 Research data

Property	*Value*
Total ore tonnage	140.6 million tonnes
Overburden/waste tonnage	1.2 million tonnes
Depth of the overburden	0.35 m
Total heavy mineral (THM)	4.7 million tonnes
Mine life	13 years
Cut-off grade	1.0%
Dip	0 degrees (orebody is generally flat lying)
Bulk Density	1.7 t/m^3
Scheduled operating hours (2 eight-hour shifts) (SH)	16 h per day
Overburden characteristics	(a) Brown red sand
	(b) 0.35 m deep
	(c) Unconsolidated
Ore characteristics	(a) Unconsolidated
	(b) Reddish to orange sand which become more pinkish as depth increases
	(c) Poorly stratified
	(d) Deposit base is composed of weathered sandstone

Source: Ausenco Limited (2006)

4.1 Other data

Other data were calculated as shown below.

Overall stripping ratio

$$\text{Overall stipping ratio} = (\text{overburden tonnage}) / (\text{ore tonnage})$$

$$\text{Overall stipping ratio} = (1,200,000 / 140,600,000) = 0.00853.$$

Tonnage factor

$$\text{The density of overburden} = 1.7 \text{ t/m}^3$$

$$\text{Tonnage factor} = 1 / \text{density} = 1 / 1.7 = 0.5882 \text{ m}^3/\text{t}.$$

Overburden volume to be stripped throughout mine life

$$\text{Volume} = \text{tonnage factor} \times \text{overburden tonnage}$$

$$\text{Volume} = 0.5882 \times 1,200,000 = 705,882 \text{ m}^3.$$

Ore volume to be mined throughout mine life

$$\text{Volume} = \text{tonnage factor} \times \text{ore tonnage}$$

$$\text{Volume} = 0.5882 \times 140,600,000 = 82,700,000\,\text{m}^3.$$

Ore volume to be mined per day

$$\text{Daily ore volume} = (\text{total ore volume}) / (\text{mine life} \times \text{working days per year})$$

$$\text{Daily ore volume} = (82,700,000) / (13 \times 250) = 25,466\,\text{m}^3 \text{per day.}$$

Average annual ore tonnage

$$\text{Ore / year} = (\text{total ore tonnage}) / (\text{mine life})$$

$$= 140,600,000 / 13 = 10,820,000 \text{ tonnes per annum.}$$

Overburden tonnage to be stripped annually

$$\text{Overburden / year} = (\text{total overburden tonnage}) / (\text{Life of mine})$$

$$= 1,200,000 / 13 = 92,300 \text{ tonnes per annum.}$$

Location of waste dump (for dumping overburden) = 500 m from the mine
Daily ore tonnage

Working days per year = 250 days

$$\text{Ore tonnage per day} = (\text{ore / year}) / 250$$

$$= 10,820,000 / 250 = 43280 \text{ tonnes per day.}$$

Accounting for 250 days per year

Public holidays in Kenya per year = 9 days

Number Sundays per year (No work on Sundays) = 52 days.

Accounting for Saturdays

Normal Mining Shift per day = 2 eight – hour shifts per day

Saturday working hours from 8 am to 1 pm = 5 h ≈ half shift

Half shifts on Saturdays : This is equivalent to : 0.75×52 days

= 39 days (2 shifts per day for mining)

Period for shutting down mine unit plant (MUP) per year

for maintenance=10 days

Total number days per year available for mining

$=360-(9+52+39+10)=250$ days per year.

Overburden to be stripped daily (assuming 250 working days per year)

$$\text{Daily overburden tonnage} = (\text{overburden / year}) / 250$$

$$= 92,300 / 250 = 369.2 \text{ tonnes per day.}$$

5 Equipment selection and sizing

5.1 Selection of overburden removal equipment

The equipments that are suitable for general overburden removal include: scrapers, dozers and excavators. Table 2 shows the conditions under which each of the above-mentioned overburden removal equipment may be applied.

Table 2 Working condition for overburden removal equipment

	Overburden removal equipment		
	Dozer	*Scraper*	*Excavator*
Suitable working condition	Suitable for both soft and hard material	Soft, fine grained material such as silt and sand	Solid bank material
	Can be applied in confined areas	Suitable for short distances	Confined areas
	Suitable for both unconsolidated and consolidated ground especially one that requires ripping before excavation	Unconsolidated material	Suitable for Compact material
	thin and thick overburden	Thin overburden	Thick overburden
	Both rocky and rock free material	Suitable for rock free material	Shaley bed rock
	Suitable for both compact and free flowing material	Free flowing material	Compact material

Source: Dagdelen (2007)

Given that Kwale mineral sand overburden is fine grained, soft, thin (0.35 m), unconsolidated, free flowing material and free of rock; the removal of overburden using either Scraper and Dozer is the most suitable of the above-mentioned equipment (see Table 2). Table 3 shows the condition under which each of the equipment is suitable for application.

Table 3 Condition under which a dozer or scraper may be applied in overburden removal

Dozer	*Scraper*
Convenient for very short haulage distance (less than 100 m) (Darling, 2011)	Convenient for haulage distances between 120 m to 1200 m (Darling, 2011)
Relatively slow and inflexible	Fast and flexible
Will require additional equipment such as trucks and loaders if the waste dump is located more than 1 km from the mine	Does not require any additional equipment

As shown in Table 3 dozers are only suitable for short haulage distances (up to 100 m) but waste damp for Kwale mineral sand was suggested to be located at a distance of 500 m from the mine site (Darling, 2011). This meant that if dozer was to be chosen as the overburden removal equipment, additional support equipment such as loaders and

trucks would be required. This raises operation cost. Additionally, dozers are not as mobile and as flexible as the scrapers. Therefore, the use *a fleet of Scrapers* was recommended for the removal overburden at Kwale mineral sand.

5.1.1 Sizing and calculation of the number of scrapers needed

Generally most scrapers that are used mining industry have capacity that range from 15 to 30.6 m^3 with caterpillar (CAT) having 26, 30.2 and 17.5 m^3 scrapers. Productivity of scraper Bank cubic metres per year (BCM/year is given by:

$$BCM/year = [(S)(A)(U)(J)(B)(CM)(LF)(60)]/C$$

BCM/year: Bank cubic metres per year
A: mechanical availability; 50–70%
U: Utilisation; 95%
S: scheduled operating hours
B: bowl fill factor; 70% and above
CM: scraper capacity in cubic metres
LF: load-factor
C: cycle-time
J: job efficiency; 70–90% (Atkinson, 1998).

The values for scraper cycle time are shown in Table 4.

Table 4 Scraper cycle time(C)

Cycle	*Time* (minutes)
Loading time	0.70
Travel time (loaded)	4.25
Dumping time	0.60
Travel time (empty)	2.10
Waiting time	0
Average delay time	0.35
CYCLE-TIME	*8.00*

Source: Atkinson (1998)

Additionally,

Load factor for sand is 0.89 (Atkinson, 1998)

Load factor for a mixture sand and clay is 0.79 (Atkinson, 1998).

Figure 2 shows typical scraper production cycle.

Trial runs

Taking a scraper of 26 m^3 capacity as the first trial run.

Scheduled operating hours (S) per year:

$$S = (\text{No. of working days per year}) \times (\text{working hours per day})$$

$$S = 250 \times 8$$

$$S = 2000 \text{ h.}$$

Therefore,

$$\text{BCM / year} = \left((\text{S})(\text{A})(\text{U})(\text{J})(\text{B})(\text{CM})(\text{LF})(60)\right) / \text{C}$$

$$\text{BCM / year} = \left((2000)(0.50)(0.95)(0.70)(0.70)(26)(0.79)(60)\right) / 8$$

$$\text{BCM / year} = 71,710.275\,\text{m}^3.$$

Total BCM required:

$$\text{BCM required} = (\text{volume of overburden to be stripped}) / (\text{mine life})$$

$$\text{BCM required} = 705,882 / 13 = 54,298.62\ \text{m}^3$$

$$\text{No. of scrapers} = (\text{BCM required}) / (\text{BCM per scraper per year})$$

$$\text{No. of scrapers} = 54,298.62 / 71,710.275 = 0.7572$$

$$\text{Scraper fleet size} = (\text{No. of scrapers}) / (\text{Mechanical Availability}$$

$$= 0.7572 / 0.6 = 1.262 \approx 2 \text{ scrapers}$$

Scraper fleet size = 2 scrapers.

Repeating the above procedure on 30.2 m^3 and 17.5 m^3 scraper gave result shown in Table 5.

Figure 2 Typical scraper production cycle

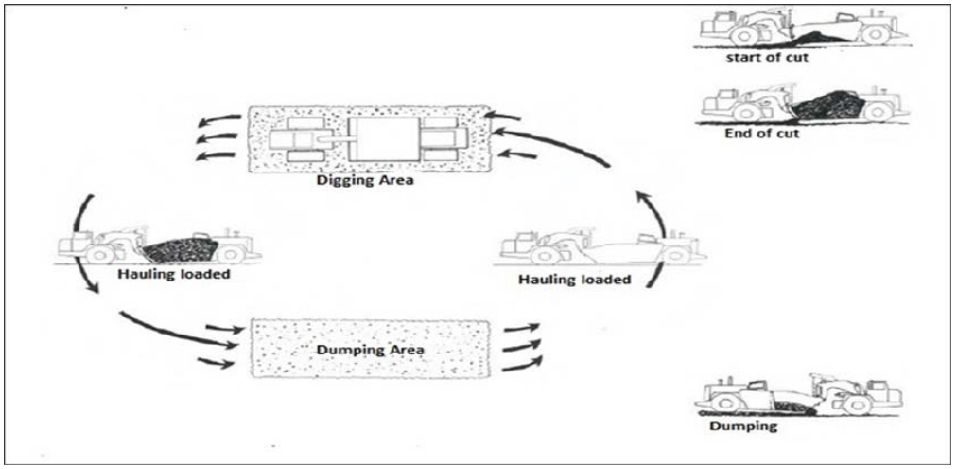

Source: Dagdelen (2007)

From the above analysis, it is observed that the number of scrapers that is required to strip and move overburden is the same (approximately two scrapers) for all the three

types of scrapers. However, the cost of acquiring a 17.5 m^3 is lower than that of other larger scrapers (26 m^3 and 30.2 m^3). Therefore, two 17.5 m^3 capacity scrapers can be used to remove the overburden and the waste. A typical example of a 17.5 m^3 scraper is CAT 632G shown in Figure 3.

Table 5 Scraper fleet size and type selection

	Scraper size (*cubic metres*)		
	26	*30.2*	*17.5*
BCM/Yr	71710.275	83294.2425	48266.53
BCM required	54298.62	54298.62	54298.62
No. of scrapers	0.7572	0.651889	1.125
Scraper fleet size	1.262 ≃ 2 scrapers	1.1 ≃ 2 scrapers	1.875 ≃ 2 scrapers

Figure 3 A 17.5 m^3 CAT 632G Scraper (2 of these or equivalent are suitable for Kwale Project) (see online version for colours)

Source: Caterpillar Inc. (n.d.)

5.2 Selection and sizing of Kwale mineral sand mining equipment

Equipment for mining Kwale mineral sand can generally be divided into: ore extraction equipment, loading equipment and haulage equipment.

5.2.1 Selection of ore extraction equipment

Generally, equipment that can be used for extraction of an ore include: scrapers, draglines, shovels (hydraulic or electric), blasting, dozers and excavators (hydraulic or electric). However, the condition under which each equipment is applicable may vary from one equipment to another. This means that a condition that may suit one mining equipment may not suit another. The table below shows these equipment and their suitable working conditions.

Just as its overburden the mineral sand (ore deposit) in Kwale is fine grained, soft, thin (0.35 m), unconsolidated, free flowing material and is free of rock. From Table 5, it can be seen that these conditions are suitable for the use of Dozers, Scrapers and

bucket wheel excavator (BWE). However, if processing plant is located at considerable distances from the mine as the case of Kwale mineral sand project, the use of scrapers may not be suitable.

According to a definitive feasibility studies that was done by Base Titanium (company that developed Kwale mineral sand project), the cost acquiring a Bucket wheel excavator and its auxiliary equipment is more than that of dozer trap mining unit (DMU) (Dozer and its auxiliary equipment). This feasibility study showed that by then, the cost of BWE was about 20 million US dollars and that of DMU was about 10 million USD. This, therefore, means that the use of *Dozer and its auxiliary equipment* is most suitable for this project.

Figure 3 shows the configuration of the DMU that was to be used at Kwale mineral sand as suggested by Base Titanium.

5.2.2 Sizing of ore extraction equipment

A DMU generally consists of: a fleet of dozers and a mining unit plant (MUP); this is shown in Figure 4 (page 13). The MUP consists of wet rotating grizzly and ore slurry pumping station. It is responsible for transporting the ore to the processing plant through slurry pumping.

Figure 4 Typical dozer trap mining unit (DMU) (see online version for colours)

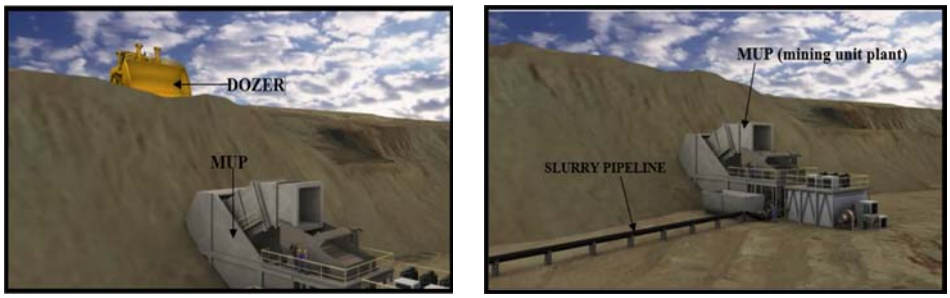

Source: Ausenco Limited (2006)

5.2.3 Dozer fleet size calculation

Dozer production (Dp) per, in LCM/h (Loose cubic metre per hour) is given by:

$$Dp = (\text{maximum production}) \times (\text{correction factors}).$$

The estimated dozer production for various dozer sizes are shown in the figure below.

Work correction factors for dozer production is shown in Table 6.

Starting with D7 CAT for the first trial run.

Note: These calculations were made on assumption that maximum distance that will be travelled by dozer while mining the ore is 30 m which is the bench width.

From Figure 5 (curve), maximum dozer production for D7 CAT dozer for 30 m haul distance is 360 loose cubic metre, LCM.

Table 6 Work correction factors for dozer production (Dp)

	Job condition	*Track-type tractor dozer*	*Wheel-type tractor dozer*
Operator	excellent	1.00	1.00
	Average	0.75	0.60
	Poor	0.60	0.50
Material	Loose, stockpile	1.2	1.2
	Hard to cut, frozen		
	With tilt cylinder	0.8	0.75
	Without tilt cylinder	0.7	–
	Hard to drift, dry non cohesive or sticky	0.8	0.80
	Rock ripped or blasted	0.75	–
Visibility	Good	1.00	1.00
	Poor	0.80	0.70
Job efficiency	50 min/h	0.84	0.84
	40 min/h	0.67	0.67
Dozer blade	U or straight blade	1.00	1.00
	U coal blade	1.20	1.20
	Other	0.60	0.60

Source: Caterpillar Inc. (n.d.)

Figure 5 Estimated dozer production for CAT D6M through to D11R

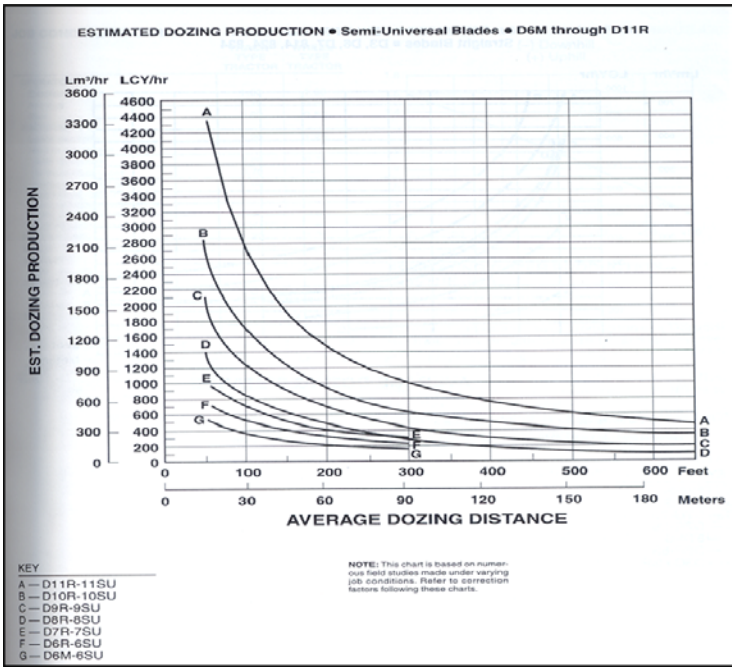

Source: Anon. (2007)

Therefore, the corrected dozer production for D7 dozer was calculated as shown below. The correction factors used in this calculation were obtained from Table 7.

$$Dp = (\text{maximum production, lcm}) \times (\text{correction factors})$$

$$D_p = 360 \times 0.75 \times 1.2 \times 1.2 \times 1.0 \times 0.84 \times 1.0 = 326.59 \text{ m}^3$$

Given,

$$\text{Daily ore production (volume)}, v = 25,466 \text{ m}^3$$

$$\text{No. of dozers required} = v / \left((\text{Dp})(\text{SH})(\text{A})(\text{U})(\text{J}) \right),$$

where

SH = scheduled operating hours = 16 h (from Table 1)

A = mechanical availability = 70%

U = Utilisation = 84%

J = job efficiency = 80%.

Table 7 Suitable working conditions for various equipment

	Ore extraction equipment				
	Dozer	*Scraper*	*Excavator*	*BWE*	*Dragline*
Suitable working condition	Suitable for both soft and hard material	Soft, fine grained material such as silt and sand	Solid bank material	Suitable for both soft and hard material	Solid bank material
	Can be applied in confined areas	Suitable for short distances	Confined areas.	Requires a large space to operate	Requires a large space to operate
	Suitable for both unconsolidated and consolidated ground especially one that requires ripping before excavation	Unconsolidated material	Suitable for Compact material	Suitable for intercalated and faulted ground. Weak unconsolidated material	Suitable for Compact material
	Thin and thick overburden	Thin overburden	Thick overburden	Thin and thick overburden	Thin and thick overburden
	Both rocky and rock free material	Suitable for rock free material	Shaley bed rock	Both rocky and rock free material	Shaley bed rock
	Suitable for both compact and free flowing material	Free flowing material	Compact material	Weak and free flowing material	Compact material

Source: Dagdelen (2007)

Therefore,

$$\text{No. of dozers required} = 25,466 / \left((326.59)(16)(0.7)(0.84)(0.8) \right) = 10.36 \approx 11 \text{ dozers.}$$

Repeating the above procedure on D8, D10 and D11 dozers gave result shown in Table 8.

Table 8 Dozer fleet size and type selection

	Dozer type			
	D7	*D8*	*D10*	*D11*
LCM	360	704		2141
Dp	326.59 m^3	639 m^3	1206.52 m^3	1942.3 m^3
No. of dozers	11 dozers	6 dozers	3 dozers	1.74 $\simeq$ 2 dozers
Price in USD as of 2011	USD 1.5 million	USD 1.6 million	USD 2.0 million	USD 2.4 million
Total capital cost required USD	11 × 1.5 = 16.5 million	6 × 1.6 = 9.6 million	3 × 2 = 6 million	2 × 2.4 = 4.8 million

When the dozer types (D7, D8, D10 and D11) are compared as done in Table 8, it is seen that it is cheaper to use 2 D11 dozers than using a fleet of the other types dozers.

The capital cost of owning the dozers can further be reduced by choosing a D11 dozer and one smaller dozer as opposed to choosing 2 D 11 dozers. This was done as shown below.

Smaller dozer production = [decimal part of dozer fleet × D11 dozer production]

Smaller dozer production = 0.74×2141=918 LCM.

Since the loose cubic metre (LCM) of a D9 dozer is 930 LCM (Figure 4 at 30 m) which is slightly more than the required LCM of 918 LCM, the D9 dozer was chosen as the smaller dozer.

Therefore, two dozers (one D11 and one D9) have been chosen for mining the ore at Kwale mineral sand project. Figure 6 shows how dozer production takes place.

Figure 6 Typical dozer productions

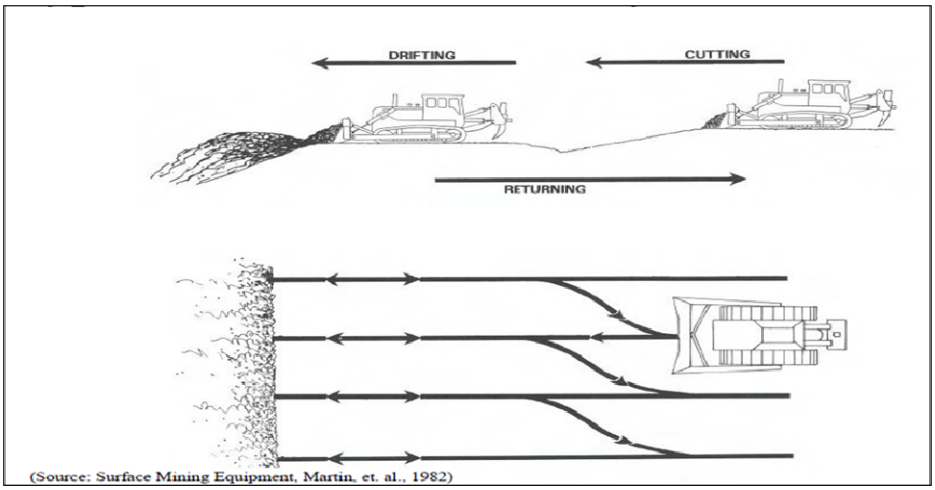

Source: Dagdelen (2007)

5.2.4 Transporting the ore to the processing plant

Just as mentioned earlier DMU consist of: a fleet of dozers and mining unit plant which consists of wet rotating grizzly and ore slurry pumping. The mining unit plant is responsible for transporting the ore to the processing plant through slurry pumping. Selection of pipeline and slurry pump was done as shown below.

Given the following conditions;

a Daily ore tonnage = 43,280 tones

b Tones per hours of sand = 2705 tones

c Specific gravity of solids, $S = 1.7$

d Average particle size d50 = 211 μm = 0.211 mm

e Solids concentration, $Cw = 30\%$ by weight

f Static discharge head (Zd) = 29.35 m (assumed to be the sum of thickness of ore body thickness and overburden thickness)

g suction head (Zs) = 1 m (positive)

h Length of pipeline = 6000 m (assumed to be the furthest distance from the plant to the mine).

The quantity of slurry to be pumped was thus calculated as follows:

Weight of solids to be in slurry per hour = daily ore tonnage = 2705tones

Weight of equal volume of water $= 2705 / 1.7 = 1591.12$ tones

Weight of water in slurry $(Cw,\ 30\%) = [2705(100-30)]/30 = 6312$ tones

Total weight of equal volume of water $= 1591.12 + 6312 = 7903.12$ tones.

Since 1 m^3 of water is 1 tonne, 7903 tones

Total weight of slurry mixture = weight of water + weight of solids

Total weight of slurry mixture = 6312 + 2705 = 9017 tones.

Specific gravity of slurry mixture = (total weight of slurry mixture)/(total weight of equal volume of water)

Specific gravity of slurry mixture $= 9017 / 7903.12 = 1.141$.

Concentration of solids by volume, Cv = [(Weight of volume of water equal to solids volume)/(total weight of equal volume of water)] × 100

Concentration of solids by volume $Cv = [1591.12 / 7903.12] \times 100 = 20.13\%$

Quantity of slurry $= 7903.12\ m^3/h$

Quantity of slurry $= (7903.12 \times 1000)/3600 = 2195.3$ L/s.

Therefore; the proposed slurry pump capacity = 2195.3 L/s.

6 Result comparison

The comparison of the result of this research with those of Base Titanium are shown in Table 9. Table shows that there is no big difference in the two outcomes.

Table 9 Research result comparison

Type of material to be handled	*Equipment size, number and type*	*Research outcome* (*results*)	*Base titanium results.*
Overburden	Equipment type	Scraper	Scraper
	Size	17.5 m^3	CAT 632G (17.5 m^3)
	Number	2	2
Ore (mining equipment)	Equipment type	Dozer	Dozer
	Size	CAT D11 and D9 or equivalent	CAT D11
	Number	2	2
Haulage	Equipment type	Slurry pipeline	Slurry pipeline

7 Conclusion and recommendation

Selection of the most appropriate equipment for material handling is one of the major problems facing mine planners throughout the mine life. These equipments must be selected and matched to the purpose they are intended for. The planners at Base Titanium were at one stage in planning faced with this problem and were able to select the various equipment for the various purposes in the proposed mine. While appreciating the work done by Base Titanium engineers at Kwale mineral sand, this separate study was carried out in order to confirm the results of Base Titanium selection. In this study, it found out that Kwale mineral sand being fine grained, soft, thin (0.35 m), unconsolidated, free flowing material and free of rock; scrapers were the most suitable equipment for removing the overburden. Further analysis showed that two 17.5 m^3 capacity scrapers were enough for this purpose. It was further found that the most suitable equipment for mining this ore deposit is dozer and two dozers (one D11 and one D9) were found to be enough. Almost the same result was obtained by the Base Titanium. The Company found out that two CAT-632G scrapers which have 17.5 m^3 capacity each were enough for stripping overburden. It was further found out the use of slurry pipeline was the most appropriate for ore haulage. Even though the results of this study were similar with those of Base Titanium selection, there was a small difference in the capacity of equipment needed for ore extraction. While Base Titanium found out that two D11 dozers with a capacity of 2141 LCM (loose cubic metre) each were enough for ore extraction, this study found that one D11 dozer and a relatively smaller capacity D9 dozer were enough for ore extraction. The D9 dozer has a capacity of 930 LCM.

References

Anon (2007) *Loading and Hauling*, s.l.:s.n., pp.83–125.

Atkinson, T. (1998) 'Selection and sizing of excavating equipment', *Mining Engineering Handbook*, 2nd ed., s.l.:Society for Mining, Metallurgy, and Exploration, Inc., pp.1311–1333.

Ausenco Limited (2006) *Kwale Mineral Sands*,Technical Report, Ausenco Limited, Kenya, Perth.

Caterpillar Inc. (n.d.) *Caterpillar Performance Handbook Edition 29*, 29th ed.,Caterpillar Inc., USA.

Dagdelen, K. (2007) *Strategic Open Pit Mine Planning Course*, Colorado School of Mines, Colorado.

Darling, P. (2011) *SMA Mining Engineering Handbook*, Society for Mining, Metallurgy, and Exploration, Inc., UAE.

Topal, E. and Kuruppu, M. (2010) *Mine Planning and Equipment Selection – MPES 2010*, Carlton Victoria, The Australasian Institute of Mining and Metallurgy.

Wills, B.A. (2008) *Wills' Mineral Processing Technology: An Introduction to the Practical Aspects of Ore Treatment and Mineral Recovery*, Butterworth-Heinemann, Great Britain.